The retinal photoreceptor topography and daily responses to illumination in a nocturnal and a diurnal South African rodent

Ingrid van der Merwe

Submitted in partial fulfilment of the requirements for the degree of doctor of Zoology in the Faculty of Natural and Agricultural Sciences

University of Pretoria

Pretoria

July 2015

Supervisor: Prof. N.C. Bennett

Co-supervisors: Prof. A.S. Haim and Dr. M.K. Oosthuizen

The retinal photoreceptor topography and daily responses to illumination in a nocturnal and a diurnal South African rodent

Student: Ingrid van der Merwe[1]

Supervisor: Prof. N.C. Bennett[1]

Co-supervisors: Prof. A.S. Haim[2] and Dr. M.K. Oosthuizen[1]

Departments: [1]Department of Zoology and Entomology, University of Pretoria, Private Bag X20, Hatfield, 0028, South Africa

[2]The Israeli Center for Interdisciplinary Studies in Chronobiology, University of Haifa, Haifa 31905, Israel

Degree: PhD (Zoology)

I, Ingrid van der Merwe declare that the thesis/dissertation, which I hereby submit for the degree PhD (Zoology) at the University of Pretoria, is my own work and has not previously been submitted by me for a degree at this or any other tertiary institution.

SIGNATURE: ……..

DATE: ……..

Disclaimer

This thesis consists of a series of chapters that have been prepared as stand-alone manuscripts for publication purposes. Consequently, unavoidable overlaps and/or repetitions may occur between chapters. Chapter 2 is essentially the text of a manuscript that has already been published in the *Canadian Journal of Zoology* (CJZ) entitled: van der Merwe, I., Bennett, N.C., Haim, A. and Oosthuizen, M.K. Locomotor activity in the Namaqua rock mouse (*Micaelamys namaquensis*) – Entrainment by light manipulations. The style of Chapter 2 is according to the specifications by the CJZ, except for the references cited, which have been incorporated into the main reference list at the end of this thesis. Therefore, the style of Chapter 2 is slightly different to that of the rest of the thesis. For ease of reading, tables and figures have been placed on separate pages at the end of each chapter.

General abstract

A number of daily rhythms were investigated under different lighting conditions and the topographical arrangements of visual (rods/cones) and non-visual retinal photoreceptors (ipRGCs) determined, in the Namaqua rock mouse (*Micaelamys namaquensis*) and the four striped field mouse (*Rhabdomys pumilio*). The present study provides evidence that *M. namaquensis* possesses a distinctly nocturnal locomotor activity rhythm that is endogenously entrained by the light-dark cycle, with a near 24h period length. Females also seem to be more active than males, this may be due to females having higher levels of estrogen.

The current investigation reveals that *M. namaquensis* and *R. pumilio* possess duplex retinas that are rod-dominated, but cone to rod ratios reflect the temporal niches of the species. *Micaelamys namaquensis* possesses far more rods than cones, whereas *R. pumilio* possesses a high amount of both rods and cones. Both species also seem to have dichromatic colour vision and although different topographical distributions of the rods, cones and ipRGCs are observed, the adaptive values of these features remain to be elucidated. The ipRGCs are sparsely distributed across the retinas of both species but in *R. pumilio* they are distinctly concentrated in the dorso-nasal quadrant.

The effects of different photophase illuminances on the photoentrainment of various daily rhythms were tested. Across the various photophase illuminances, both species expressed daily activity patterns that are generally typical to the species, but brighter illuminances might be needed to increase diurnal activity in *R. pumilio* to levels that reflect its activity under natural

conditions. The amplitude, but not the temporal expression of daily activity is affected and *M. namaquensis* seems to be more susceptible to different illuminances than *R. pumilio*. Unexpectedly, dim photophase lighting reduces daily activity in *M. namaquensis*. These responses appear to reflect the photoenvironments of the species under natural conditions. Furthermore, day/night urine production values generally reflect the activity patterns of the species. In *M. namaquensis,* the 6-SMT rhythm is attenuated by a brighter as opposed to a dimmer photophase cycle and likely indicates a sensitivity threshold of the melatonin rhythm that is below 330 lux. *Rhabdomys pumilio* appears to express an ultradian 6-SMT rhythm with similar mean daily values, yet with different temporal patterns, under both dim and bright photophases.

Lastly, the effects of differing photophase wavelengths on the photoentrainment of various daily rhythms were investigated. Long wavelength photophase lighting slightly increases daytime activity in both species. In *M. namaquensis*, this is probably due to the visual capabilities of the species, but in *R. pumilio*, lower stress levels under a long wavelength photophase, is the most likely cause. In both species, short wavelength photophase lighting attenuates the overall daily urine production rhythm, while medium and long wavelengths exert similar effects. Furthermore, there is an inverse correlation between the wavelength of the photophase and the level of daily 6-SMT as well as with corticosterone. The results also indicate the involvement of the ipRGCs, in mediating urine, melatonin and corticosterone production in *M. namaquensis* and in *R. pumilio*. It is clear that light plays an integral role in adjusting physiology and behaviour in these animals and a wide range of anatomical and physiological features reflect different adaptations according to their respective temporal niches.

Acknowledgements

It is evident that without the assistance, support and guidance of a number of people, the completion of this project would not have been possible. I would like to express my sincere gratitude towards Nigel Bennett, Marietjie Oosthuizen and Abraham Haim; it has been an immense blessing and privilege to have you as my supervisors. I am especially grateful to Nigel Bennett for arranging various opportunities, which apart from being necessary for this project also enriched me as a person.

A number of people assisted me with various aspects of this project and for this I thank Sonja, Carol, Katarina, Sasha, Michael, Jacques and Louwrens. I also thank Ákos Lukáts for his contribution to Chapter 3, Neville Pillay for providing mice at one occasion, as well as Paul Manger and Nina Patzke for their assistance with the perfusions. I am immensely thankful to Andre and Stefanie Ganswindt from Onderstepoort for their invaluable assistance with the hormone assays. I am particularly grateful to Marietjie for patiently and willingly assisting me with, amongst many other things, the statistical analyses of the data. To all of my wonderful friends (Sonja, Michael and Jacques) who have helped out on the dreaded 'urine collection days', thank you so much! I also extend my sincere gratitude to Veronika Blahova, for helping out with lab work and for her friendship. Very special thanks to my cousin Anél and to Sonja for all of their invaluable support and motivation. To my heavenly Father, thank you for revealing to me over these last few years that "the branch cannot bear fruit of itself unless it abides in the vine".

To my parents Hannes and Liza, and to my brother Schalk, I extend my deepest gratitude towards you for loving me, supporting me and especially for encouraging me. It is impossible to express in words what the three of you mean to me. To my treasurable husband, Jacques, thank you for being with me all of the way, through the many frustrations and accomplishments!

Finally, I would like to thank the Department of Zoology and Entomology at the University of Pretoria, for their support and for making this project possible.

Glossary of important abbreviations

6-SMT	6-Sulfatoxymelatonin
GCL	Ganglion cell layer
HPY	Hypothalamic-pituitary-axis
IDA	International Dark-Sky Association
ILC	Illuminance light cycle
INL	Inner nuclear layer
IPL	Inner plexiform layer
ipRGC	Intrinsically photosensitive retinal ganglion cells
LAN	Light at night
M/L-cones	Medium wavelength sensitive cones
ONL	Outer nuclear layer
OPL	Outer plexiform layer
PEL	Pigment epithelial layer
RHT	Retino-hypothalamic-tract
SCN	Suprachiasmatic nuclei
S-cones	Short wavelength sensitive cones
TPP	Total photoreceptor population
TVPP	Total visual photoreceptor population
WLC	Wavelength light cycle

Table of contents

List of figures

List of Tables

CHAPTER 1:

GENERAL INTRODUCTION

Light and dark: Resources for life

Whether we receive it from the sun or from a bulb in the ceiling, a world completely void of light is unimaginable to say the least. Even in the dark and frigid regions of the deep ocean where sunlight seldom or ever reaches, a type of light called bioluminescence ensures the survival of many sea creatures (Haddock & Moline 2010). Prior to the invention and the popularization of the incandescent light bulb less than 150 years ago, the prospect of artificial light at night becoming a pollutant one day, let alone a global threat, would simply have been inconceivable (Fig. 1.1). The International Dark-Sky Association (IDA; http://www.darksky.org), one of the world's foremost protectors of the nighttime environment, defines light pollution as "*Any adverse effect of artificial light, including sky glow, glare, light trespass, light clutter, decreased visibility at night, and energy waste"*. Since its effects span beyond the borders of the cities from where light is so freely emitted, light pollution does not only threaten human health, but also biodiversity and evidence for this is intensifying (Stevens & Rea 2001; Longcore & Rich 2004; Navara & Nelson 2007; Chepesiuk 2009; Kloog *et al*. 2009, 2010; Fonken *et al*. 2010). What exactly about light is so threatening, beyond of course abolishing one of our most splendid natural vistas, i.e. the night sky (Fig. 1.1)? The key to this question lies in understanding how organisms utilize both light and dark to live and survive.

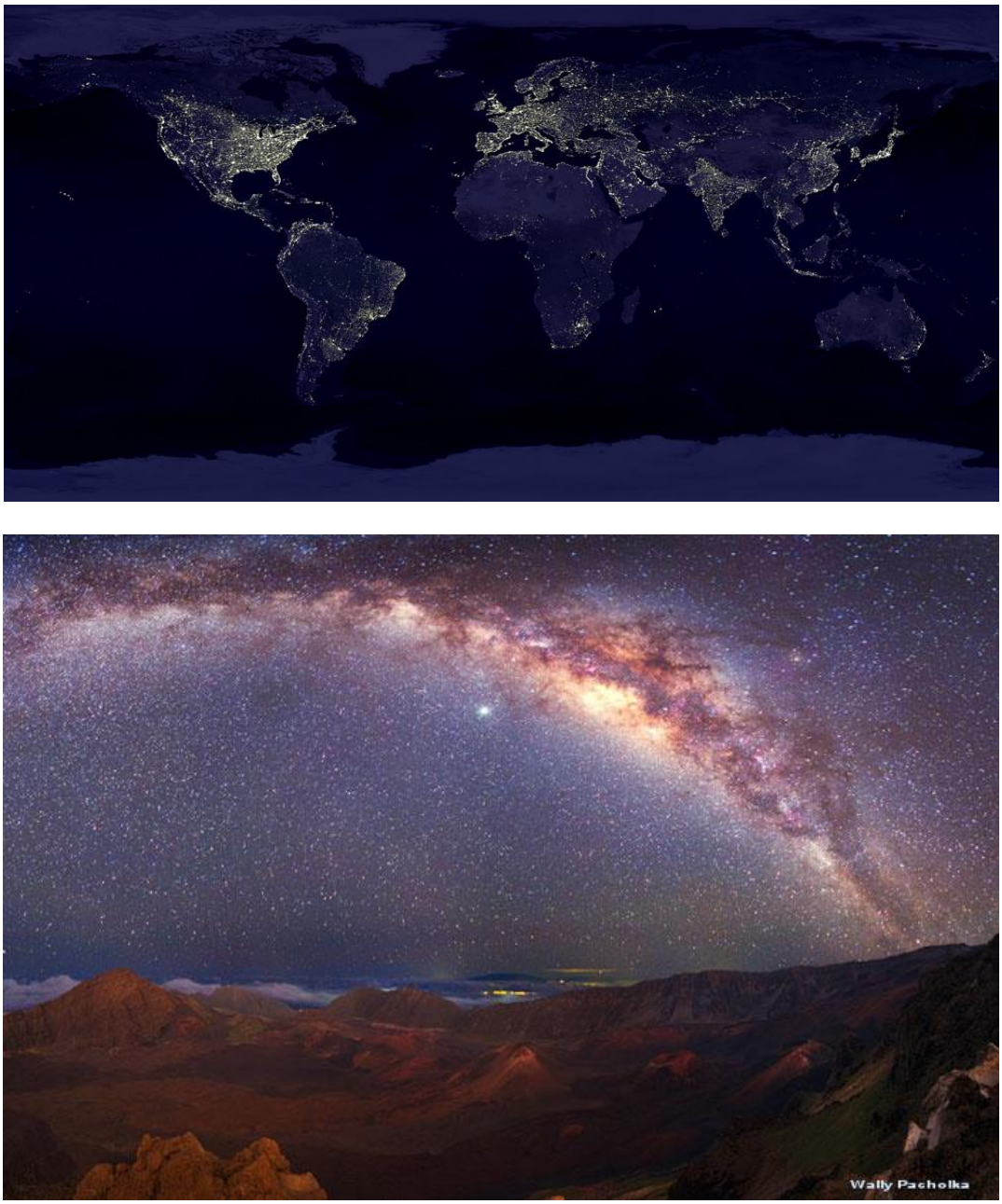

Figure 1.1: At the top: a composite satellite image of the whole Earth at night showing the extent to which various regions are illuminated at night. Image courtesy of Chris Mayhew and Robert Simmon, NASA GSFC. http://visibleearth.nasa.gov/view_rec.php?id=1438. At the bottom: A beautiful night sky at the world's first International Dark Sky Park (IDSP) at the Haleakala Crater in Utah.

Circadian rhythms

In the natural environment, nearly all organisms are exposed to the perpetual cycling of day and night (the light-dark cycle), which in conjunction with the length of day reliably exposes daily and seasonal time. Myriads of biological processes transpire rhythmically and in synchrony with geophysical time, as presented by photic cues (Pittendrigh & Minis 1964; Gachon *et al.* 2004; Mohawk *et al.* 2012). Such rhythmicity is achieved through biological clock mechanisms that allow organisms to register and respond to the temporal environment, a process that evidently ensures survival in many species (Navara & Nelson 2007; Paul *et al.* 2008). The photic entrainment of biological rhythms in terrestrial animals has been extensively studied, with the most familiar and widespread rhythm being the circadian rhythm.

Circadian rhythms are daily fluctuations in biochemical, cellular, physiological and behavioural processes that have a cycle length close to 24h, even under constant environmental conditions (Reppert & Weaver 2002; Holzberg & Albrecht 2003). As a consequence of these oscillations being not exactly 24 h, the system needs regular external input for it to be synchronized to geophysical time. Light is considered the principal *zeitgeber* (time signal) for circadian adjustment in most terrestrial animals and may even drive circadian rhythms in various subterranean species, including those that are rarely exposed to light (Lovegrove & Papenfus 1995; Begall *et al*. 2002; Vasicek *et al*. 2005; Tachinardi *et al.* 2014). At its core, the circadian timing system is genetically driven and rhythmicity is preserved as a result of numerous positive and negative autoregulatory feedback loops of circadian clock genes (Reppert & Weaver 2001). In support of this, mutations within several mammalian clock genes alter the cycle length or even

abolish circadian rhythmicity altogether (Ralph & Menaker 1988; Zheng *et al.* 1999; Cermakian *et al.* 2001).

In vertebrates, circadian entrainment is initiated through ocular light exposure. Photic cues are absorbed by the retinal photoreceptors and then communicated *via* the retino-hypothalamic-tract (RHT) to the central pacemaker, namely the suprachiasmatic nuclei (SCN) of the hypothalamus (Cassone *et al*. 1988; Ralph *et al*. 1990). Several studies have established that a group of photoreceptors that reside in the inner retina, i.e. the intrinsically photosensitive retinal ganglion cells (ipRGCs), is fundamentally involved in entrainment of the SCN (Foster *et al*. 1991, 1993; Freedman *et al*. 1999; Lucas *et al*. 1999, 2001). Nevertheless, despite the discovery of a rodless, coneless photoreceptive pathway for non-visual responses, evidence suggests that conventional photoreceptors (rods and cones) also play a contributive role in non-visual processes related to the SCN (Aggelopoulos & Meissl 2002; Dkhissi-Benyahya 2007; Altimus *et al.* 2010; Gooley *et al.* 2010; van Diepen *et al.* 2013; Weng *et al.* 2013). The mammalian SCN consists of a vast amount of closely opposed neurons (~20 000) that functions as a network with remarkable coherence in neuronal firing and clock gene expression (Yan *et al.* 2008; Welsh *et al.* 2010). Ablation of the SCN has been demonstrated to disrupt both circadian as well as seasonal rhythms (Stephan & Zucker 1972; Ruby *et al.* 1996), whilst transplantation thereof rescues lost circadian rhythms (Ralph *et al*. 1990). Interestingly, isolated SCN neurons display cell autonomous circadian rhythms but ultimately, the complete neuronal SCN network is essential for optimal SCN functioning (Welsh *et al.* 2010).

Temporal locomotor activity rhythms

A large proportion of daily rhythms are SCN-generated. Examples include the sleep-wake cycle, body temperature, urinary function, mitosis, mitochondrial oxidative capacity and the secretory patterns of numerous hormones (Benstaali *et al.* 2001; Piccione *et al.* 2002; Matsuo *et al.* 2003; Noh *et al*. 2011; Peek *et al.* 2013). One of the most frequently studied circadian rhythms is that of locomotor activity. Since the availability of environmental resources change in concurrence with changing levels of illumination across the day, the temporal organization of the locomotor activity rhythm of a species is vital. In mammals, the temporal locomotor activity rhythm is typically described in relation to the light-dark cycle and classifies organisms as being either nocturnal, diurnal, crepuscular or arrhythmic. Although the photic entrainment of the locomotor activity rhythm by the SCN underpins the temporal expression of locomotor activity, several internal and external factors interactively shape the temporal niche of a species. Consequently there is in reality a continuum of temporal niches that exists between a strictly nocturnal lifestyle and a strictly diurnal lifestyle (Refinetti 2008).

Some factors such as body size, insulative properties, retinal photoreceptor composition and morphology of the central timing system may have an overall constraining effect on the temporal niche. Others factors such as the pressure experienced from resource competition, aggression or environmental temperature may drive changes in the temporal niche. In addition to the entrainment of the activity rhythm by the SCN, another internal mechanism that is referred to as masking also shapes the temporal niche of a species. Similar to entrainment, masking is also mediated by the visual system (Hattar *et al.* 2003). Whereas entrainment by the SCN is the direct

synchronization of the clock by a *zeitgeber* (i.e. the light-dark cycle), masking refers to the immediate effect that an agent (in some cases light) has on the overt rhythm, without changing the SCN-timing (Mrosovsky 1999). In effect, entrainment stabilizes circadian rhythms by using repetitive and predictable cues while masking provides individuals the ability to respond to unforeseen environmental changes (Kronfeld-Schor & Dayan 2008). In contrast to entrainment, which is comparable in nocturnal and diurnal species, masking (particularly by light) differs between nocturnal and diurnal species (Mrosovsky 1999). In diurnal species, bright light has a stimulating effect on activity (positive masking) whereas in nocturnal species, it has an inhibiting effect (negative masking). Positive masking has been observed in nocturnal mice that were exposed to a 1 hour dim light source during the scotophase (nighttime); locomotor activity increased rather than decreased during the period of dim light exposure (Mrosovsky *et al.* 1999). In some species, such as the Nile grass rat (*Arvicanthis niloticus*), masking may even vary between individuals. Although masking differences seem to be connected to the chronotype of the individual (day active versus night active individuals), the phase of circadian rhythms as entrained by the light-dark cycle remains unaffected by the chronotype (Mahoney *et al.* 2001).

Interestingly, some species show drastic changes in their activity rhythms when presented with certain external conditions under standard laboratory conditions. For example, in the degu (*Octodon degus*), *ad libitum* wheel running induces shifts from diurnal to nocturnal activity (Kas & Edgar 1999). Similarly, in Nile grass rats (*Arvicanthis niloticus*), wheel running changes activity from predominantly diurnal to primarily nocturnal (Redlin & Mrosovsky 2004). Nevertheless, evidence suggests that in both of these species the activity shifts were at least partly due to the effects of masking (Redlin & Mrosovsky 2004; Vivanco *et al.* 2009).

Furthermore, drastic nocturnal to diurnal activity shifts have also been observed in knockout mice (OPN4-/-; RPE65-/-) lacking retinal melanopsin as well as the protein essential for the regeneration of visual pigment (Doyle *et al*. 2008). As previously mentioned, mutations within clock genes are also capable of changing circadian rhythmicity and hence its outputs (Ralph & Menaker 1988; Zheng *et al.* 1999; Cermakian *et al.* 2001).

Basis for nocturnality or diurnality

At present, the task of distinguishing and defining the physiological mechanisms that determine nocturnality or diurnality remains largely unresolved, with the reason being that many underlying features of the SCN seem largely similar in nocturnal and diurnal species. Some studies have shown that among others, electrical firing, glucose metabolism and clock gene expression within the SCN share similar phases in nocturnal and diurnal species (Schwartz *et al.* 1983; Sato & Kawamura 1984; Challet 2007). Clock genes such as *mPer1* is induced by light and expression peaks during the subjective day in nocturnal rodents (mice, rats and hamsters), diurnal rodents such as ground squirrels (*Spermophilus tridecemlineatus*), grass rats (*Arvicanthis ansorgei*), and even in the blind mole rat (*Spalax ehrenbergi*; Mrosovsky *et al.* 2001; Oster *et al.* 2002; Caldelas *et al.* 2003). The circadian expression of some neuropeptides of the SCN such as arginine-vasopressin also share similar phases in nocturnal mice (*Mus musculus*) and diurnal mice (*Arvicanthis ansorgei*), but nevertheless, other SCN-neuropeptides such as vasoactive intestinal polypeptide and gastrin-releasing peptide peak at different phases (Dardente *et al.* 2004). Interestingly, in contrast to mice, the latter two peptides appear to be under the direct control of light rather than the circadian clock in rats (Dardente *et al.* 2004). Therefore, even

though it cannot be conclusively stated, evidence suggests that nocturnality or diurnality is based on species specific differences that lie downstream or upstream from the SCN (Nunez *et al.* 1999, Smale *et al.* 2003; Doyle *et al.* 2008; Refinetti 2008; Karnas *et al.* 2013).

Melatonin

One pathway, through which light-dark information is communicated to individual cells downstream from the SCN, is *via* the rhythmic secretion of the neurohormone melatonin (*N*-acetyl-5-methoxytryptamine; Fig. 1.2) by the pineal gland (Klein & Moore 1979). Circadian cues are projected from the SCN *via* the paraventricular nuclei to the intermediolateral cell column of the upper spinal cord and subsequently to the superior cervical ganglia (Kappers 1965). The pineal is then activated by postganglionic sympathetic innervations through the release of norepinephrine, which then leads to the synthesis of melatonin (Moore 1996; Reiter *et al.* 2011). In mammals, pineal melatonin is synthesized and secreted during nighttime under dark conditions, irrespective of whether the animal is nocturnal or diurnal and consequently classifies melatonin as an arousal-independent factor (Challet 2007). In contrast, arousal-dependent factors such as body temperature and serotonin level have opposing phase relationships to the light-dark cycle depending on whether the species is nocturnal or diurnal (Challet 2007). Melatonin is quickly released into the blood and cerebrospinal fluid after it is synthesized and hence effectively translates and disseminates information on circadian time for daily adjustments and also seasonal adjustments in photoperiodic species (Reiter 1993).

Several features of light including intensity, spectral wavelength, duration, frequency and timing of exposure to light, affect the circadian rhythm of melatonin synthesis (Gorman *et al.* 2003; Duffy & Wright 2005; Aral *et al*. 2006; Zubidat *et al.* 2009, 2010b). There are also large variations in the capacity of light to suppress melatonin rhythms among different species. Each species seems to have a characteristic sensitivity threshold to light that is most likely reflective of the habitat to which the species is adapted and evidently this goes hand in hand with specific visual adaptations (Peichl 2005; Zubidat *et al.* 2009, 2010b). There is some evidence to suggest that nocturnal species are more sensitive than diurnal species to the effects of light at night or LAN (Reiter *et al.* 1982). Since it has been shown that conventional rod and cone pathways contribute to non-visual pathways (van Diepen *et al.* 2013), different photoreceptor compositions may potentially explain, at least in part, inter-species differences in melatonin responses to different lighting conditions.

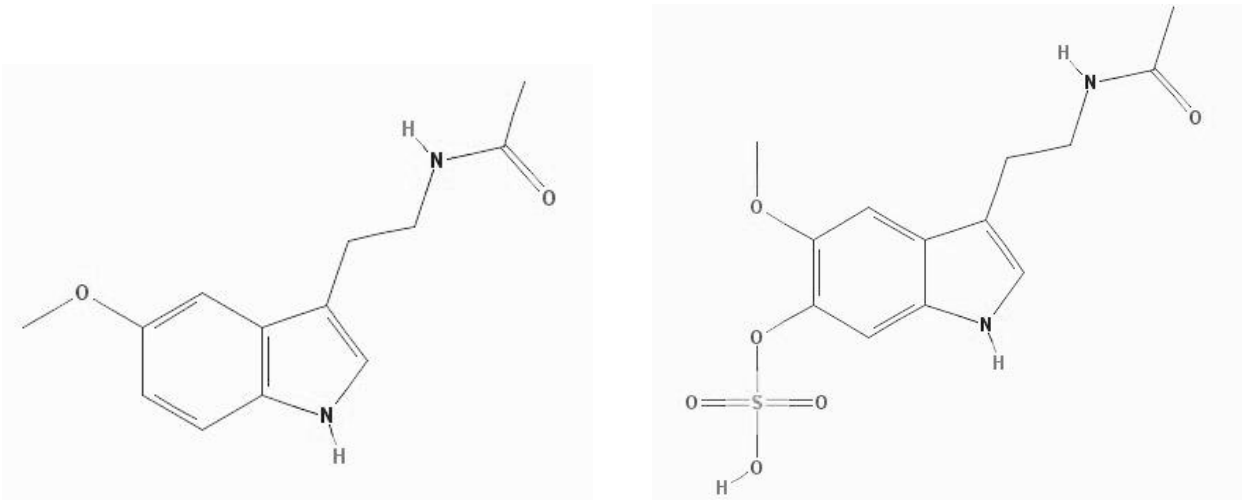

Figure 1.2: The molecular structure of melatonin (on the left) and of 6-sulfatoxymelatonin (6-SMT; on the right).

In general, the melatonin response to light is intensity dependent with higher intensities of light at night (LAN) being more effective in suppressing nocturnal melatonin secretion than low light intensities (Deveson *et al.* 1990; Thapan *et al.* 2001). This effect has also been shown to be true across a range of different wavelengths of light. In a study by Thapan *et al.* (2001) on human subjects, an increase in the light intensity caused a decrease in plasma melatonin levels at several different wavelengths of monochromatic light. There is however, also contradicting evidence from the literature regarding melatonin suppression by light. Both a high intensity (2500 lux) of LAN and a low intensity (300 lux) of LAN were capable of suppressing nighttime melatonin levels in humans (Bojkowski 1987). Nevertheless, evidence suggests that the high sensitivity of the pineal to dim light intensities (200 lux) in humans could be a result of disorders such as bipolar affective disorder or seasonal affective disorder (Nathan *et al.* 1999). Also, ocular light adaptation prior to LAN exposure also plays an important role in determining the melatonin response (Jasser *et al.* 2006). In terms of the spectral composition of the light source, short wavelengths (~420nm-500nm, blue light) are deemed the most potent spectra for suppressing melatonin in both humans and animals (Brainard *et al.* 2001, Thapan *et al.* 2001; Rahman *et al.* 2008). However, at sufficient intensities, light with longer wavelengths are also able to suppress melatonin (Hanifin *et al.* 2006). Nighttime melatonin production is not only altered by light exposure during darkness, but also by the quality of daytime lighting with brighter daytime lighting usually resulting in higher levels of nocturnal melatonin (Hashimoto *et al.* 1997; Griffith & Minton 1992; Park & Tokura 1999). Amongst the various metabolites of melatonin, 6-sulfatoxymelatonin (6-SMT) can easily be measured from urine and accurately represents the concentration of pineal secreted melatonin (Bojkowski *et al.* 1987; Stieglitz *et al.* 1995; Fig. 1.2).

Stress and corticosterone

The stress system is comparable to the circadian system in that it also enables animals to adapt to immediate changes in the environment. However, unlike the circadian system, which uses predictive indicators (i.e. the light-dark cycle) for biological coordination, the stress system reacts to unpredictable environmental changes or stressors. Stress is best described as a condition during which an organism experiences a real or perceived disruption in its physiological or psychological homeostasis by an unpredictable and uncontrollable agent (Chrousos 2009; Koolhaas *et al.* 2011). Although stress most commonly elicits negative experiences, the response to a stressor may be beneficial since it consists of a series of adaptive mechanisms that are activated to defend the individual and to restore homeostasis (Bomholt *et al.* 2004; de Kloet *et al.* 2005). The list of potential stressors is far reaching; examples include noise, physical restraint, heat/cold and even social defeat (De Boer 1989; Keeney *et al.* 2006; Sonna *et al.* 2002; Wong 2006). Recently, it was shown that light interference at night causes a stress response, measured as increased heat shock protein HSP70, in Golden spiny mice (*Acomys russatus*; Ashkenazi & Haim 2012).

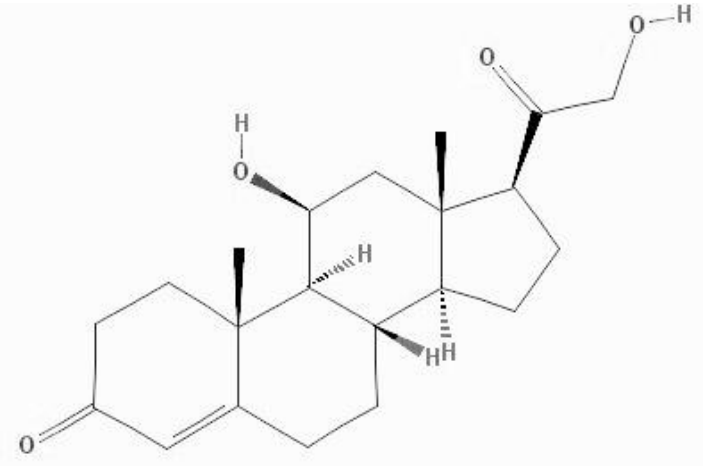

Figure 1.3: The molecular structure of corticosterone.

The magnitude of the stress response does not only depend on the qualities of the stressor, but are also affected by earlier life experiences and genetic predisposition to stress (Edwards *et al.* 1999; Landgraf & Wigger 2003; O'Connor *et al.* 2013). The principal effectors of the central nervous system comprises of a wide range of peptides, steroids and biogenic amines, which then subsequently also function downstream in the circulatory system (Holsboer & Ising 2010).

The principal effectors of the peripheral system consist of glucocorticoids and catecholamines of which the former is mediated by the hypothalamic-pituitary-adrenal (HPA) axis and the latter by the sympatho-adreno medullary system (Habib *et al.* 2001; Möstl & Palme 2002). Activation of the HPA axis by a stressor causes the release of corticotropin releasing hormone by the hypothalamus, which causes the release of adrenocorticotrophic hormone (ACTH) by the anterior pituitary and subsequently the release of glucocorticoids from the adrenal cortex (de Kloet *et al.* 2005). Glucocorticoids are widely used as agents to counteract stress in a wide range of animals and although cortisol is the main glucocorticoid manufactured in many mammals (eg. primates, dogs, cats, horses and pigs), corticosterone is the primary glucocorticoid in rodents (Möstl & Palme 2002; Palme *et al.* 2005; Fig. 1.3). The HPA axis is under direct regulation of the circadian timing system and corticosterone levels exhibit distinct daily rhythms (Ishida *et al.* 2005; Oster *et al.* 2006; Thorpe *et al*. 2012). The light-dark cycle is thus essential for the maintenance of normal corticosterone rhythms and consequently unnatural light exposure or insufficient light exposure causes stress (van der Meer *et al.* 2004; Gonzalez & Aston-Jones 2008; Thorpe *et al.* 2012). Similar to melatonin, light induced corticosterone levels are correlated with the intensity of light, but whereas LAN has an inhibiting effect on melatonin levels, it has a stimulating effect on corticosterone levels (Ishida *et al.* 2005). In laboratory mice, relatively dim

light (40 lux) is sufficient to induce maximal plasma corticosterone production (Ishida *et al.* 2005). It has also been suggested that large inter-individual variations in corticosterone levels, in response to stress, could potentially account for observed differences in circadian clock functioning. For example, in a study by Weibel *et al.* (2002), When Sprague-Dawley rats were exposed to an acute stressor and subsequently subjected to an abrupt shift in the light-dark cycle two weeks later, a positive correlation was observed between the stress-induced corticosterone levels with the time it took the animals to entrain and resynchronize to the new light cycle, as well as with the length of the free-running period. This study also showed that corticosterone levels were negatively correlated with daily locomotor activity.

The eye

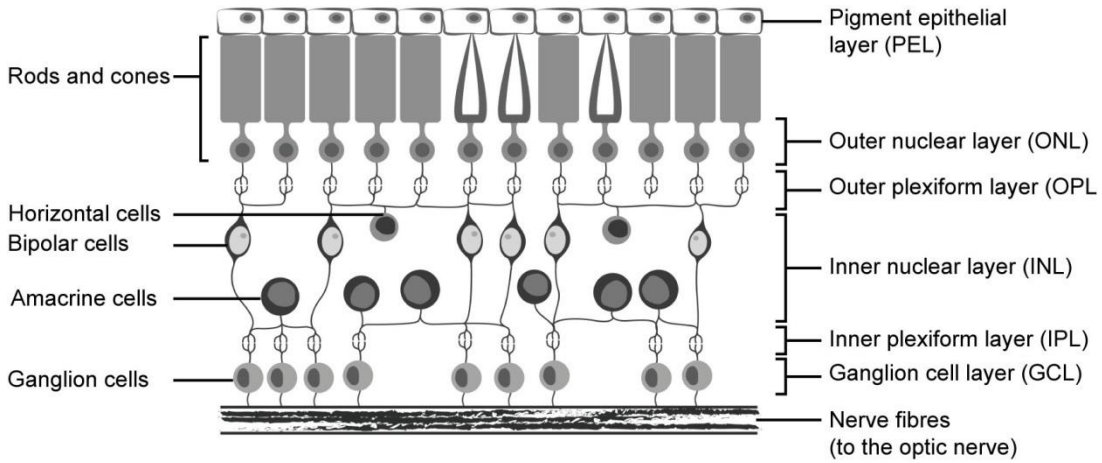

Figure 1.4: Schematic representation of the main layers of the retina.

The vertebrate eye, and in particular the stratified net-like membrane that lines the back of the eye, i.e. the retina, serves as a mediator between the spectrum of photic information from the environment, and the brain of an animal. Incredibly, despite being only ~200μm thick (Masland 2012), the retina comprises several specialized layers (Fig. 1.4) that are capable of transducing electromagnetic energy into neurological quanta. Around 55 functionally distinct cell types have been identified in the mammalian retina (Haverkamp & Wässle 2000; Masland 2001). The outermost margin of the retina is characterized by the pigment epithelial layer (PEL). The PEL reduces light scatter and plays a fundamental role in both the maintenance of the photoreceptors and in the visual process; i.e. the re-isomerization of all-*trans*-retinal into 11-*cis*-retinal (Strauss 2005).

Conventional photoreceptors (rods and cones) are densely arranged below the PEL with their outer segments bordering the apical face of the PEL and their cell bodies forming the outer nuclear layer (ONL). The rods and cones synapse with bipolar and horizontal cells in the outer plexiform layer (OPL) and the cell bodies of both of these interneurons as well as that of the amacrine cells reside in the inner nuclear layer (INL). In turn, the inner plexiform layer (IPL) connects the INL synaptically to the ganglion cell layer (GCL) and the latter contains the retina's output neurons, the ganglion cells, whose axons converge to form the optic nerve. A small subpopulation of these ganglion cells is currently recognized as a third photoreceptor class; the intrinsically photosensitive retinal ganglion cells (ipRGCs).

Light absorption and interpretation in the retina does not only produce visual perception, but also a range of non-visual behavioral and physiological responses, by means of two parallel circuitry

networks that extend *via* the optic nerve to the associated brain regions (Freedman *et al.* 1999; Berson 2003; Lockley & Gooley 2006). Examples of non-visual processes include circadian entrainment, the regulation of eye movements and the control of pupillary light reflex (Provencio *et al*. 2000; Berson *et al.* 2002; Hattar *et al*. 2002; Lockley & Gooley 2006). Photoreception is orchestrated by three classes of photoreceptors namely rods, cones and ipRGCs (Hattar *et al.* 2003; Sand *et al.* 2012). All photoreceptors are sensitive to different ranges of the electromagnetic spectrum, due to the photopigments they enclose. Cone photopigments are termed cone-opsins, rods enclose rhodopsin (rod opsins) and ipRGCs enclose melanopsin.

Classical photoreceptors (rods and cones) innervate the outer retina and are the starting point of the circuitry that is for image-based detection of the spatial environment (Jacobs 1993). In mammals, three basic cone types (S-, M- and L-cones) form the basis for trichromatic vision. They are distinguished by the short (blue, λ_{max}*=420 nm),* medium (green, λ_{max}*=530 nm),* and long wavelengths (red-orange, λ_{max}*=560 nm)* of light to which their photopigments are maximally absorptive (Schnapf 1987). Nevertheless, most mammals are typically dichromatic i.e. they possess one cone type (S-cones), which is sensitive to short wavelengths of light (maximally sensitive to either blue, violet, or near-ultraviolet light) and a second cone type (generally denoted as M/L-cones) that is sensitive to parts of the spectrum between medium to long wavelengths (maximally sensitive to either green, yellow, or orange light; Jacobs 1993; Peichl 2005). The density and topographical array of conventional photoreceptors vary immensely between mammalian species with the greatest difference amongst rodents (Peichl 2005). In some cases rod and cone arrangements are believed to cater for different adaptations to a diverse array of environments. One basic example is that of the rod to cone ratio in rodents,

which commonly corresponds with the circadian activity pattern of the animal and is hence low in strongly diurnal species and high in strongly nocturnal species (Jacobs 1993; Peichl 2005). Furthermore, M/L-cones usually outnumber S-cones by a considerable amount and their topographical density arrangement is not always homogenous; either one or both of the S-cone and M/L-cone populations may be restricted to certain retinal domains (Szél *et al*. 1996; Peichl 2005). Cone segregation has been observed in the house mouse (*Mus musculus*), mound builder mouse (*M. spicilegus*), agouti (*Dasyproctaaguti*) and rabbit (Szél *et al*. 1992; 1994; Rocha *et al*. 2009*).*

Circuitry projecting to the SCN is primarily innervated by the ipRGCs, which reside in the ganglion cell layer of the inner retina (Provencio *et al.* 1998; von Schantz *et al.* 2000; Hattar *et al*. 2002). Amongst the more or less 15 different ganglion cell types identified, only a small subpopulation (1-2%) is intrinsically light sensitive (Hattar *et al*. 2002; Masland 2001). Prior to the discovery of ipRGCs slightly more than a decade ago, the rods and cones were considered the two sole retinal photoreceptor classes and naturally all light responses were attributed to them. However, several studies have confirmed that the ipRGCs is a functional retinal photoreceptor class that is fundamentally involved in entrainment of the SCN (Foster *et al*. 1991, 1993; Freedman *et al*. 1999; Lucas *et al*. 1999, 2001). Unfortunately, the discovery of a rodless, coneless photoreceptive pathway for non-visual responses i.e. *via* the ipRGCs, caused the incorrect impression that conventional rods and cones do not contribute to photic entrainment. At present, it is becoming increasingly clear that rods and cones also contribute to non-visual processes (Aggelopoulos & Meissl 2002; Dkhissi-Benyahya 2007; Altimus *et al.* 2010; Gooley *et al.* 2010; van Diepen *et al.* 2013; Weng *et al.* 2013). Likewise, despite being directly

photosensitive (Lucas *et al*. 1999; Semo *et al*. 2003), ipRGCs share connections with rod and cone networks and are involved in vision patterns (Foster & Helfrich-Förster 2001; Schmidt *et al*. 2011b).

Study animals

The Namaqua rock mouse (*Micaelamys namaquensis*)

The Namaqua rock mouse or *Micaelamys namaquensis* (formerly *Aethomys namaquensis*, A. Smith, 1834; Fig. 1.5) is a small rodent with a reddish-brown to yellowish-brown pelage (Skinner & Chimimba 2005). Their distributional range encompasses parts of Angola, Zambia, Malawi, northern Mozambique, and nearly the entire southern African subregion where they abundantly inhabit a range of biomes (Skinner & Chimimba 2005; Russo *et al.* 2010). As their colloquial name indicates, *M. namaquensis* prefers rocky environments above other habitat types and frequently find refuge among rock crevices (Skinner & Chimimba 2005). Notably their foot morphology may contribute to them preferring rocky terrain: they have naked soles with robust tubercles which may improve traction on harder surfaces (Baker & Brow 2011; Kotler *et al.* 2001). Furthermore, despite having a low basal metabolic rate as is typical of desert rodents, *M. namaquensis* survives cold nights in the Namib Desert due to its highly insulative pelage (Buffenstein 1984). The diet of *M. namaquensis* consists of foliage, seeds, insects and nectar (Skinner & Chimimba 2005). *Micaelamys namaquensis* is also a well-known flower pollinator and has been observed pollinating plants such as Mountain-rose sugar bush (*Protea nana*) and the African lily (*Massonia depressa*) in the Western Cape Province of South Africa (Johnson *et*

al. 2001; Biccard & Midgley 2009). *Micaelamys namaquensis* has been described as communal or social (Skinner & Chimimba 2005), but such groups may potentially only consist of family members (Fleming & Nicolson 2004). This species is polygynous and shows no sexual dimorphism (Skinner & Chimimba 2005). The reproductive system of the Namaqua rock mouse, as well as that of the closely related Tete veld rat (*Aethomys ineptus*), has been shown to respond to photoperiod and the species is classified as a seasonal breeder (Muteka *et al*. 2006). In the southern Western Cape Province, sex differences exist in space use behaviour as males appear to occupy larger overlapping areas compared to the smaller non-overlapping areas occupied by females. Lovegrove and Heldmaier (1994) have described the species' daily body temperature rhythm and briefly reported on its daily locomotor activity rhythm under a long day photoperiod (16L: 8D) and a high ambient temperature (30°C). Both rhythms were described as displaying a bimodal nocturnal pattern. The Namaqua rock mouse is purportedly nocturnal, based on field observations, but little is known regarding how it expresses activity throughout the day and its locomotor activity rhythm has not been described (Skinner & Chimimba 2005).

The four striped field mouse (*Rhabdomys pumilio*)

The four-striped field mouse, *Rhabdomys pumilio* (Sparrman 1784; Fig. 1.5), is a small grey-brown rodent (~40-70g) that has four characteristic black stripes on their back (Skinner & Chimimba 2005). The species has an extensive, yet discontinuous distribution throughout the Southern African subregion and is also discontinuously distributed towards East Africa, as far as Uganda and Kenya (Skinner & Chimimba 2005). *Rhabdomys pumilio* is highly adaptable to a variety of habitats, but typically prefers areas densely covered with grass and avoids open areas

and is furthermore an opportunistic omnivore that feeds on foliage, seeds and insects (Skinner & Chimimba 2005). The species breeds opportunistically and males show no reproductive photoresponsiveness (Jackson & Bernard 1999). Interestingly, *R. pumilio* displays a body temperature rhythm comparable to that of nocturnal spcies, with the acrophase of the rhythm occurring during nighttime. Such a rhythm has also been observed in another small diurnal rodent, the golden spiny mouse (*Acomys russatus*), and is suggested to enable the animal to avoid hyperthermia during activity (Haim *et al.* 1998). *Rhabdomys pumilio* has also been described as having flexibility in its social behaviour and social structure. Some evidence suggests that their social structure depends upon the availability of cover, with individuals being more asocial in savannahs as opposed to in the Kalahari Desert where social interactions are increased by the limited vegetation cover (Nel 1975).

Figure 1.5: On the left: The Namaqua rock mouse (*Micaelamys namaquensis*); image source: www.mammalogy.org; photo by J. Visser. On the right: The four striped field mouse (*Rhabdomys pumilio*); image source: www.biodiversityexplorer.org; photo by T. Hardaker.

In the Cape Flats (Western Cape, South Africa), male *R. pumilio* form dominance hierarchies with the alpha male having an exclusive territory whereas in females, territoriality is only observed in breeding individuals (Johnson 1980). Interestingly, males help to care for offspring in both natural and laboratory environments (Schradin & Pillay 2003). The activity rhythm of this species has been described both in the laboratory and in the field as fundamentally diurnal but with marked activity at dusk and dawn (Schumann *et al.* 2005; Skinner & Chimimba 2005). Moreover, the free-running rhythm of this species under constant darkness ranges between 23.10h to 24.80h and under constant light between 24.30h to 24.79h (Schumann *et al*. 2005).

Aims

If the temporal activity rhythm of a rodent species is an adaptation, then differences in response to illumination conditions are expected. The following aims were set in order to test this.

The primary focus of this thesis was to study and compare the daily rhythms responses of a nocturnal rodent, the Namaqua rock mouse (*Micaelamys namaquensis*), with a diurnal rodent, the four striped field mouse (*Rhabdomys pumilio*), after subjecting them to different intensities and wavelengths of light. Since the retina is the primary mediator of light for visual as well as non-visual (circadian) processes, we also aimed at describing the retinal topographies of classical- (rods and cones) and melanopsin-containing photoreceptors (ipRGCs) in both species. The idea was that differences in the retinal photoreceptor topographies may provide insights into any observed differences in the daily responses to different lighting regimes between the two species. An additional objective was to deduce whether locomotor activity in the Namaqua rock

mouse results from endogenous entrainment to the light-dark cycles and also to provide a quantitative description of its daily locomotor activity rhythm in response to various lighting conditions under controlled laboratory conditions. This was necessary since the locomotor activity was used as a parameter for measuring daily responses to various light intensities and wavelengths.

Chapter 2

The focus of this chapter was to determine whether the locomotor activity rhythm of *M. namaquensis* entrains to the light-dark cycle and further to quantitatively describe its daily activity rhythm in response to various lighting regimes under controlled laboratory conditions.

A priory prediction:

Micaelamys namaquensis would exhibit a light entrained locomotor activity rhythm in which activity would be suppressed by light and induced by darkness. The period length of the free running rhythm under constant darkness would be less than 24 hours.

Reference of the publication of Chapter 2: van der Merwe, I., Bennett, N.C., Haim, A. and Oosthuizen, M.K. (2014) Locomotor activity in the Namaqua rock mouse (*Micaelamys namaquensis*) – Entrainment by light manipulations, *Canadian Journal of Zoology 92(12): 1083-1092.*

Chapter 3

The objective of this chapter was to characterize the retinal photoreceptor topographies (rods, cones and ipRGCs) of *M. namaquensis* and *R. pumilio*.

A priory predictions:

The compositions of the classical retinal photoreceptors (rods and cones) would reflect the temporal activity patterns of the two species, with the retina of *M. namaquensis* being rod-rich and the retina of *R. pumilio* being cone-rich. Furthermore, the ipRGCs would be sparsely distributed.

Chapter 4

The aim of this chapter was to investigate the response in locomotor activity and urine production to various levels of photophase illuminance as well as to investigate the response in the urinary 6-SMT levels to a low level of photophase illuminance and a high level of photophase illuminance.

A priory predictions:

Micaelamys namaquensis: Locomotor activity and urine production would decrease as the photophase illuminance level increases and the 6-SMT rhythm would be more pronounced under the higher level of photophase illuminance as opposed to the lower level of photophase illuminance.

Rhabdomys pumilio: Locomotor activity and urine production would increase as the photophase illuminance level increases and the 6-SMT rhythm would be more pronounced under the higher level of photophase illuminance as opposed to the lower level of photophase illuminance.

Chapter 5

The aim of this chapter was to investigate the response in locomotor activity, urine production, urinary 6-SMT and urinary corticosterone to various wavelengths of photophase lighting.

A priory predictions:

In *M. namaquensis* and in *R. pumilio* locomotor activity and urine production would increase whereas nighttime 6-SMT levels and corticosterone levels would decrease with an increase in the wavelength of light during the photophase.

Chapter 6

In this chapter, the collective findings of this study are discussed in view of existing data on the relationship between the light-dark cycle and biological systems in other mammalian species.

CHAPTER 2:

DAILY LOCOMOTOR ACTIVITY IN THE NAMAQUA ROCK MOUSE (*MICAELAMYS NAMAQUENSIS*) – ENTRAINMENT BY LIGHT MANIPULATIONS

This chapter is essentially the text of a paper entitled: van der Merwe, I., Bennett, N.C., Haim, A. and Oosthuizen, M.K. (2014) Locomotor activity in the Namaqua rock mouse (*Micaelamys namaquensis*) – Entrainment by light manipulations, *Canadian Journal of Zoology 92(12): 1083-1092* (CJZ). The format of the text in this chapter is according to the specifications by the CJZ, except for the references cited, which are in the main reference list at the end of this thesis.

Abstract

The locomotor activity rhythms of wild-caught Namaqua rock mice (*Micaelamys namaquensis* Smith, 1834) were examined under four light cycle regimes in order to quantitatively describe the daily expression of locomotor activity and to study the innate relationship between activity and the light-dark cycle. Activity was always significantly higher at night than in the day: 1) The LD1 light cycle (12L: 12D) established a distinct light-entrained and strongly nocturnal activity rhythm (99.11% nocturnal activity). The activity onset was prompt (ZT 12.2 ± 0.04) and activity continued without any prominent peaks or extended times of rest until the offset of activity at ZT 23.73 ± 0.08. 2) Evidence for the internal maintenance of locomotor activity was obtained from the constant dark cycle (DD) in which locomotor activity free ran (mean τ = 23.89 h) and 77.58% of the activity was expressed during the subjective night. 3) During re-entrainment (LD2; 12L: 12D), a nocturnal activity rhythm was re-established (98.65% nocturnal activity) and, 4) the inversion of the light cycle (DL; 12D: 12L) evoked a shift in activity that again revealed dark-induced locomotor activity (95.69% nocturnal activity). Females were consistently more active than males in all of the light cycles but only under the DD and LD2 cycles were females significantly more active than males. Although this species is considered nocturnal from field observations, information regarding its daily expression of activity and the role of light in its entrainment is lacking. To the best of our knowledge this study is the first to report quantitatively on the species' daily rhythm of activity and to investigate its relationship to the light-dark cycle.

Key words: Circadian rhythm, entrainment, free-run, locomotor activity, *Micaelamys namaquensis*, Namaqua rock mouse

Introduction

The perpetual rotation of the earth on its axis and the revolution of the earth around the sun are undoubtedly some of the strongest cyclical events to which organisms are exposed. As a consequence, the light-dark cycle reliably exposes daily and seasonal time and is considered the primary *zeitgeber* (environmental cue) that entrains daily physiological and behavioral rhythms (Benstaali et al. 2001; Reppert and Weaver 2002). Since the availability of environmental resources change in concurrence with changing levels of illumination across the day, the temporal organization of the locomotor activity rhythm of a species is vital. During the process whereby the temporal niche of a species is shaped, the locomotor activity rhythm may become entrained to other non-photic cues and thereby mask the underlying photically-entrained rhythm (Edmonds and Adler 1977; Francis and Coleman 1988; Hut et al. 1999; Rajaratnam and Redman 1999). Consequently, light-entrained daily rhythms that persist (free-run) in an environment devoid of *zeitgebers* confirm the existence of an internal biological clock mechanism which in turn controls the circadian rhythm (Aschoff 1981). In mammals, the suprachiasmatic nucleus (SCN) is considered the central moderator of the circadian timing system (Moore and Eichler 1972; Stephan and Zucker 1972). The importance of the circadian timing system and its coordination by the light-dark cycle is best demonstrated by the prevalence of increased health risks and in some cases disturbances within ecological systems, that result from disruptions of the circadian clock network and distrainment by a natural light-dark cycle (Bird et al. 2004; Navara and Nelson 2007; Haim et al. 2010; Rotics et al. 2011; Haim and Portnov 2013).

Mammalian daily locomotor activity rhythms have been extensively used in studying photic entrainment of the circadian timing system and in unraveling its underlying mechanisms (Aschoff, 1981; Benstaali et al., 2001). A small number of laboratory-reared mammalian species (e.g. strains of mice, rats and hamster) are typically used in chronobiological studies, as they breed readily and are maintained easily in captivity. Moreover, studies on wild animals usually focus on species from temperate regions of the Northern hemisphere. Here, we study light entrainment of the locomotor activity rhythm in a southern African rodent namely the Namaqua rock mouse (*Micaelamys namaquensis* Smith, 1834). The species is polygynous, shows no sexual dimorphism and inhabits a range of biomes but usually prefers rocky environments above other habitat types (Skinner and Chimimba 2005; Russo et al. 2010). The Namaqua rock mouse is described as communal or social, though such groups may potentially only consist of family members (Fleming and Nicolson 2004). The reproductive system of the Namaqua rock mouse, as well as that of the closely related Tete veld rat (*Aethomys ineptus*), has been shown to be photoresponsive and the species is classified as a seasonal breeder (Muteka et al. 2006). Although various aspects of the Namaqua rock mouse are well-known, basic characteristics of its temporal locomotor activity rhythm have not been studied (Skinner and Chimimba 2005). The species is considered nocturnal mostly based on field observations, but it is possible that the innate circadian rhythm of this species is not expressed in its natural environment due to masking by other non-photic factors (Mrosovsky 1999). Lovegrove and Heldmaier (1994) have described the species' daily body temperature rhythm and briefly reported on its daily locomotor activity rhythm under a long day photoperiod (16L: 8D) and a high ambient temperature (30°C). Both rhythms were described as displaying a bimodal nocturnal pattern.

The present study aimed to quantitatively describe the daily expression of locomotor activity in male and female Namaqua rock mice and to study the relationship between activity and the level of illumination using various lighting regimes, under controlled laboratory conditions. The mice were also subjected to constant darkness in order to describe the endogenous locomotor activity rhythm of the Namaqua rock mouse and thus to calculate the period of the free running rhythm, which we predicted to be less than 24 h as it is for most nocturnal species (Aschoff 1981). Furthermore, the objective was to re-entrain the mice to a regular light-dark cycle and subsequently expose them to an abrupt inversion of the light-dark cycle as a means to further validate light entrainment of the activity and to further establish whether darkness induces activity.

2. Materials and methods

2.1 Animal housing

The project was approved by the Animal Ethics Committee of the University of Pretoria, Pretoria, South Africa (EC063-11). In mid-August, eight adult *M. namaquensis* (four males; four females; mean body mass = 36.3 ± 2.66 g) were collected from amongst the rocky hills of the Goro Game Reserve in the Soutpansberg region (Limpopo Province, South Africa). The animals were kept individually in semi-transparent plastic cages (58 x 38 x 36 cm) in a light and temperature controlled animal room at an ambient temperature of 25 °C (± 1°C) and approximately 60% relative humidity. Each cage contained a layer of wood shavings (± 3 cm thick) for bedding and the animals were given a small plastic shelter and tissue paper for nesting

material. The mice had *ad libitum* access to food and water and were fed at random times every second or third day to avoid activity entrainment to the feeding schedule. Water and food (parrot seed mix) were topped up and fresh food was replaced. The room was illuminated at day time by white fluorescent lights (± 400 lux) and two weeks prior to the experimentation period, the animals were maintained on a 12L: 12D light-dark cycle (L: 06:00 – 18:00h).

2.2 Activity recording and experimental procedure

Activity was recorded using infra-red motion captors (Quest PIR internal passive infrared detector; Elite Security Products (ESP), Electronic Lines, London, UK) that were attached to the top of each cage and detected movement over the whole cage floor area. The number of locomotory movements detected during each minute was stored on a computer using VitalView software (VitalView^{TM}, Minimitter Co., Sunriver, OR, USA; http://www.minimitter.com). Methods were similar to those employed in Van der Merwe et al. 2011. Four consecutive light cycle regimes, each lasting for fourteen days (the second light cycle lasted 15 days), were used to measure locomotor activity responses: 1) The LD1 light cycle comprised of 12L: 12D (ZT 0 at 06:00 and ZT 12 at 18:00h) for recording any patterns of activity entrainment to the L/D cycles and in order to ensure that animals are entrained to a known light cycle to obtain a starting point for determination of endogenous rhythms. 2) Animals were exposed to constant darkness (DD) to assess whether animals possess endogenous rhythms of locomotor activity and if it is the case, to determine the period of the free running rhythm (tau; τ). 3) A second light cycle comprising of 12L: 12D (ZT 0 at 06:00 and ZT 12 at 18:00h) served to re-entrain the animals to a 12L:12D light cycle before exposing them to the last light cycle regime. 4) An inverse light

cycle (DL; ZT 0 at 18:00 and ZT 12 at 06:00h), in order to subject the animals to a drastic change in the L/D-cycles and evaluate the response observed in locomotor activity. Inversing the light cycle will establish whether animals use light to entrain their activity rhythms as opposed to some other cue, and in addition provide an indication of the rate of re-entrainment to a novel light cycle. During the transition from the LD2 light cycle to the inverse DL light cycle, the animals were exposed to a 24 h period of light, which was then followed by D12: L12. Note: Zeitgeber time (ZT) refers to time in hours during the LD or DL light cycles (ZT 0 = light phase onset; ZT 12 = dark phase onset).

2.3 Data analysis

The recorded activity data were analyzed and the daily activity rhythms visually presented as double-plotted actograms using the computer program ActiView (ActiView™, Minimitter Co., Sunriver, OR, USA; http://www.minimitter.com). Only the last 10 days of each light cycle were used in the calculations as to exclude the transitory periods between light cycles. Moreover, under the LD2 and DL light cycle, only the days in which the animals were fully re-entrained were included in the analyses. Activity counts and percentages of activity were compared between the four light cycles as well as within each light cycle (light phase vs. dark phase) for all of the mice combined as well as for males and females separately. The sums of the activity counts per light phase and per dark phase of each day were calculated for each individual across all four light cycles. These values were then used to estimate the mean number of activity counts (of all individuals combined) for each entire light cycle as well as for the light phase and dark phase of each light cycle separately. The number of activity counts during either the light or dark

phase (or subjective light or dark phase under DD) of each day was further expressed as a percentage against the total number of activity counts for each day and was calculated for all animals individually. The mean of these values within each of the light cycle regimes were then presented as the percentage of activity. The period length (in hours) during the DD cycle was calculated using the chi-squared periodogram function in the rhythm analysis software Clocklab (ClockLab TM, Actimetrics, Evanston, IL, USA). The activity percentages for the subjective light and dark phases were calculated for each individual according to its own τ. Where it was possible, we determined the mean daily onset and offset times for each animal. Activity onset was defined visually as activity within ten consecutive minutes and activity offset as inactivity for 20 minutes. From this we extrapolated the phase angle of entrainment (ψ; the time difference between the lights on or off and activity onset or offset) and the active phase (α; the period from activity onset to activity offset).

Statistical analyses were performed using Microsoft Excel (Microsoft Corp., Redmond, WA, USA) and IBM SPSS Statistics version 21.0 (SPSS Inc., Chicago, IL, USA). Statistical significance for light cycle (LD1, DD, LD2 and DL), light phase (light/dark phase and subjective light/dark phase), sex, and the interaction effects of light cycle with light phase as well as light cycle with sex on activity were determined. Data were not normally distributed and thus a generalized linear mixed model was used to evaluate activity; the *post hoc* least significant difference test was used where significant differences were detected. $P<0.05$ were considered significantly different and all means were indicated with standard error (SE).

3. Results

3.1 The LD1 light cycle

The Namaqua rock mouse displayed a robust daily locomotor activity rhythm in accordance with the alternation of light and dark, and was invariably nocturnal across all light cycles (Figs. 1, 2 and 3). All of the animals were nearly exclusively active during the dark phase of the LD1 light cycle (99.11% nocturnal activity); the mean amount of activity counts were significantly higher during the dark phase (1047.87 ± 76.57) than during the light phase (9.37 ± 2.88; F=184.161, df_1=1, df_2=487, P<0.001; Fig. 1). The mean amount of activity counts for the 24h day for the whole LD1 cycle was 528.62 ± 38.37 with no significant effect of sex on the activity counts (males: 537.34 ± 54.99, females: 519.91 ± 53.51, F=0.052, df_1=1, df_2=487, P=0.820; Fig. 4). The mean activity onset during LD1 was precise (ZT 12.2 ± 0.04) and coincided closely with the start of the dark phase. The mean activity offset (ZT 23.73 ± 0.08) occurred prior to the end of the dark phase and the mean ψ and α for LD1 was 0.2 ± 0.04 h and 11.53 ± 0.11 h, respectively. Individual differences in the activity rhythms, as presented by the actograms were minor; generally activity continued throughout the dark phase without any pronounced peaks or troughs (See Fig. 2). Only in one female mouse (animal no. 8) was activity expressed more intermittently during the latter half of the dark phase.

3.2 The DD light cycle

Under the DD cycle, all of the mice retained a distinct daily activity rhythm, thus validating the presence of an internal time-keeping mechanism. Compared to the LD1 cycle, the mean amount of activity counts during the DD cycle was slightly lower (741.90 ± 29.42) but with the difference being not significant between the two groups (F=3.654, df_1=3, df_2=487, P=0.240). The mice were significantly more active during the subjective night than the subjective day (77.58% nocturnal activity; F=79.030, df_1=1, df_2=487, P<0.001) with the mean number of activity counts being 732.22 ± 65.56 and 211.57 ± 15.71 for these two light phases respectively (Fig. 1). The mean number of total activity counts was also significantly higher in females (603.76 ± 52.17) than in males (340.04 ± 27.19, F=20.095, df_1=1, df_2=487, P<0.001; Fig. 4). Only animal no. 5 (male) displayed an increasingly arrhythmic activity pattern following DD. The mean free run period or τ was slightly less than 24 h (23.89 ± 0.08 h) and the range was small (23.4 – 24.13 h); only two animals had a τ marginally above 24 h (animal no. 3, female: 24.05 h and animal no. 5, male: 24.13 h).

3.3 The LD2 light cycle

During the re-entrainment period (LD2), only mouse no. 7 did not straightaway re-entrain to the new light schedule (Fig. 2) and consequently, for this individual, only the last day of its recorded activity was included in the analysis. The overall mean number of activity counts was 413.04 ± 32.80; this value was significantly lower than the value obtained under the LD1 light cycle (F=3.654, df_1=3, df_2=487, P=0.022) yet not significantly different to the value under the DD

cycle (F=3.654, df_1=3, df_2=487, P=0.180). The percentage of nocturnal activity was 98.65%, with a significantly higher mean amount of activity counts during the dark phase (814.91 ± 65.41) than the light phase (11.16 ± 2.91; F=151.266, df_1=1, df_2=487, P<0.001; Fig. 1). Under this light cycle, females expressed significantly more activity than males (males: 289.87 ± 33.28, females: 536.20 ± 56.52, F=14.104, df_1=1, df_2=487, P<0.001, Fig. 4). The activity onsets were restored to again coincide close to the start of the dark phase (ZT 12.27 ± 0.04) and the mean ψ was 0.27 ± 0.04 h. Activity offset was on average less precise and occurred slightly earlier than during LD1 (ZT 23.43 ± 0.14) because of inter-individual differences in the rate of re-entrainment to the LD2 light cycle. Subsequently, the mean α was 0.39 h shorter during LD2 (ZT 11.14 ± 0.14 h).

3.4 The DL light cycle

The locomotor activity rhythm of the Namaqua rock mouse was immediately affected by the inverted light-dark cycle (DL). Once more a strong nocturnal rhythm was observed (percentage nocturnal activity: 95.69%) with the mean number of activity counts during the dark phase (680.36 ± 85.19) being significantly higher than during the light phase (30.62 ± 4.72; F=58.116, df_1=1, df_2=487, P<0.001; Fig. 1). Over the 24h day, females were more active than males, but the difference was not significant (males: 300.99 ± 35.69, females: 409.99 ± 70.60, F=1.628, df_1=1, df_2=487, P=0.203; Fig. 4). The overall mean number of the activity counts (355.49 ± 42.71) was significantly lower than during the LD1 light cycle (F=3.654, df_1=3, df_2=487, P=0.003) as well as the DD light cycle (F=3.654, df_1=3, df_2=487, P=0.025). Activity onset (ZT 12.09 ± 0.02) remained in close proximity to the start of the dark phase (ZT 12 = 06:00) and the

mean ψ was 0.09 ± 0.02 h. The actograms revealed a relative amount of inter-individual differences in the activity profiles displayed; re-entrainment times ranged between 0 and 10 days. Only two mice (both males) displayed immediate re-entrained activity rhythms to the DL light cycle. In one of these males, the pattern of activity was less pronounced under DL (Fig. 2.) and in the other male, the mode of activity changed from continuous (during LD2) to bimodal (during DL; Fig. 5) but with the percentage of nocturnal activity being similar between these two light cycles (DL: 98.11 ± 0.33%; LD2: 99.79 ± 0.09%). In the six remaining individuals (four females and two males), re-entrainment was gradual and took approximately 10 days to complete. In two of these mice, only the last five days of the recorded activity data were used in the analyses and in the remaining four mice, only the last three days were used in the analyses. The slowly re-entraining mice generally exhibited a period of continuous activity at the beginning of the night, which then increased daily until the offset of activity coincided with the end of the night (ZT 12 = 18:00h). Simultaneously there was a decrease in the daytime activity and furthermore, shorter bouts of activity were also observed in the latter part of the night (Fig. 5). From three individuals, it was possible to calculate that the continuous active period increased by 0.89 ± 0.5 h each day. Overall, the mice expressed ~3.2% more daytime activity during the DL cycle than during the LD1 and LD2 cycles, even after the activity offsets were fully restored.

4. Discussion

The locomotor activity rhythms of mammals are typically described in relation to the strongest environmental *zeitgeber*, the light-dark cycle, as being nocturnal, diurnal, crepuscular or cathemeral, but may entrain to *zeitgebers* other than photic cues (Hut et al. 1999). Therefore,

before claiming that an organism possesses a circadian locomotor activity rhythm, the endogenous maintenance of a free running rhythm should be demonstrated. Despite various aspects of the Namaqua rock mouse being well-known, basic characteristics regarding its temporal locomotor activity rhythm have not been studied (Skinner and Chimimba 2005). The Namaqua rock mouse is considered nocturnal based on field observations, yet it is possible that non-photic factors within its natural environment is responsible for shaping its purportedly nocturnal behavior and thereby mask its underlying endogenous activity rhythm (Mrosovsky 1999). Such differences in activity patterns have been observed in for example golden hamsters (*Mesocricetus auratus*) and East African root rats (*Tachyoryctes splendens*), where animals exhibit nocturnal activity in a controlled environment, but not in their natural environments (Gattermann et al. 2008; Katandukila et al. 2013). The results of the present study are the first to quantitatively demonstrate the entrainment by the light-dark cycle, of the locomotor activity rhythm of the Namaqua rock mouse and to provide evidence that the species possesses an endogenously controlled nocturnal activity rhythm.

As demonstrated by the actograms, our results revealed a clearly defined phase relationship between the locomotor activity rhythm of the Namaqua rock mouse and the daily light-dark cycle, and furthermore that this relationship is endogenously maintained. When subjected to a 12L: 12D light cycle (LD1 and LD2) all of the animals were almost (~ 99%) exclusively active when it was dark. In addition, an inversion of the light-dark cycle (DL) again produced very high (~96%) nighttime activity, which if given more time would most likely have resulted in an even higher nocturnal percentage. Most rodents are nocturnal, yet trends in their activity rhythms seem to be predominantly constrained by phylogeny and the subfamily Murinae, to which the

Namaqua rock mouse belongs, is described as being primarily nocturnal (Roll et al. 2006). Some benefits of a nocturnal lifestyle, particularly in open habitats, include decreased visibility to predators, which thus leaves more time for foraging (Brown et al. 1988; Kotler et al. 1991; Kotler et al. 2002; Rotics et al. 2011).

Although the percentage of activity gives a good measure of the strength of an animal's preference for a particular phase of the day, it does not express how activity is distributed; this can be achieved in the laboratory by the construction of actograms. During entrainment (LD1), activity started only a few minutes after the lights went off and was generally continuous throughout the night with no pronounced peaks or extended times of rest and ended less precisely. It is interesting to note that despite being relieved from many aspects of its daily activity it would normally have in the wild, of which foraging is probably most significant, the Namaqua rock mouse was almost always active throughout the night and had a mean α of 11.53 h under laboratory conditions (during LD1).

Free running rhythms reveal an internal sense of external time and also demonstrate the dependence of the internal clock mechanism on environmental cues for adjusting circadian rhythms to the specific time of the day. In the present study, the activity rhythm was maintained under constant darkness (DD) and a small amount of drift was observed. The τ varied only slightly between individuals and only two mice exhibited a τ marginally above 24 h; the overall mean τ was 23.89 h. This supports the statement that this species is nocturnal since a τ shorter than 24 h in constant darkness is predominantly associated with nocturnal species (Aschoff 1981). Even though the sample size of males versus females was small, sex significantly affected

the activity response of the mice in the present study. Females were consistently more active than males and under the DD and LD2 cycles, the differences were significant. This finding is consistent with reports on other rodents in which females generally exhibit higher levels of activity than males, suggested being due to higher levels of estrogen (Lightfoot 2008). Reproductive hormones acutely affect many non-sexual behaviors including locomotor activity and estrogens usually induce an increase in activity; most likely through the estrogen-α receptor pathway (Ogawa 2003; Lightfoot 2008).

Inversing the light-dark cycle quickly evoked an activity response in the Namaqua rock mouse and revealed that light suppresses activity and darkness induces activity in this species. During the transition of the LD2 light cycle to the inverse DL light cycle, the animals were exposed to 24 h period of light and hence all of the mice postponed activity by a further 12 h. The animals then showed different ways of re-entraining to the DL light cycle since the majority of the mice showed a gradual resetting of the activity offsets towards the end of the night. Only two mice showed an immediate resetting of the activity rhythm to the DL light cycle. The percentage of nocturnal activity after the mice were fully re-entrained was high (~96%) and given more time, the percentage of nocturnal activity would probably have increased even more. Similar results were obtained in another murid rodent from the Soutpansberg region, the spiny mouse (*Acomys spinosissimus*), that was exposed to experimental conditions similar to that of present study. Activity resetting in spiny mice was also gradual (re-entrainment took approximately 9 days) and the proportion of light versus dark phase activity also did not differ much between the inverse light cycle and the preceding regular 12L: 12D light cycle (Hoole et al. 2012). The rate of circadian re-entrainment is influenced by several factors such as the magnitude and the direction

of the phase shift and interestingly, melatonin has been shown to affect the re-entrainment process (Singaravel et al. 1996; Ruby and Heller 1998; Cohen and Kronfeld-Schor 2006). Furthermore, inter-individual differences in re-entrainment may be age-related and even stress-related. In mice, younger individuals have been shown to adjust their circadian timing quicker to shifts in the light schedule than older individuals, and in rats and degus, restraint stress causes a significant delay in re-entrainment (Mohawk and Lee 2005; Davidson et al. 2008; Sellix et al. 2012). It is therefore possible that, in the present study, mice with slower re-entrainment times were either older or more stressed individuals.

The present study revealed that the Namaqua rock mouse possesses a strong nocturnal locomotor activity rhythm that is endogenously entrained by the light-dark cycle. The Namaqua rock mouse was generally active continuously and consistently throughout most of the night under a normal entrainment period (12L: 12D) and activity onset and offset coincided closely with dusk and dawn, respectively. The activity rhythm persisted under constant darkness with a small amount of drift and with almost all of the activity being expressed during the subjective night. A sudden inversion of the light-dark cycle demonstrated that locomotor activity is prompted by darkness in this species. It is highly probable that this species displays similarly high nocturnal activity in the wild due to the potent effect the light-dark cycle has on its circadian locomotor activity rhythm.

Acknowledgements

The research was supported by a South African Research Chair of Mammal Behavioural Ecology and Physiology awarded to N. C. Bennett. The work was further supported by a

collecting permit from the Department of Nature Conservation in Limpopo Province and I. van der Merwe acknowledges a scholarship from the University of Pretoria (UP). We would also like to thank Sonja Faul and Sasha Hoffman for assistance with fieldwork. The authors also thank two anonymous reviewers for their constrictive remarks on an earlier draft of this manuscript.

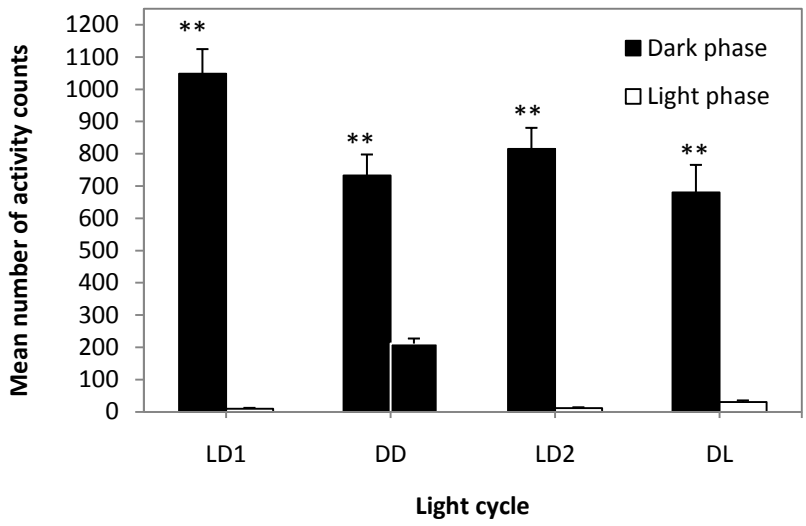

Figure 2.1

Mean numbers of activity counts for the Namaqua rock mouse (*Micaelamys namaquensis*) showing significantly higher ($P<0.001$) values in the dark phases (12h) (or subjective dark phase of DD (~12h)) than in the light phases (or subjective light phase of DD) of all four light cycles. **=$P<0.001$.

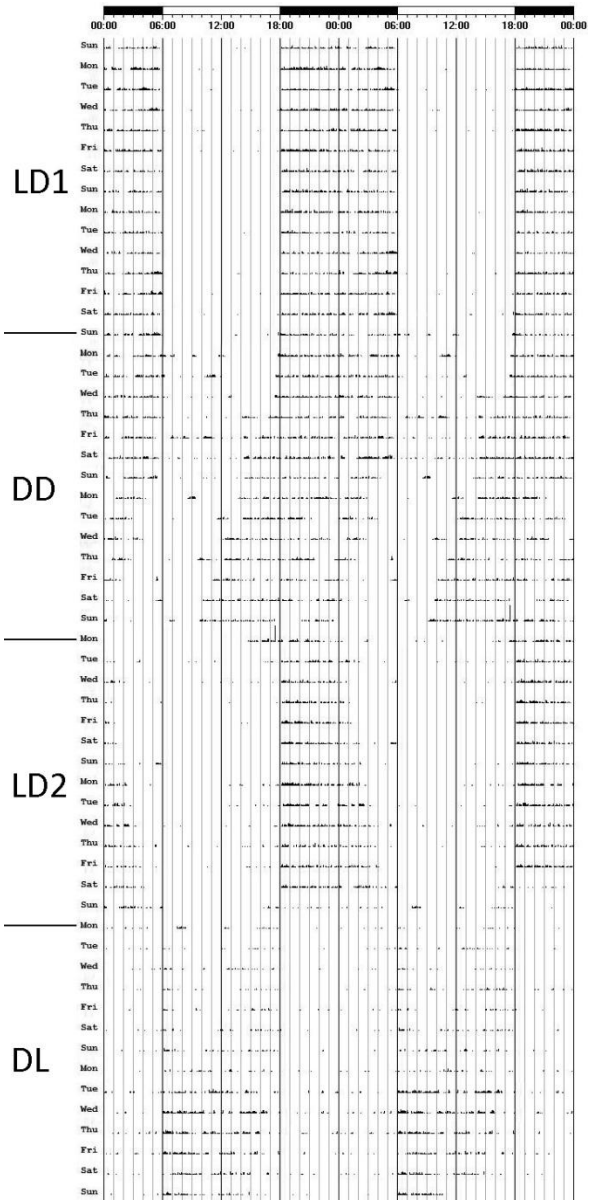

Figure 2.2

An actogram of the locomotor activity rhythm of animal no. 7 across all four light cycles revealing a strong nocturnal activity rhythm during entrainment to a 12L: 12D light cycle (LD1), a free running activity rhythm (τ = 23.7 h) during constant darkness (DD), slow re-entrainment to the dark phase during a second 12L: 12D light cycle (LD2), and finally a shift in activity following an inverse of the light cycle (DL).

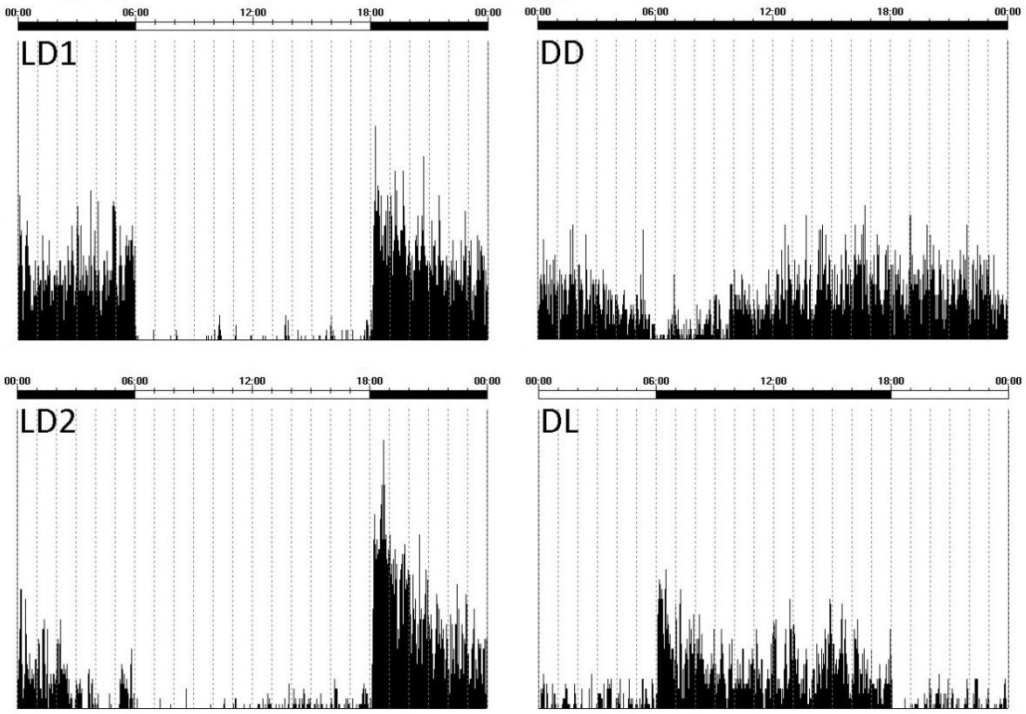

Figure 2.3

Average activity profiles for animal no. 1 (male) for the last ten days of each of the four light cycles (LD1, DD, LD2 and DL). Zeitgeber time (LD1, LD2 and DL) and circadian time (DD) is indicated on the x-axis and mean counts/min on the y-axis.

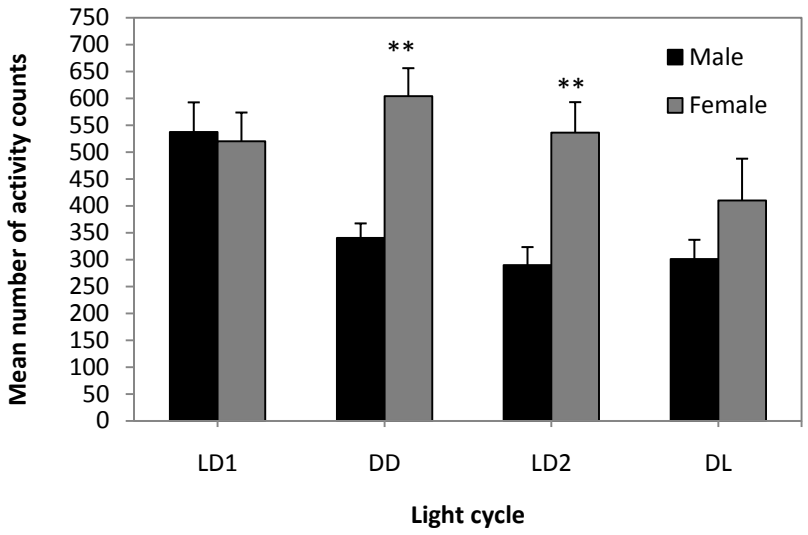

Figure 2.4

Mean numbers of activity counts over the 24h day for the Namaqua rock mouse (*Micaelamys namaquensis*) under four light cycles (LD1, DD, LD2 and DL) showing values obtained for males and females separately. Females were significantly more active than males during the DD, LD2 and DL light cycles. **=P<0.001.

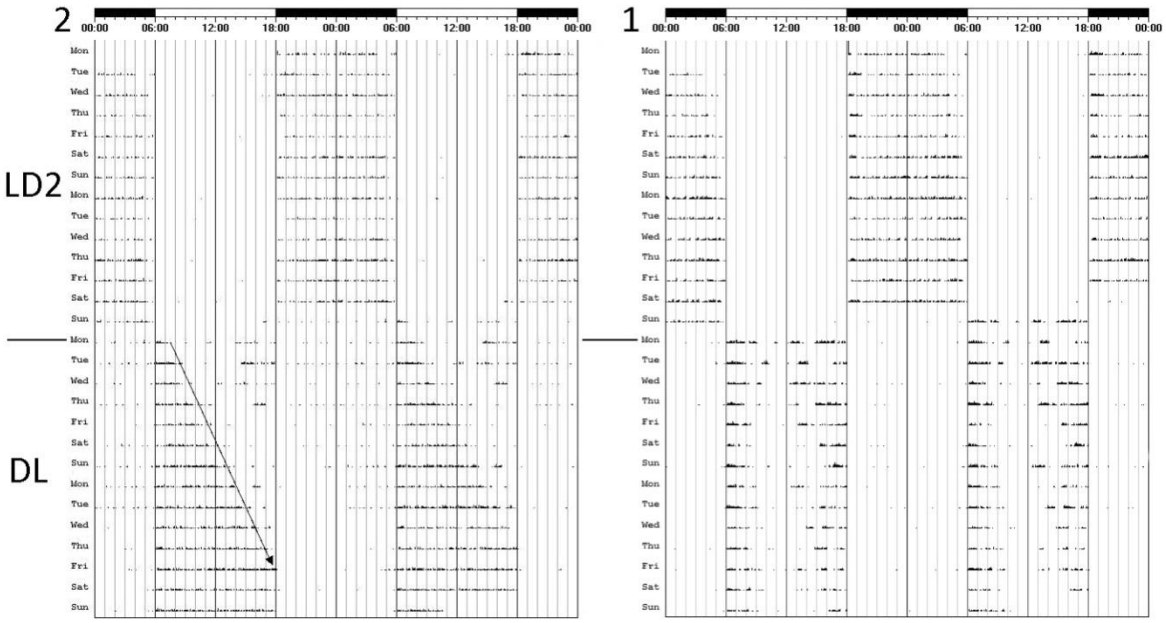

Figure 2.5

Actograms for the Namaqua rock mouse (*Micaelamys namaquensis*) showing either a progressive shift (on the left; animal no. 2) or a direct shift (on the right; animal no. 1) in the locomotor activity rhythm in response to the inversing of the lighting regime from 12L: 12D (LD1) to 12D: 12L (DL). Note that activity in animal no. 1 changed from continuous during LD2 to bimodal during DL.

CHAPTER 3:

THE TOPOGRAPHY OF RODS, CONES AND INTRINSICALLY PHOTOSENSITIVE RETINAL GANGLION CELLS IN THE RETINAS OF A NOCTURNAL (*MICAELAMYS NAMAQUENSIS*) AND A DIURNAL (*RHABDOMYS PUMILIO*) RODENT

Abstract

We used immunocytochemistry to determine the topographical density arrangements of visual (rods/cones) and non-visual photoreceptors (intrinsically photosensitive retinal ganglion cells; ipRGCs) in the four striped field mouse (*Rhabdomys pumilio*) and the Namaqua rock mouse (*Micaelamys namaquensis*). Both species possess duplex retinas with cone to rod ratios that generally reflect the species' daily activity patterns. Although *R. pumilio* is characterised as diurnal, the species is largely active around dawn and dusk, i.e. when there are large changes in the photoenvironment. Accordingly, *R. pumilio* possesses a high density of both cones and rods and has a cone to rod ratio (1:1.23) slightly above the usual range for diurnal species. Similarly, the ratio of cones to rods in *M. namaquensis* (1:12.4) reflects its distinct nocturnal lifestyle. As in most mammals, rods are the dominating photoreceptor class in both species and similar density peaks are observed (*R. pumilio*: ~84467 rods/mm^2; *M. namaquensis*: ~81088 rods/mm^2). Despite this, rods display a centro-peripheral gradient in *R. pumilio* (central region:~56618 rods/mm^2; periphery:~32689 rods/mm^2), but are homogenously distributed in *M. namaquensis*. *Micaelamys namaquensis* has on average ~12000 more rods per mm^2 than *R. pumilio*. The present results also suggest that both species possess dichromatic colour vision and thus that their cones comprise of one populations of short wave sensitive cones (S-cones) and a second population of medium to long wave sensitive cones (M/L-cones). There are no signs of topographical separation between S-cones and M/L-cones in either of the species, but cones are homogenously distributed only in *M. namaquensis*. In *R. pumilio*, M/L-cones are distinctly concentrated in the ventral retina between the optic nerve and the periphery whereas S cones show a centro-peripheral gradient. The S- to M/L-cone ratio is ~1:7.8 in central and peripheral regions of *M. namaquensis* and also

in the central retina of *R. pumilio*. The ratio is 1:6.8 in the peripheral region of *R. pumilio* and 1:15 when it is calculated only in the region where the M/L-cones are highly concentrated. Only small amounts of ipRGCs are observed (*R. pumilio*: total number=1012 ipRGCs; *M. namaquensis*: total number=862 ipRGCs) and in *R. pumilio*, ipRGCs are densest in the dorso-nasal quadrant whereas in *M. namaquensis*, the ipRGCs appear to be uniformly distributed. Although the cone to rod ratios reflect the temporal niches of the species, the adaptive values of the specific topographical photoreceptor distributions remain unclear.

Introduction

The vertebrate eye and in particular the retina, mediates between the spectrum of photic-information from the environment, and the brain of an animal. The absorption and interpretation of light does not only produce the visual perception of sight, but also a range of non-visual behavioural and physiological responses (Freedman *et al.* 1999; Berson 2003; Lockley & Gooley 2006). Vision is the end-point of the circuit that projects to the visual cortex *via* the lateral geniculate nucleus (Schiller 2010). Non-visual processes result mainly from projections to the SCN (for circadian entrainment and which in turn project to other brain regions such as the pineal gland; Provencio *et al*. 2000; Berson *et al.* 2002; Hattar *et al*. 2002), the superior colliculus (the centre for the regulation of eye movements) and the pretectum (for the control of pupillary light reflex; Lockley & Gooley 2006). Accordingly, visual and non-visual responses are achieved through two parallel circuitry networks that originate in the retina and extend *via* the optic nerve to the associated brain regions.

Circuitry for image-based detection of the spatial environment originates at the classical photoreceptors (rods and cones) that innervate the outer retina (Jacobs 1993). Rods have a low acuity for the visual scenery but remarkably, are capable of detecting even single photons (Rodieck & Rushton 1976; Baylor *et al.* 1979). Conversely, cones are less light sensitive, but discriminate detailed information regarding colour, space and time (Rieke & Baylor 1998; Sugita & Tasaki 1988). Rods and cones thus permit scotopic and photopic vision, respectively. In contrast, the circuitry projecting to the SCN is primarily stimulated by the non-image forming photoreceptors (intrinsically photosensitive retinal ganglion cells; ipRGCs) that reside in the ganglion cell layer of the inner retina (Provencio *et al.* 1998; von Schantz *et al.* 2000; Hattar *et al*. 2002). Amongst the more or less 15 different ganglion cell types identified, only a small subpopulation (1-2%) is intrinsically light sensitive (Hattar *et al*. 2002; Masland 2001). Prior to the discovery of ipRGCs slightly more than a decade ago, the rods and cones were considered the two sole retinal photoreceptor classes and naturally all light responses were attributed to them. However, after observing at first normal circadian entrainment in mice with severely degenerated photoreceptors (*rd/rd* mice) and later in mice lacking all functional rods and cones (*rd/rd cl* mice), the presence of a novel retinal photoreceptor class was imperative (Foster *et al*. 1991, 1993; Freedman *et al*. 1999; Lucas *et al*. 1999, 2001). Unfortunately, the discovery of the ipRGCs and hence a rodless, coneless photoreceptive pathway for non-visual responses, caused the general impression that conventional rods and cones do not contribute to photic entrainment. At present, it is becoming increasingly clear that rods and cones also contribute to non-visual processes (Aggelopoulos & Meissl 2002; Dkhissi-Benyahya 2007; Altimus *et al.* 2010; Gooley *et al.* 2010; van Diepen *et al.* 2013; Weng *et al.* 2013). Likewise, despite being directly photosensitive (Lucas *et al*. 1999; Semo *et al*. 2003), ipRGCs share connections with rod and

cone networks and are involved in pattern vision (Foster & Helfrich-Förster 2001; Schmidt *et al.* 2011b). Moreover, many morphologically, physiologically and functionally distinct subtypes of ganglion cells (M1 through to M5) have been identified since its discovery (Ecker *et al*. 2010; Schmidt *et al.* 2011a).

All photoreceptors are sensitive to different ranges of the electromagnetic spectrum, due to the photopigments they enclose. Photopigments share the same chromophore (11-*cis*-retinal or 11-*cis*-3,4-dehydroretinal) but has opsin molecules with different amino acid residues that when changed produce varying spectral characteristics (Asenjo *et al.* 1994; Imai *et al*. 1997; Nathans 1999; Kuwayama *et al*. 2002). Cone photopigments are termed cone-opsins, rods enclose rhodopsin (rod opsins) and ipRGCs enclose melanopsin. Interestingly, melanopsin shares a greater sequence homology with invertebrate opsins than with any other vertebrate opsins (Provencio *et al*. 2000; Gooley *et al*. 2001; Berson *et al.* 2002; Hattar *et al*. 2002). In mammals, three basic cone types (S-, M- and L-cones) form the basis for trichromatic vision. They are distinguished by the short (blue, λ_{max}*=420 nm),* medium (green, λ_{max}*=530 nm),* and long wavelengths (red-orange, λ_{max}*=560 nm)* of light to which their photopigments are maximally absorptive (Schnapf *et al.* 1987). Trichromacy was believed to be limited to Simian primates (Ahnelt & Kolb 2000), but at present it is known to occur also in certain marsupials such as the fat-tailed dunnart (*Sminthopsis crassicaudata*) and the honey possum (*Tarsipes rostratus*; Arrese *et al*. 2003). Most other mammals are typically dichromats, i.e. they possess one cone type (S-cones), which is sensitive to short wavelengths of light (maximally sensitive to either blue, violet, or near-ultraviolet light) and a second cone type (generally denoted as M/L-cones*)* that is sensitive to medium to long wavelengths (maximally sensitive to either green, yellow, or orange

light; Jacobs 1993; Peichl 2005). Beyond this general pattern, some animals possess dual cones that simultaneously express S-pigment and M/L-pigment in certain areas of the retina (Lukáts *et al.* 2005). The presence of dual cones is generally widespread and has been observed in mammals such as mice, rabbits, guinea pigs, voles, African mole rats, pocket gophers and even in humans, but are often only a transient feature of developing retinas (Röhlich *et al.* 1994; Applebury *et al.* 2000; Cornish *et al*. 2004; Lukáts *et al.* 2005; Williams *et al.* 2005). Remarkably, retinae of the adult Siberian hamsters (*Phodopus sungorus*) and the pouched mouse (*Saccostomus campestris*) are characterized by a single, uniformly distributed cone population that coexpresses S- and M/L-pigments (Lukáts *et al*. 2002).

The density and topographical array of conventional photoreceptors vary immensely between mammalian species with the greatest difference amongst rodents (Peichl 2005). In some cases rod and cone arrangements are believed to reveal different adaptations to different environments. One basic example is that of the cone to rod ratio in rodents, which commonly corresponds with the circadian activity pattern of the animal and is hence high in strongly diurnal species and low in strongly nocturnal species (Jacobs 1993; Peichl 2005). For instance, in the diurnal Californian ground squirrel (*Spermophilus beecheyi*), the total visual-photoreceptor population (TVPP) contains 86% cones (Kryger *et al*. 1998). Other diurnal rodents with cone rich retinas include the Sudanian unstriped grass rat (*Arvicanthis ansorgei*: 33%), striped desert mouse (*Lemniscomys barbarus*: 33%), Nile grass rat (*A. niloticus*: 35-40%), Fat sand rat (*Psammomys obesus*: 41%) and Mongolian gerbil (*Meriones unguiculatus*: 12-14%; Govardovskii *et al*. 1992; Bobu *et al*. 2006; Gaillard *et al*. 2008; Saïdi *et al*. 2011). Conversely, in the retinas of nocturnal species, generally a very small proportion (less than 3%) of the TVPP comprises of cones, e.g. in the

Gambian pouched rat (*Cricetomys gambianus*: 0.3-0.5%), Emin's pouched rat (*C. emini*: 0.5-0.8%), eastern woodrat (*Neotoma floridana*: 1%), and conventional laboratory mice and rats (<3%; Carter-Dawson & La Vail 1979; Szél & Röhlich 1992; Jeon *et al.* 1998; Peichl & Moutairou 1998; Feldman & Phillips 1984). Thus, although rods still outnumber cones in most diurnal rodents, the proportion of cones is comparatively much higher in diurnal species compared to nocturnal species.

Many mammals possess dichromatic vision and hence possess two cone types that have opsins with maximal sensitivities at spectral wavelengths characteristic of the species (Peichl 2005). The M/L-cones usually outnumber S-cones by a considerable amount (Szél *et al*. 1996). In addition, the topographical layout of the cones is not always homogenous as it has been described for the Mongolian gerbil (*M. unguiculatus*), rat (*Rattus norvegicus*) and the wood mouse (*Apodemus sylvaticus*), to name a few (Govardovskii *et al*. 1992; Szél & Röhlich 1992; Szél *et al*. 1994). Either one or both the S-cone and M/L-cone populations may be restricted to certain retinal domains. Cone segregation has been observed in the house mouse (*Mus musculus*), mound builder mouse (*Mus spicilegus*), agouti (*Dasyprocta aguti*) and rabbit (Szél *et al*. 1992; 1994; Rocha *et al*. 2009).

The present study aimed at characterizing retinal photoreceptor topographies in two South African rodents. For this, the density and topographical arrangement of rods, cones and ipRGCs are investigated and compared by means of immunocytochemistry in the diurnally active four striped field mouse (*Rhabdomys pumilio*) and the nocturnally active Namaqua rock mouse (*Micaelamys namaquensis*). Retinal photoreceptor compositions are expected to reflect the

temporal activity patterns of the studied species and as in all mammals studied so far, the ipRGCs are expected to be sparsely distributed. Knowing that the eye is the gateway to both "image-forming vision" and "circadian vision", a thorough description of the photoreceptor compositions may provide further insights in the circadian responses that these species might show when they are subjected to different lighting conditions (See Chapters 4 & 5).

Materials and methods

Some procedures in the immunocytochemistry and mode of photoreceptor counting differed slightly between the photoreceptor types. Both cone types in *M. namaquensis* as well as S-cones and rods in *R. pumilio* were immunostained, and the photoreceptors counted, as described by Á. Lukáts (Ph.D. dissertation 2004). For an overview of these methods see *Brief outline on the methods by Á. Lukáts* on page 58. For immunostaining of the rods in *M. namaquensis*, M/L-cones in *R. pumilio* and the ipRGCs in both *M. namaquensis* and *R. pumilio*, see below. Apart from the counting protocol, all calculations for analyses were similar. Collaboration of the data provided the opportunity to present a complete set of the topographical layouts of all photoreceptors in both species.

Animal and tissue preparation

The project was approved by the Animal Ethics Committee of the University of Pretoria, Pretoria, South Africa (EC063-11). The eyes from adult laboratory-bred four striped field mice (*R. pumilio*) and wild-caught Namaqua rock mice (*M. namaquensis*) were studied. *Rhabdomys*

pumilio was obtained from a breeding colony at the University of the Witwatersrand (Johannesburg, South-Africa) while *M. namaquensis* were collected from the rocky outcrops of the Goro Game Reserve in the Soutpansberg region (Limpopo Province, South Africa). Before the animals were euthanized and enucleated they were maintained individually in semi-transparent plastic cages (58 x 38 x 36 cm) in a light and temperature controlled animal room at an ambient temperature of 25 °C (± 1°C) and approximately 60% relative humidity. Each cage contained a layer of wood shavings (± 3 cm thick) and the animals were given a small plastic shelter and tissue paper for nesting material. The mice had *ad libitum* access to food and water and were fed at random times every second or third day. Water and food (parrot seed mix) were topped up and fresh food was replaced. The mice were exposed to a 12L: 12D photoperiod (L: 06h00 – 18h00) and the room was illuminated at day time by white fluorescent lights (± 400 lux).

All animals were euthanized using an overdose of halothane anaesthetic (Zeneca, Johannesburg, South Africa) and then perfused intracardially with 0.9% saline followed by 4% paraformaldehyde (PFA; Saarchem, Johannesburg, South Africa) in phosphate-buffered saline (PBS, 0.1M). The heads were removed and post fixed in 4% PFA for approximately 4 hours before being transferred to 0.5% PFA diluted in PBS. Each eye was marked dorsally for orientation, enucleated, cut at the orra serrata, the lens and vitreous body were removed. The retina was carefully separated from the pigment epithelial layer and stored in PBS with 0.05% sodium azide at 4 °C until the preparation of retinal sections or whole mounts for immunocytochemistry. For vertical 14 µm sections, quarter sections of the retinas were embedded with Jung Tissue Freezing Medium (Leica Instruments, Germany), cut with a cryostat

and mounted onto slides. For whole mounts, retinas were sequentially incubated in phosphate buffer containing 10%, 20% and 30% sucrose for cryoprotection and then shock-frozen to increase antibody penetration. Whenever patches of the pigment epithelium remained attached to the retina, the retinae were incubated in a solution comprising of 5 ml 1.8% saline (NaCl in H_2O), 4 ml 30% H_2O_2, 1 ml H_2O and one drop of a 25% NH_3 solution (modified from Hemmi & Grünert 1999; Petry *et al.* 1993), until the remaining pigment epithelium were bleached.

Antibodies

Vertical retinal sections from several retinas were used in the initial testing of the anitibodies. Vertical sections were immunolabelled in order to validate the presence of the photoreceptor classes and to test the specificity of the antibodies in the two species. Whole mounts were used to study the topographical distribution and densities of the photoreceptors. For each species, one whole retina was used per analysis of one photoreceptor class. See Table 3.1 for a list of the primary antibodies and their dilutions that were used in the present study; the antibodies listed in the Ph.D. dissertation (2004) of dr. Á. Lukáts is included here. In *M. namaquensis*, three mouse monoclonal antibodies namely Rho4D2 (1:1000), OS-2 (1:5000) and COS-1 (1:50) labelled rods, S-cones and M/L-cones, respectively. In *R. pumilio*, OS-2 (1:100) labelled S-cones, a rabbit polyclonal antibody (cat no. AB5405, 1:500) labelled M/L-cones, and a rat polyclonal antibody (AO, 1:100) labelled rods. For the labelling of the ipRGCs in both species, a rabbit polyclonal antibody (PA1-781, 1:1000) was used. With the exception of the photoreceptors analyzed by dr. Á. Lukáts (see *Brief outline on the methods by Á. Lukáts* on page 58), concentrations of the antibodies were doubled for whole mounts.

Immunocytochemistry

In order to block nonspecific binding sites, retinal sections were incubated in a blocking solution comprising 10% normal goat serum or normal donkey serum (NGS/NDS), depending on the antibody to be used, and 3% Triton in PBS for 30 minutes. Subsequently, the sections were immunostained through overnight incubation (at room temperature) in a solution comprising of the primary antibodies diluted in PBS with 3% NDS/NGS and 0.3% Triton. The following day the tissue was washed in PBST and then incubated in a solution containing the secondary antibodies (Alexa 488 or Alexa 700), 3% NDS/NGS and 0.3% Triton in PBS for 90 minutes in order to reveal the primary antiserum-antibody binding sites. For retinal whole mounts all primary antibody concentrations were doubled, and diluted in 3% NDS/NGS, 0.3% Triton and 0.05% sodium azide. The free floating retinas were incubated in the solution for three days on an orbital shaker (at room temperature). Once incubation was completed, the retinal tissue for sections and whole mounts were carefully transferred onto glass slides with a soft paint brush and cover slipped using Aqua PolyMount solution. The labelled slides were stored in a fridge until inspection.

Data capture and photoreceptor density analyses

Rods, cones and ipRGCs were observed using a fluorescence microscope (Olympus BX51FT, Olympus Optical Co., LTD.) fitted with a camera (SPOT RT Slider 2.3.1.1, Diagnostic Instruments, Inc.) and micrographs captured and analyzed with SPOT Advanced 5.0 software. For rod and cone cell counting, a grid was superimposed over the whole mounted retina that

divided it into 1mm^2 squares. A photographic image (117 x 88μm; x1000 magnification) was captured within each square and the number of the respective cells manually counted within the photo. The values were then converted to indicate the amount of photoreceptors per mm^2. Vector illustrations were created for whole retinae using Adobe Illustrator CS5 (Adobe Systems Inc., CA) and the density values plotted in to create topographical maps. Camera lucida drawings were made for ipRGCs and the cells counted directly. Several ratios between photoreceptor classes were determined using the mean values of the photoreceptors (per mm^2) that were calculated for either the central, peripheral or whole retinal regions. The recognition of ipRGCs as a photoreceptor class is relatively recent and thus the majority of published data typically refer to the collection of rods and cones as the total photoreceptor population. In order to avoid confusion, a distinction is made in the present study between the total photoreceptor population (TPP) and the total visual-photoreceptor population (TVPP), of which the latter excludes the ipRGCs. Standard error was indicated where applicable.

Brief outline on the methods by Á. Lukáts

The following section is adapted from Lukáts (PhD dissertation, 2004) and briefly outlines the methods related to the immunocytochemistry and photoreceptor counting of the S- and M/L-cones in *M. namaquensis* as well as the S-cones and rods in *R. pumilio*. The mice were euthanized using halothane anaesthetic (Zeneca, Johannesburg, South Africa) followed by a combination of ketamine (150 mg/kg) and rompum (30mg/kg). The animals were then perfused intracardially with heparinized saline (37 °C) followed by Zamboni's fixative (Na_2HPO_4, NaH_2PO_4, PFA and saturated picric acid; 4°C) and the heads stored in the same solution. Each

eye was marked dorsally for orientation, enucleated and the retina removed from the posterior eyecup. Retinas that were being used for whole mount immunostaining were collected and rinsed in 0.1M PBS for at least 24 hours prior to further processing. For vertical 1 μm sections, several samples were cut from various sites of the retina, rinsed overnight in PBS, dehydrated, embedded in araldite, flatmounted and cut using an ultramicrotome. Whole retinas and sections were incubated in 1% BSA (bovine serum albumin) diluted in PBS (containing 0.4% Triton X-100 for whole retinas).

Immunostaining and photoreceptor counting: S-cones, ML-cones and rods were immunostained using OS-2, COS-1 and AO (See Table 3.1). The incubation period for whole retinas were 5-7 days and the bound monoclonal antibodies (OS-2 and COS-1) were visually revealed by subsequent incubation in a biotinylated anti-mouse antibody (12-24 hours), then with either of the two avidin conjugates with a red fluorochrome: Texas Red avidin D (50 μg/ml) or streptavidin Alexa Fluor 594 conjugate (100 μg/ml). The immunostained retinas were inspected either on a Leica DMR or Zeizz Axiophot microscope, using Nomarski optics or the appropriate filter set for the fluorescent antibodies. A computerized system plotted the locations of fluorescent labeled cone photoreceptors in whole mounts. Cones were counted with a 50x or 100x oil immersion objective in 70-90 evenly distributed sample fields across the retina. Since the cell densities of the photoreceptors were high and the outer segments of the photoreceptors long, counting was carried out manually.

Results

Immunolabelling validated the presence of four photoreceptor populations in *R. pumilio* and *M. namaquensis*; rods, S-cones, M/L-cones as well as ipRGCs. With the exception of the relatively uniform distribution of rods and ipRGCs in the retina of *M. namaquensis*, all of the photoreceptor classes in both species displayed some topographical heterogeneity. The retinas of both species were characterized by high rod densities but interestingly, cone density in the retina of *R. pumilio* was nearly as high as the density of rods. From the mean photoreceptor densities (per mm^2) that were calculated for the retina as a whole (not considering topographical layout), cones made up to ~44.9% of the TVPP in *R. pumilio* and only ~7.5% in *M. namaquensis*. Despite this high density of both rods and cones in *R. pumilio*, the mean ratio of cones to rods (1:1.23) fell within the typical range, yet at the higher end, which has been reported for many diurnal small mammals. In *M. namaquensis*, the mean cone to rod ratio was 1:12 and was also as expected for a nocturnal mammal. When the cone/rod ratios were compared between central and peripheral retinae, it was slightly higher centrally (1:1.49) than peripherally (1:1.32) in *R. pumilio* but lower centrally (1:10.5) than peripherally (1:14.1) in *M. namaquensis*. In stark contrast to the conventional photoreceptors, ipRGCs were very sparsely distributed and constituted approximately 0.024% of the TPP for both species. The mean ipRGC/rod and ipRGC/cone ratios were 1:2280 and 1:1861 in the diurnal species and, 1:1390 and 1:316 in the nocturnal species.

Rod photoreceptors

Rods were labelled with rhodopsin specific antibodies AO (*R. pumilio*) and Rho4D2 (*M. namaquensis*) and had the highest densities (per mm^2) of all photoreceptor classes. In *R. pumilio* retina, rod density was highest in the central region (mean: 56618 rods/mm^2) and steadily decreased towards the periphery (mean: 32689 rods/mm^2); see Fig. 3.1. The density peaked at 84467 rods/mm^2 in the ventro-nasal region close to the optic nerve and was lowest at the far ventro-terminal periphery (14739 rods/mm^2). The retina of *M. namaquensis* displayed no heterogeneity in its topographical distribution. Density values ranged between 20712 rods/mm^2 and 81088 rods/mm^2 (Fig. 3.1). Although the values at the densest regions were nearly the same in the two species, the overall mean density was higher in the nocturnal (50820 rods/mm^2) compared to the diurnal species (38766 rods/mm^2).

Cone photoreceptors

The overall mean cone density was almost 8 times higher in *R. pumilio* (31640 cones/mm^2) than in *M. namaquensis* (4113 cones/mm^2). Two separate cone populations were identified. OS-2 positively labelled short wave sensitive opsins in both species while red/green sensitive opsins were labelled using the AB5405 antibody in *R. pumilio* and COS-1 in *M. namaquensis*. Both species had M/L-cone dominant retinas where M/L-cones made up ~89% of the total cone population. In *R. pumilio*, M/L-cones had an overall mean density of 28302 M/L-cones/mm^2. Topographically these cones formed neither a visual streak nor a centro-peripheral gradient, but were densely concentrated in a spherical region located about 0.75-1.5 mm ventral to the optic

disc where the density peak was 71319 M/L-cones/mm^2 (Fig. 3.2). Beyond this very dense region, the M/L-cones were distributed relatively uniformly (25920 M/L-cones/mm^2), yet the region with the lowest count (16218 M/L-cones/mm^2) was furthest peripherally. Unlike the M/L-cones, the S-cones displayed a centro-peripheral gradient, but with a mild density streak directed in a ventro-temporal to dorso-nasal direction (Fig. 3.2). S-cone density ranged from 2401 to 5019 S- cones/mm^2. In *M. namaquensis*, both cone populations displayed a centro-peripheral density gradient. The minimum and maximum M/L-cones/mm^2 was 2018 and 5066, whilst that for the S-cones was 151 and 800, respectively (Fig. 3.3). Naturally, the ratio between the two cones populations varied between different regions of the retinas. Using the density means of central and peripheral regions, the S-cone to M/L-cone ratios were estimated to be approximately 1:7.8 in central and peripheral regions of *M. namaquensis* as well as in the central region of *R. pumilio*. This ratio was slightly lower (1:6.8) in the peripheral region of the latter species and much higher (1:15) when it is calculated only in the spherical region where the M/L-cones are highly concentrated. See figs. 3.2 and 3.3.

Intrinsically photosensitive ganglion cells (ipRGCs)

In both species, we used a rabbit polyclonal antibody, PA1-781, that recognizes the C-terminus of melanopsin to expose the ipRGCs. Compared to rods and cones, the amount of positively labelled ipRGCs was very low, while *Rhabdomys pumilio* had a mean of 17 ± 14 ipRGCs/mm^2 and a total of 1012 ipRGCs across the entire retina, *M. namaquensis* had a mean of 13 ± 6 ipRGCs/mm^2 and a total of 862 ipRGCs across the entire retina. The density distribution of the ipRGCs portrayed different patterns in the two species; see Fig. 3.4. In *R. pumilio*, the ipRGCs

were concentrated in the dorso-nasal quadrant where the density peak was 56 ipRGCs/mm^2. Across the remaining retinal surface the ipRGCs were uniformly distributed (~11-20 ipRGCs/mm^2). In the retina of *M. namaquensis*, the ipRGCs appeared to be uniformly distributed across the retinal field. However, slightly lower densities (~10-15 ipRGCs/mm^2) were observed in the central retina (Fig. 3.4) and slightly higher densities in dorsal retina. In both species, the vertical sections used for testing whether PA1-781 recognized melanopsin in the two study species displayed M1 type ipRGCs with somata located in the ganglion cell layer (GCL) and their dendrites stratifying the outermost margin (OFF lamina) of the inner plexiform layer (IPL; Fig. 3.5). Immunolabelled ipRGCs in whole mounted retinae also revealed the photoreceptive net and a beaded appearance of the axons and dendrites projecting from the somata (Fig. 3.6).

Discussion

Animals depend on their senses to live and survive in their environment and hence most sensory systems display adaptations to the specific lifestyle of a species. Adaptations of the visual system range from the anatomical, for example eye size, shape, and positioning on the animal's head (Hall & Ross 2007; Martin 2007; Ross & Kirk 2007), to the physiological, for example the arrangement of retinal circuitry and the topographical distribution of the photoreceptors (Jacobs 1993; Ahnelt & Kolb 2000).

In the present study, we assessed not only conventional photoreceptors (rods and cones) but also the relatively novel photoreceptor class (ipRGCs) in two murid rodents; the diurnally active *Rhabdomys pumilio* and the nocturnally active *Micaelamys namaquensis*. A few features of the

conventional photoreceptors of these two species have been briefly reported by Lukáts *et al.* (2005). Here we present and compare the density and topographical distributions of the various photoreceptor classes in *R. pumilio* and *M. namaquensis*. We used antibodies that have repeatedly been shown to reliably label rods, S-cones, M/L-cones and ipRGCs in various species.

Immunostaining has revealed duplex retinas that were rod-dominated in both species. This is a typical feature of mammalian retinae whether the species is diurnal or nocturnal (Jacobs 1993; Peichl 2005). As expected, in both species the ratios of cones to rods generally reflected the species' daily activity patterns. In the diurnal *R. pumilio*, the total cone population represented a large proportion of the TVPP (~44%); rods were 56% of the TVPP. This proportion of cones is higher yet comparable to that reported for other small diurnal mammals; around 10% more than in *Arvicanthis ansorgei* and *Lemniscomys barbarous,* between 4-8% more than in *Arvicanthis niloticus* and *Psammomys obesus*, and around 30% more than in *Meriones unguiculatus* (Govardovskii *et al*. 1992; Bobu *et al*. 2006; Gaillard *et al*. 2008; Saïdi *et al*. 2011). Interestingly, in the strictly diurnal *Spermophilus beecheyi w*here cones comprise 86% of the TVPP, cone density peaked at 49550 cones/mm^2 (Kryger *et al.* 1998). This is one and a half times lower than only the M/L-cone density peak of *R. pumilio* (~71319 M/L-cones/mm^2). Consequently, *R. pumilio* has a high density of both rods and cones with a ratio of cones to rods (1:1.23) slightly above the usual range of diurnal species. Although *R. pumilio* is classified as diurnal, most of its activity centres around the period of dawn and dusk (Schumann *et al*. 2005). Thus more specifically, *R. pumilio* displays diurnal-crepuscular activity and presumably its high density of rods and cones is advantageous during dusk and dawn when the environment is transformed from illuminated to dark. In contrast, only ~7.5% of the TVPP in *M. namaquensis* comprised of

cones (rods were 92.5% of the TVPP) and the overall mean cone to rod ratio (1:12.4) was high compared to that of *R. pumilio*. This proportion of cones is similar in other nocturnal mammals (*Cricetomys gambianus, Cricetomys emini, Neotoma floridana* and laboratory mice and rats) where cones comprised between 0.3-3% of the TVPP (Carter-Dawson & La Vail 1979; Szél & Röhlich 1992; Jeon *et al.* 1998; Peichl & Moutairou 1998; Feldman & Phillips 1984). Furthermore in *M. namaquensis*, rods did not display any noticeable heterogeneity, whilst the opposite was true in *R. pumilio* where a centro-periphero density gradient was observed. This explains why, despite the similarly high density peak values (*R. pumilio*: ~84467 rods/mm^2; M. namaquensis: ~81088 rods/mm^2), *M. namaquensis* had on average ~12000 more rods per mm^2 than *R. pumilio*. In the Californian ground squirrel (*S. beecheyi*) rods are distinctively segregated across the dorso-ventral axis of the retina with a density peak in the ventral retina (Kryger *et al.* 1998). Exactly how such a rod distribution might be beneficial to *S. beecheyi*, remains to be tested. Such a pattern has not been observed in murid rodents thus far.

In both species, immunocytochemistry revealed the presence of one cone population that expresses S-opsin and a second that expresses M/L-opsin. This strongly suggests dichromatic colour vision in both species. Very few rodents are monochromats and it is usually limited to nocturnal species. In all cases the retinae of such animals are void of S-cones; examples of such species include the pygmy field mouse (*Apodemus microps*), African giant rats (*C. gambianus* and *C. emini*) and even the Syrian golden hamster (*Mesocricetus auratus*; Szél *et al.* 1994; von Schantz *et al.* 1997; Peichl & Moutairou 1998). Furthermore, the topographical array of cones across the retinal field varies immensely between mammalian species; S- and M/L-cones could be arranged in a variety of manners (Peichl 2005). One pattern common to mice (e.g. *M.*

musculus and *M. spicilegus*) is a dorso-ventral separation of S- and M/L-cones where S-cones are completely or primarily concentrated in the ventral retina and M/L cones in dorsal retina (Szél *et al.* 1994). *R. pumilio* and *M. namaquensis* showed no signs of topographical separation of the two cone classes. Cone topographies were nonetheless heterogeneous and as a consequence the S-cone to M/L-cone ratio depended upon the retinal region. In *R. pumilio* M/L-cones were distinctly concentrated in the ventral retina between the optic nerve and the periphery. This pattern differs from the centro-peripheral density gradients described in *A. sylvaticus* and *A. microps*, since M/L-cones density did not show a gradual decrease towards the periphery but were rather uniformly dispersed outside of this concentrated sphere. On the other hand, S-cones displayed a centro-peripheral gradient but with a mild density streak directed in a ventro-temporal to dorso-nasal direction. Consequently, the mean ratio of S-cones to M/L-cones was very high in the M/L-cone rich centre (1:15) and low in the region where the S-cone density peaked (1:4). In *M. namaquensis*, both cone populations displayed a centro-peripheral density gradient with little variation in the ratio of S-cones to M/L-cones between central and peripheral retina. The mean ratios of S-cones to M/L-cones in *R. pumilio* (1:8.5) and *M. namaquensis* (1:7.8) resembling those of most small mammals, which generally lie in the vicinity of 1:10 irrespective of whether the species has a rod dominant or cone dominant retina (Szél *et al*. 1996; Ahnelt & Kolb 2000). Most unusually, the opposite pattern has been observed in some mole-rats belonging to the family Bathyergidae, where the majority of the immunostained cones expressed S-opsins (Peichl *et al.* 2004).

Melanopsin expressing ipRGCs make up only a small subpopulation of the total retinal ganglion cell population (1-2%; Hattar *et al*. 2002). Presently, five distinct ipRGC subtypes have been

identified (M1 through M5) that differ in somata size, dendritic morphology, the location of their dendritic stratification, the strength of their intrinsic responses, the brain regions to which they project etc. (Ecker *et al*. 2010; Estevez *et al.* 2012). Immunolabelling with PA1-781 exposed ipRGCs in both the diurnal *R. pumilio* and nocturnal *M. namaquensis*. Although the ipRGCs were quantitatively comparable in both species (*R. pumilio*: ~17 ipRGCs/mm^2; *M. namaquensis*: ~13 ipRGCs/mm^2), their topographical distributions were distinctly different. In *R. pumilio*, ipRGCs displayed were most dense in the dorso-nasal retina. In addition, this density gradient did not correspond to either rod or cone density topographies. In *M. namaquensis*, the ipRGC population showed a topographical distribution as homologous as that of its rods. Furthermore, the ipRGCs identified in this study were most likely M1 and M2 types. From the vertical sections it could be seen that somata of the PA1-781 labelled cells resided in the GCL with their dendrites stratifying the outermost margin (OFF lamina) of the IPL. This is characteristic of the M1 type (Hattar *et al* 2002; Berson *et al.* 2010). Although we did not inspect enough vertical sections to observe it, some of the ipRGCs were most likely M2 cells. In *A. ansorgei*, immunolabelling only detected M1 and M2 types, with ~74% being M1 cells and 24% M2 cells (an insignificantly small amount of displaced ipRGCs were also seen; Karnas *et al*. 2013). Furthermore, evidence suggests that the ratio between M1 and M2 cell types could potentially contribute to differences in the temporal niches of species and that M1 cells are possibly higher in diurnal than nocturnal species (Karnas *et al.* 2013).

In conclusion, *R. pumilio* and *M. namaquensis* retinas were characterized by cone to rod ratios that reflected the species' temporal niches. The present results indicate that both species are dichromats and there were no signs of topographical separation between S- and M/L-cones in

either of the species. However, in *R. pumilio* M/L-cones were distinctly concentrated in the ventral retina between the optic nerve and the periphery. In both species, rods were the dominating photoreceptor class and ipRGCs were by far the least abundant photoreceptor type. Interestingly, neither rods nor ipRGCs were homogenously distributed in *R. pumilio*. The adaptive values of the various topographical photoreceptor distributions in the retinae of the present species remain unclear.

Table 3.1: List of primary antibodies used in the present study.

Specificity	Antibody (dilution)		Antigen
	Micaelamys namaquensis	*Rhabdomys pumilio*	
Rods	Mab; Rho4D2 (1:2000*)[a]	Pab; AO (1:100)	Rhodopsin N terminal[d,e]
M- and L-cones	Mab; COS-1 (1:50)	Pab; AB5405 (1:1000*)[b]	M/L-pigment C terminal[e]
S-cones	Mab; OS-2 (1:5000)	Mab; OS-2 (1:5000)	S-pigment C terminal[e]
ipRGCs	Pab; PA1-781 (1:2000*)[c]	Pab; PA1-781 (1:2000*)[c]	Melanopsin C terminal[f]

*Dilutions were halved for vertical sections.

Abbreviations: Mab=Monoclonal antibody; Pab=Polyclonal antibody

[a]Abcam; [b]Millipore; [c]Thermo Scientific; [d]Hicks & Molday 1986; [e]Röhlich & Szél 1993; [f]Hattar *et al*. 2002.

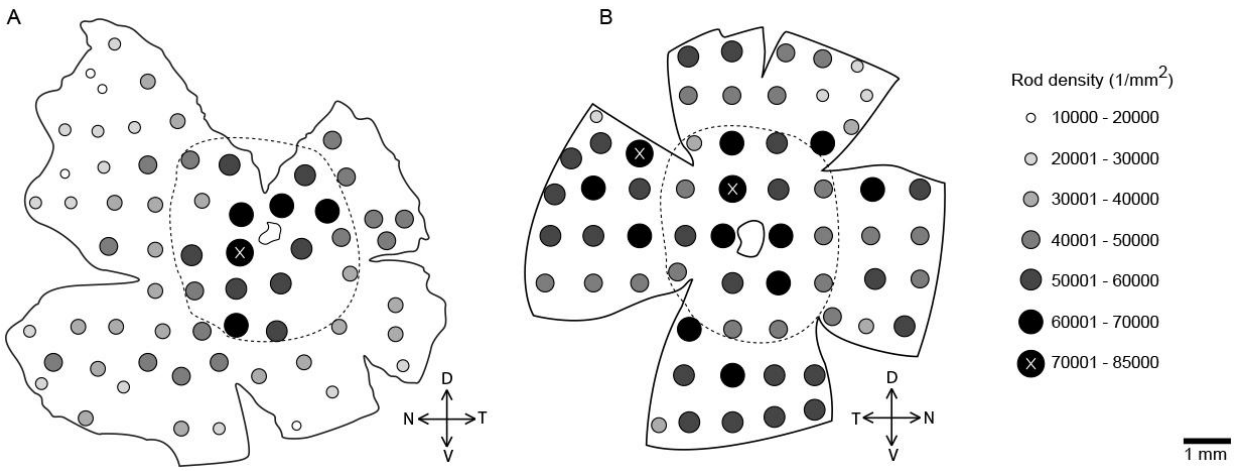

Figure 3.1: Topographical map of the rod density distribution in (A) *Rhabdomys pumilio* and (B) *Micaelamys namaquensis*. The filled circles indicate rod density and the irregular outline that is more or less in the center of the retina, indicates the position of the optic nerve head. The dashed lines separate central from peripheral retinal regions and designates the areas that were used in calculating photoreceptor ratios between central and peripheral retina. D, dorsal; V, ventral; T, temporal; N, nasal.

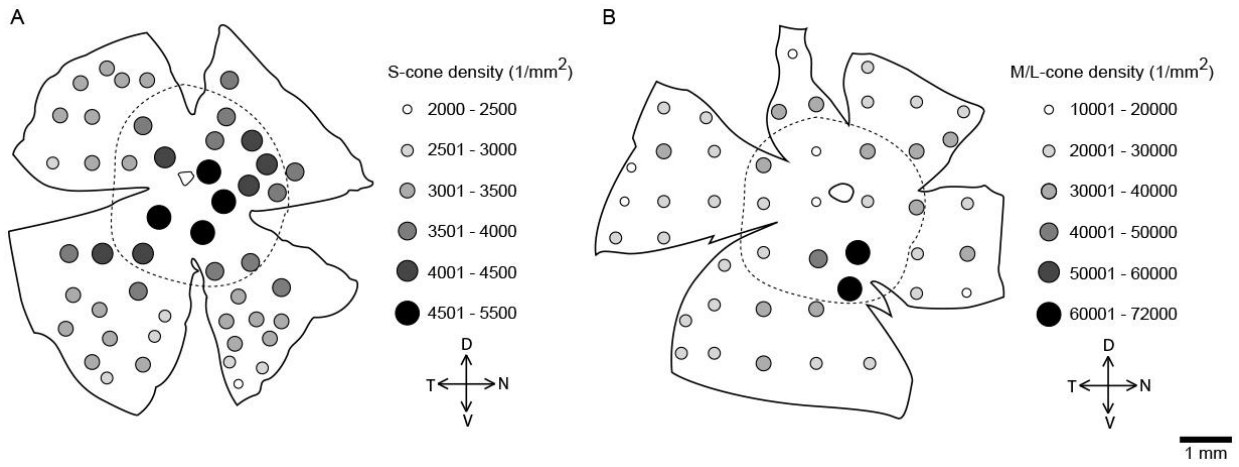

Figure 3.2: Topographical map of the (A) S-cone and (B) M/L-cone density distribution in *Rhabdomys pumilio*. The filled circles indicate rod density and the irregular outline that is more or less in the center of the retina, indicates the position of the optic nerve head. The dashed lines separate central from peripheral retinal regions and designates the areas that were used in calculating photoreceptor ratios between central and peripheral retina. D, dorsal; V, ventral; T, temporal; N, nasal.

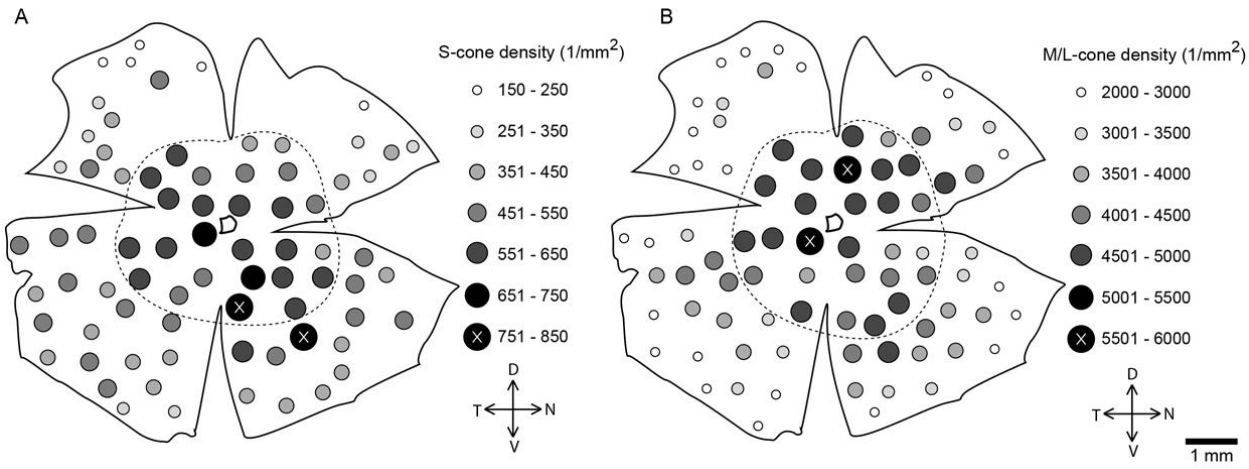

Figure 3.3: Topographical map of the (A) S-cone and (B) M/L-cone density distribution in *Micaelamys namaquensis*. The filled circles indicate rod density and the irregular outline that is more or less in the center of the retina, indicates the position of the optic nerve head. The dashed lines separate central from peripheral retinal regions and designates the areas that were used in calculating photoreceptor ratios between central and peripheral retina. D, dorsal; V, ventral; T, temporal; N, nasal.

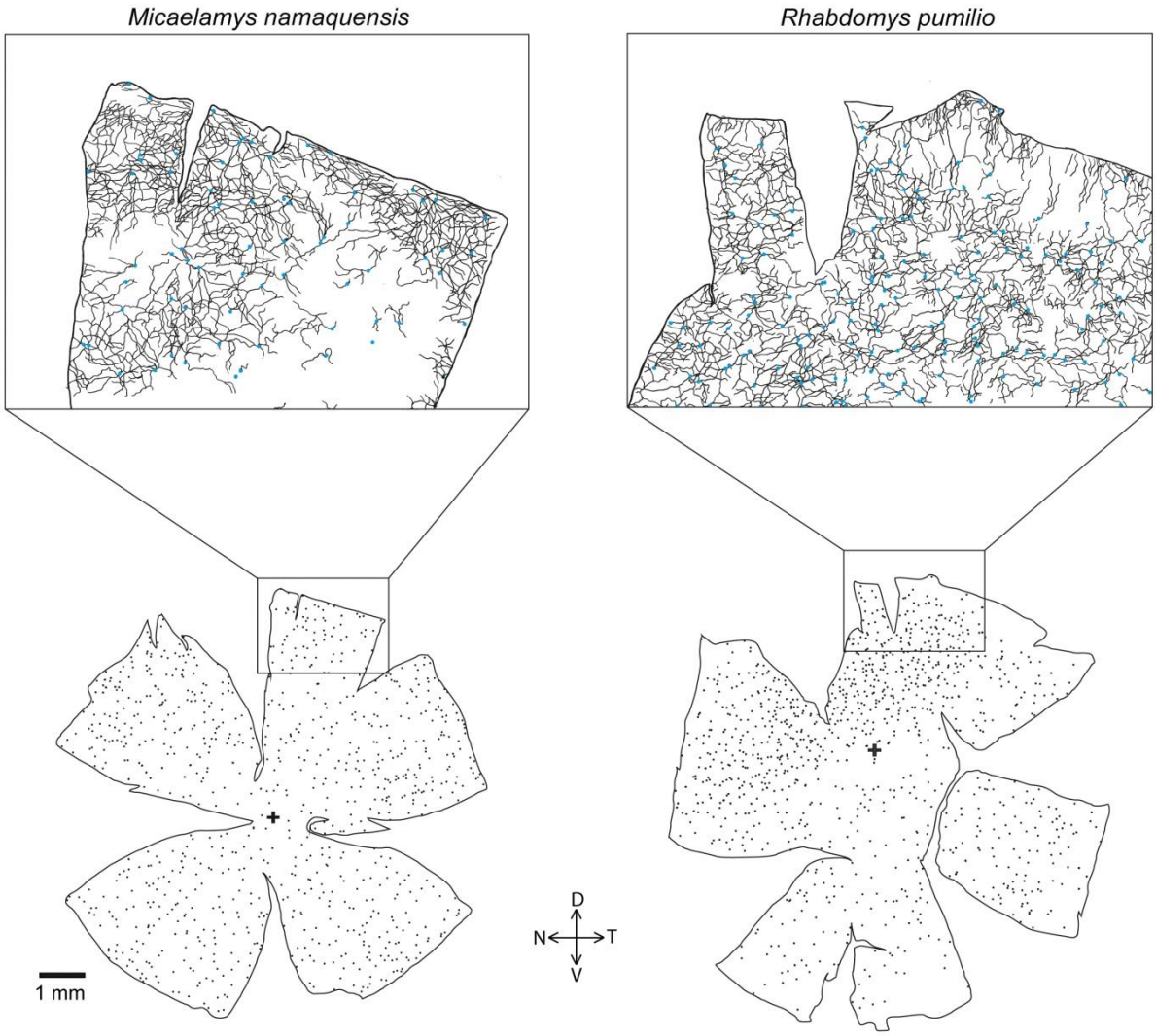

Figure 3.4: Topographical distribution of ipRGCs in whole mounted retina of *Micaelamys namaquensis* (left) and *Rhabdomys pumilio* (right); each dot represents one ipRGC. The enlarged retinal segments (in the top two rectangles) display camera lucida drawings of the photoreceptive nets that are formed the ipRGCs and their overlapping dendrites.

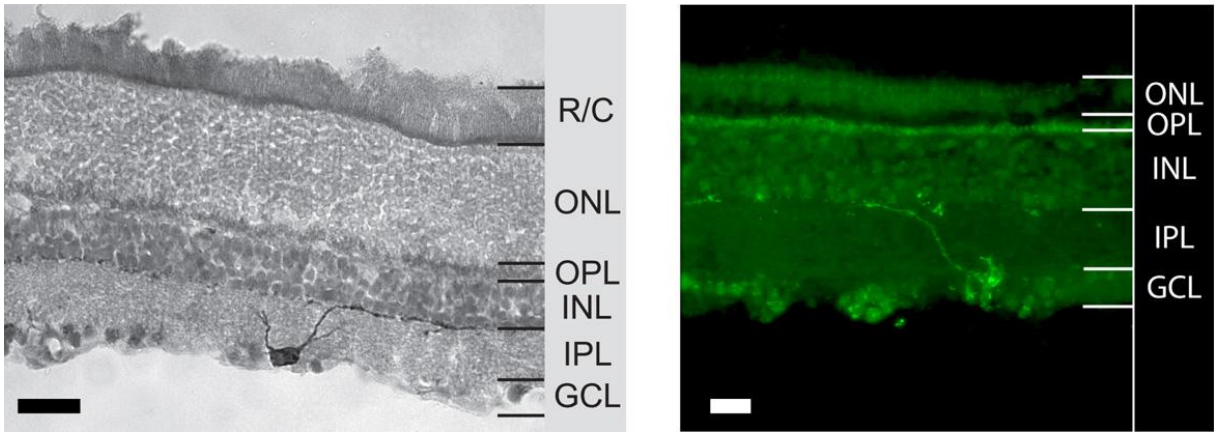

Figure 3.5: Immunolabelling of vertical retinal 14.0 μm sections revealing melanopsin positive ganglion cells in *Micaelamys namaquensis* (on the left) and *Rhabdomys pumilio* (on the right). Somata of ipRGCs are situated in the GCL with axonal projections stratifying in the outermost margin (OFF lamina) of the IPL. ONL, outer nuclear layer; OPL, outer plexiform layer; INL, inner nuclear layer; IPL, inner plexiform layer; GCL, ganglion cell layer. Antibodies were detected with diaminobenzidine staining (DAB) in *M. namaquensis* and fluorescent staining in *R. pumilio*. Scale bars = 50μm.

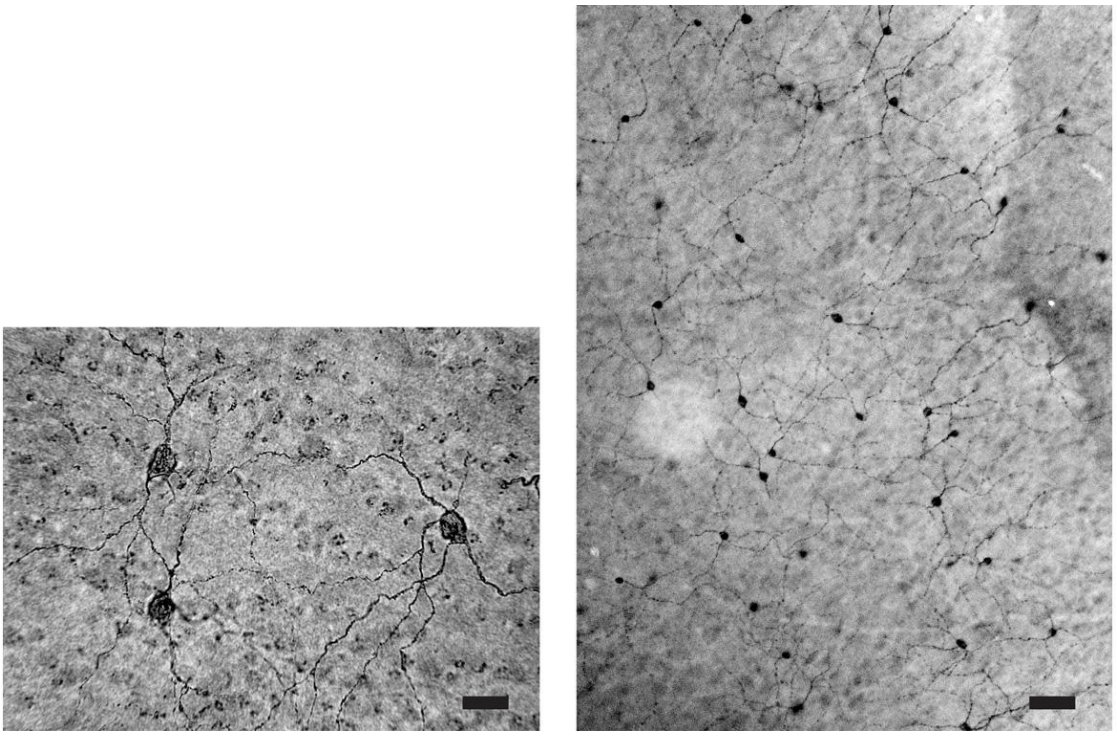

Figure 3.6: Flattened retina showing ipRGCs with axonal projections in *Micaelamys namaquensis* (on the left; scale bar = 25μm) and *Rhabdomys pumilio* (on the right; scale bar = 100μm).

CHAPTER 4:

EFFECTS OF PHOTOPHASE ILLUMINANCE ON LOCOMOTOR ACTIVITY, URINE PRODUCTION AND URINARY 6-SULFATOXYMELATONIN IN A NOCTURNAL AND A DIURNAL SOUTH AFRICAN RODENT

Abstract

The effects of different photophase illuminance levels (1, 10, 100 and 330 lux of white incandescent lighting) on daily rhythms of locomotor activity, urine production and 6-sulfatoxymelatonin (6-SMT; 10 lux vs. 330 lux) were investigated in the nocturnally active Namaqua rock mouse (*Micaelamys namaquensis*) and the diurnally active four striped field mouse (*Rhabdomys pumilio*). Whereas all individuals of *M. namaquensis* were consistently and fundamentally nocturnal (~90-94% nocturnal activity), there was considerable individual variation in the activity patterns in *R. pumilio*; nevertheless, activity was mostly pronounced around dusk and dawn (~49-52% diurnal activity) and brighter photophase illuminances might be needed to further induce diurnal activity. In both species, the photophase illuminance did not change the temporal pattern of activity expression but significantly affected the amplitude thereof and this effect was greater in *M. namaquensis* than in *R. pumilio*. Since *R. pumilio* is expected to tolerate a wider range of illuminances than *M. namaquensis*, these responses seem to be related to the lighting conditions of the species' temporal niches. *Micaelamys namaquensis*, but not *R. pumilio*, displayed distinctive daily urine production rhythms, which correlated with the species' nocturnal activity rhythm. Mean daily urine production values were higher under the two brighter, as opposed to the two dimmer, photophase illuminances, but differences were only significant in *R. pumilio*. The results furthermore suggest that the circadian regulation of locomotor activity and of urine production each possesses their own sensitivity threshold to the level of photophase illuminance. *Micaelamys namaquensis* expressed significant daily 6-SMT rhythms that peaked during the late night. Interestingly, the rhythm was attenuated by the brighter photophase cycle (330 lux); this indicates that the sensitivity threshold for *M.*

namaquensis lies below this illuminance level. *Rhabdomys pumilio* appears to express ultradian melatonin rhythms under both lighthing regimes and although the present illuminance levels did not change the mean daily 6-SMT values, the temporal expression of the rhythm seems to be different. The present results illustrate the importance of photophase light intensity in the entrainment of daily rhythms, not only in diurnal species that are evidently awake during the photophase, but also in nocturnal species that are resting or sleeping during the photophase.

Introduction

Nearly all mammals maintain biological synchrony with geophysical time by means of reading and adjusting to daily changes in ambient light and dark, a task that evidently ensures survival in many species (Navara & Nelson 2007; Paul *et al.* 2008). The main biological clock that controls daily or circadian rhythms is situated in the suprachiasmatic nucleus (SCN; Cassone *et al*. 1988; Ralph *et al*. 1990). In vertebrates, entrainment to the light-dark cycle is initiated through ocular light exposure. Photic cues are absorbed in the retina by classical photoreceptors (rods and cones) and by melanopsin-expressing intrinsically photosensitive retinal ganglion cells (ipRGCs); known also as image forming photoreceptors (IFP) and non-image forming photoreceptors (NIFP), respectively. The photic information is relayed, *via* the retino-hypothalamic-tract (RHT), to the SCN (Cassone *et al*. 1988; Ralph *et al*. 1990). It was only after observing distinct light responses, pupil constriction, and normal circadian photoentrainment in mice lacking all functional rods and cones (*rd/rd cl* mice), that the presence of an additional retinal photoreceptor class first became unequivocally clear (Freedman *et al*. 1999; Lucas *et al*. 1999, 2001). However, an increasing amount of evidence suggests that rods and cones do still

contribute to non-visual processes that are related to the SCN (Aggelopoulos & Meissl 2002; Dkhissi-Benyahya 2007; Altimus *et al.* 2010; Gooley *et al.* 2010; van Diepen *et al.* 2013; Weng *et al.* 2013). Not only has it been shown that the rods and cones influence the SCN *via* the ipRGCs (Weng *et al.* 2013), but also that the SCN responds sustainably to light signals in melanopsin deficient mice, solely through the rods and cones (van Diepen *et al.* 2013). It is thus possible that different photoreceptor compositions between species may at least partly explain differences in circadian responses to photic stimuli observed in different species.

One pathway, through which light-dark information is further relayed to individual cells downstream from the SCN, is *via* the rhythmic secretion of melatonin by the pineal gland (Klein & Moore 1979). Melatonin effectively translates and disseminates information on circadian time for daily adjustments and also seasonal adjustments in photoperiodic species (Reiter 1993). Since melatonin production is mostly induced by darkness (Challet 2007), its concentration is highest during the active phase of nocturnally active species and during the sleep/rest phase of diurnally active species. Amongst its various metabolites, 6-sulphatoxymelatonin (6-SMT) can easily be measured from urine and accurately represents the concentration of pineal secreted melatonin (Bojkowski *et al.* 1987). Furthermore, evidence suggests that species possess characteristic sensitivity thresholds in their circadian rhythms, such as the melatonin rhythm, to different light intensities and wavelengths. It is believed that these thresholds most likely reflect the habitat to which the species are adapted and that it may accordingly also reflect specific visual adaptations of the species (Kumar & Rani 1999; Peichl 2005; Zubidat *et al.* 2009, 2010a, 2010b).

In the present study, the responses of different circadian controlled processes to different intensities of lighting during the photophase are evaluated in a nocturnal and in a diurnal rodent. The Namaqua rock mouse (*Micaelamys namaquensis*) and the four striped field mouse (*Rhabdomys pumilio*) are two terrestrial species that display different retinal photoreceptor arrangements and occupy contrasting temporal niches. The daily locomotor activity rhythm of *M. namaquensis* is discussed in Chapter 2 of the present study: *M. namaquensis* is described as a strongly nocturnal species with an activity rhythm that is entrained by the light-dark cycle. Under a 12L: 12D photoperiod, ~99% of the species' activity was expressed during the nighttime and under constant darkness, the mean period length of the endogenous locomotor activity rhythm was 23.89 h. Likewise, in *R. pumilio*, locomotor activity is also robustly entrained by the light-dark cycle and the species has been described both in the laboratory and in the field as being fundamentally diurnal, but with marked activity at dusk and dawn (Schumann *et al.* 2005; Skinner & Chimimba 2005). Moreover, the free-running rhythm of *R. pumilio* under constant darkness ranges between 23.10 h to 24.80 h and under constant light between 24.30 h to 24.79 h (Schumann *et al*. 2005). Furthermore, *M. namaquensis* and *R. pumilio* also have different retinal photoreceptor densities and compositions, which seem to reflect the temporal niche of the species. Please refer to Chapter 3 of the present study for a detailed discussion regarding the retinae of *M. namaquensis* and *R. pumilio*.

The aim of the present study was to evaluate and compare the expression of different photoperiod-mediated processes in *M. namaquensis* and *R. pumilo*, after subjecting mice of each species to different levels of photophase illuminances. Locomotor activity, urine production and

melatonin secretion were selected as parameters of rhythmicity because it is well recognized that these processes are regulated by the light-dark cycle and the SCN (Negoro *et al.* 2012).

Materials and methods

Animal housing

Nine wild Namaqua rock mice (*Micaelamys namaquensis*: four males, five females; mean body mass = 34.9 g) and nine wild striped field mice (*Rhabdomys pumilio*: six males, three females; mean body mass = 35.1 g) were used in this experiment. *Rhabdomys pumilio* was live-trapped at Birha farms near Birha in the Eastern Cape Province (33°22'S, 27°19'E), while *M. namaquensis* was captured in the rocky outcrops of the Soutpansberg region at Goro Game Reserve, Limpopo Province, South Africa (22°58'S, 29°25'E). The animals were kept individually in semi-transparent plastic cages (58 x 38 x 36 cm) in a light (See *Experimental protocol* below) and temperature controlled animal room at an ambient temperature of 25 °C (± 1°C) and approximately 60% relative humidity. Each animal was given a small plastic shelter and tissue paper for nesting material. The mice had *ad libitum* access to food and water and were fed at random times every second or third day to avoid activity entrainment to the feeding schedule. Water and food (parrot seed mix) were topped up and fresh food was replaced. The project was approved by the Animal Ethics Committee of the University of Pretoria, Pretoria, South Africa (EC063-11).

Experimental protocol

One incandescent lamp (white light, 100W, OSRAM, Germany) was positioned centrally above every two neighboring cages, approximately 50 cm above the cage floor level. All of the lamps were coupled to a dimmer circuit and a timer which permitted the light intensity to be manually adjusted and the lights to automatically switch on at 06h00 (start of photophase) and switch off at 18h00 (start of scotophase) each day. The animals were exposed for a period of three weeks to each of four illuminance light cycles (ILCs), during which the light intensity/illuminance of the photophase differed; starting with a 1 lux-ILC, followed by a 10 lux-ILC, a 100 lux-ILC and ending with a 330 lux-ILC. Locomotor activity was recorded throughout the second and third week while urine samples were collected at day 21 of each ILC. Urine samples were used to determine the rate of urine production and for measuring the urinary 6-SMT levels under exposure to a dim photophase (10-lux ILC) and a bright photophase (330 lux-ILC). A hand-held digital light meter (Major Tech; basic accuracy: ± 5% + 10dgt) was used to measure illuminance (lux) at the central floor level of each cage in order to adjust the illuminance manually to the desired level.

Locomotor activity: Recording and data analysis

Activity was recorded using infra-red motion captors (Quest PIR internal passive infrared detector; Elite Security Products (ESP), Electronic Lines, London, UK) that were attached to the top of each cage and detected movement over the whole cage floor area. The number of locomotory movements (activity counts) detected during each minute was stored on a computer

using VitalView software (VitalView™, Minimitter Co., Sunriver, OR, USA; http://www.minimitter.com).

The recorded activity data were analyzed and the daily activity rhythms visually presented as double-plotted actograms using the computer program ActiView (ActiView™, Minimitter Co., Sunriver, OR, USA; http://www.minimitter.com). Activity counts and percentages of activity were compared between the four ILCs as well as within each ILC (light phase vs. dark phase) for all of the mice within a species. The sums of the activity counts per 12 hour light phase and per 12 hour dark phase of each day were calculated for each individual across all four light cycles. These values were then used to estimate the mean number of activity counts (of all individuals combined) for each entire ILC as well as for the light phase and dark phase of each ILC separately. The number of activity counts during either the light or dark phase of each day was further expressed as a percentage against the total number of activity counts for each day and was calculated for all animals individually. The mean of these values within each of the ILCs were then presented as percentages of activity.

Urine production rate: Collection and analysis

During the last day of each ILC (day 21), urine samples were collected from *M. namaquensis* and *R. pumilio* at 3h intervals for the duration of 24h. For this, the animals were transferred to specially constructed 'urine cages' that were then placed at the animals' original positions in the experimental room. These 'urine cages' matched the regular cages (semi-transparent, 58 x 38 x 36 cm) but had stainless steel wire mesh floors that were fixed 2 cm above the cage bottoms.

Each cage also had an open slit at its shortest side, right below the stainless steel mesh, through which a plastic plate was slid to cover the cage floor and that could be removed whenever the screened urine had to be collected. Urine was transferred to Eppendorf tubes using disposable glass Pasteur pipettes, weighed immediately after collection using a Mettler digital scale (Mettler, Zurich, Switzerland) and stored at -30ºC until further analysis. When calculating urine volume (sample mass divided by urine specific gravity), urine specific gravity was assumed to be 1 g/ml (Schoorlemmer *et al.* 2001; Tendron-Franzin *et al.* 2004). Urine volume was converted to indicate the hourly urine production rates (μl/h) and the collective means are presented per species for each ILC as well as for the dark phase and light phase of each ILC, respectively. In addition, the mean values for all of the animals within a species were calculated at each 3h point to present the 24h rhythms in urine production rate.

Urinary 6-sulfatoxymelatonin (6-SMT) levels: Hormone analysis

Urinary 6-SMT was compared between a low level of photophase illuminance (10 lux-ILC) and a high level of photophase illuminance (330 lux-ILC. Urinary 6-SMT concentrations were determined using enzyme-linked immunosorbent assay kits (ELISA, IBL, Hamburg, Germany, cat. no. RE54031). All of the samples were analyzed in duplicate and a standard curve was drawn from seven standard samples of known 6-SMT concentrations (0.0-, 1.7-, 5.2-, 15.6-, 46.7-, 140.0- and 420.0 μl). A volume of 10 μl of each urine sample, containing an unknown amount of antigen, was diluted with 500 μl Assay Buffer. 50 μl of the diluted solution was subsequently incubated for 2h with a known amount of enzyme labelled antigen (50 μl Enzyme Conjugate and 50 μl Melatonin Sulfate rabbit-Antiserum) in a well of the Microtiter Plate.

During incubation, the unknown amount of antigen in the urine sample and the known amount of enzyme labelled antigen competed for the binding sites of the antibodies that coated the Microtiter Plates. The competition reaction was stopped by rinsing the wells with a wash buffer. Further incubation (30 min.) with a TMB (tetramethylbenzidine) Substrate Solution (100 μl) revealed the bound enzymatic activity. 100 μl TMB Stop Solution ended the substrate reaction and the intensity of the developed colour was indicative of the sample antigen concentration. The absorbance of the immunoreaction was measured spectrophotometrically at a wavelength of 450 nm with a universal plate reader and the 6-SMT concentration values determined using the standard curve. The intra- and inter-assay coefficients of variation were 5.2-12.2% and 4.0-6.0%, respectively.

Furthermore, the 6-SMT concentrations were corrected for urine concentration, which was indicated by the level of creatinine in the samples. Creatinine determination was also carried out in microplates, samples analyzed in duplicate and a standard curve drawn using eight standard samples of known createnine concentration (0.0-, 0.05-, 0.1-, 0.5-, 1.0-, 1.5-, 2.0- and 2.5 μl). A volume of 7 μl of a urine sample was incubated in 210 μl of freshly prepared Picric reagent for 2 h in the dark. The latter comprised of one volume of saturated picric acid solution, one volume of alkaline triton solution and 10 volumes of distilled water. In turn, the alkaline triton solution comprised of 4.2 ml triton and 12.5 ml NaOH 1N dissolved in 66.0 ml distilled water. After incubation, the absorbancy of the samples were measured at 492 nm with a universal plate reader and the creatinine concentration values determined using the standard curve.

Statistical analysis

Data and statistical analyses were performed using Microsoft Excel (Microsoft Corp., Redmond, WA, USA) and IBM SPSS Statistics version 21.0 (SPSS Inc., Chicago, IL, USA). Data were not normally distributed and hence were analyzed for statistical significance by generalized linear mixed models; the *post hoc* least significant difference test was used where significant differences were detected. $P<0.05$ were considered significantly different and all values are expressed as means ± standard error (SE). The generalized linear mixed models (GLMM) tested for mean effects of illuminance on the different variables and also tested for the interaction effects of illuminance with the phase of the day (light/dark phase), as well as the interaction effects of illuminance with the time of the day (h), on the different variables. A gamma distribution with an identity link function were selected for the statistical analyses of locomotor activity and urinary 6-SMT, whereas a gamma distribution with a log link function was selected for the analyses of urine production.

Results

Locomotor activity

- **Namaqua rock mouse: *Micaelamys namaquensis***

Micaelamys namaquensis displayed a robust daily locomotor activity rhythm in accordance with the alternation of light and dark, and was invariably nocturnal across all ILCs (See Fig. 4.1 for a representative actogram). The level of photophase illuminance had an overall significant effect

on locomotor activity in *M. namaquensis* ($F_{3,985}$=7.883, P<0.001). The mice were least active during the dimmest ILC and most active during the brightest ILC. During the 1 lux-ILC, the mean number of activity counts were 244.92 ± 15.17; this value differed significantly from the 10 lux-ILC value (327.96 ± 20.38; $F_{3,985}$=7.883, P<0.05), the 100 lux-ILC value (292.38 ± 18.58; $F_{3,985}$=7.883, P<0.05) and the 330 lux-ILC value (358.43 ± 22.34; $F_{3,985}$=7.883, P<0.001; Fig. 4.2). Furthermore, there was a significant difference in the mean activity counts between the 100 lux-ILC and the 330 lux-ILC ($F_{3,985}$=7.883, P<0.05; Fig. 4.2). As expected, *M. namaquensis* was strictly nocturnal during all ILCs and the percentages of nocturnal activity did not differ much between the ILCs, but exposure to the brightest ILC provoked a slight decrease in nocturnal activity (1 lux-ILC: 89.56%; 10 lux-ILC: 92.75%; 100 lux-ILC: 94.28%; 330 lux-ILC: 93.63%). The mean numbers of activity counts were significantly higher during nighttime than daytime under all ILCs (Fig. 4.3).

- **Four striped field mouse: *Rhabdomys pumilio***

Compared to *M. namaquensis*, *R. pumilio* was far more inactive and displayed a less robust locomotor activity pattern. There was also a large inter-individual variation in the daily activity rhythms of *R. pumilio* (Fig. 4.4). In general, half of the mice expressed activity fundamentally around dusk and dawn, but in two of these individuals activity became less concentrated around dusk and dawn only under the 330 lux-ILC (See Fig. 4.4). In three mice, activity was intermittent throughout the 24 day: In two of these mice, activity was slightly elevated around dusk and during the latter part of the dark phase, whereas in the third mouse, activity showed a slight peak around dusk and dawn. Finally, the remaining two mice were primarily active during the daytime, but without any distinguishable dawn and dusk peaks. In *R. pumilio*, the level of

photophase illuminance significantly affected locomotor activity ($F_{3,941}$=2.759, P<0.05). The mean number of daily activity counts was lowest during the 10 lux-ILC (103.31 ± 19.42) and this value differed significantly from the values obtained under the 100 lux-ILC (110.94 ± 19.47; $F_{3,941}$=2.759, P<0.05) and the 330 lux-ILC (111.08 ± 19.49; $F_{3,941}$=2.759, P<0.05), but not the 1 lux-ILC (111.70 ± 19.69; $F_{3,941}$=2.759, P=0.101; Fig. 4.2). Interestingly, *R. pumilio* displayed nearly equal proportions of nighttime and daytime activity percentages during all four ILCs, but with the lowest percentage of nighttime activity occurring during the brightest ILC. The percentages of nocturnal activity were 50.84% (1 lux-ILC), 50.55% (10 lux-ILC), 49.00% (100 lux-ILC) and 47.76% (330 lux-ILC). The mean numbers of activity (day vs. night) did not differ significantly in any of the ILCs (Fig. 4.5).

Urine production rate

- **Namaqua rock mouse: *Micaelamys namaquensis***

The level of illuminance during photophase had a definite, yet non-significant influence on urine production in *M. namaquensis* ($F_{3,186}$=1.335, P=0.264). Exposure to the dimmest light cycle (1 lux-ILC) produced the lowest total mean urine production rates (68.83 ± 23.87 μl/h) and under the 10 lux-ILC the value was nearly the same (69.56 ± 23.82 μl/h). The urine production rate was highest under the 100 lux-ILC (98.46 ± 34.18 μl/h) and second highest under the brightest light cycle (330 lux-ILC: 85.58 ± 29.55 μl/h; Fig. 4.6). Urine production rates were consistently higher during nighttime than daytime in all of the ILCs (Fig. 4.7a). The interaction between illuminance and the phase of day (light/dark) revealed a significant difference between night and day values only during the 1 lux-ILC (light phase: 37.68 ± 14.07 μl/h; dark phase: 125.72 ±

44.59, $F_{3,186}$=6.670, P=0.011) and the 10 lux-ILC (light phase: 45.45 ± 16.33 μl/h; dark phase: 106.46 ± 37.54, $F_{3,186}$=5.889, P=0.016).

The daily rhythms in urine production rate for *M. namaquensis* are displayed in Fig. 4.8. The interactive effect of photophase illuminance with the time of the day did not produce a significant effect in any of the ILCs. Under the 1 lux-ILC, the rate peaked one hour after the onset of the scotophase (19h00: 178.71 ± 79.80 μl/h), the rate then dropped to a moderate level at 22h00 (73.07 ± 29.92 μl/h) and increased again after midnight (01h00: 151.03 ± 6.32 μl/h). From this time point, the rate decreased consistently until it reached its lowest point right after midday (13h00: 20.22 ± 9.03 μl/h); the greatest decline in the rate was between 04h00 and 07h00. Exposure to the 10 lux-ILC produced a pattern in which the urine production rate remained relatively high throughout the night, with the highest value at 04h00 (116.79 ± 48.95 μl/h). The rate then declined over the next six hours towards its lowest point, which was at 10h00 (23.99 ± 11.20 μl/h). Under the 100 lux-ILC, with the exclusion of a decrease after midnight (01h00: 85.15 ± 35.69 μl/h), the rate was again relatively high throughout the night. The urine production rate peaked at 04h00 (168.08 ± 72.44 μl/h) and was at its lowest at 13h00 (51.69 ± 22.23 μl/h). Exposure to the 330 lux-ILC once again yielded relatively high nighttime values but with a dip at 04h00 and peaked slightly earlier than during the preceding two ILCs (22h00: 137.13 ± 56.18 μl/h). The lowest value for this rhythm was again during the middle of the day (13h00: 46.18 ± 20.61 μl/h).

- **Four striped field mouse: *Rhabdomys pumilio***

The level of illuminance of the photophase had a significant influence on urine production rate in *R. pumilio* ($F_{3,173}$=4.104, P=0.008). Interestingly, the response pattern in *R. pumilio* to the four successive ILCs was similar to that of *M. namaquensis* (Fig. 4.6). Exposure to the dimmest light cycle (1 lux-ILC) produced the lowest total mean urine production rate (33.09 ± 7.65 μl/h), exposure to the 10 lux-ILC increased urine production (45.11 ± 10.06 μl/h) and the highest rate was obtained under the 100 lux-ILC (69.45 ± 15.58 μl/h). Subsequently, a further increase in the photophase illuminance to 330 lux resulted in a reduction in the rate of urine production (60.94 ± 14.21 μl/h; Fig. 4.6). Significant differences were obtained between the 1 lux-ILC and the 100 lux-ILC ($F_{3,173}$=4.104, P=0.001), between the 1 lux-ILC and the 330 lux-ILC ($F_{3,173}$=4.104, P=0.007) and furthermore between the 10 lux-ILC and the 100 lux-ILC ($F_{3,173}$=4.104, P=0.019). Daytime urine production rates were higher than nighttime rates at the 1 lux-ILC, the same was true under the 10 lux-ILC, except that this time the difference was significant (light phase: 58.80 ± 14.30 μl/h; dark phase: 34.61 ± 8.76 μl/h, $F_{3,173}$=4.622, P=0.033; Fig. 4.7b). Under the 100 lux-ILC, night and day values were comparable and interestingly, under the highest photophase illuminance cycle the rate was slightly higher during the dark phase than the light phase (Fig. 4.7b).

The daily rhythms in urine production rate for *R. pumilio* are illustrated in Fig. 4.9. The interactive effect of photophase illuminance with the time of the day did not produce significant effects in any of the ILCs. There appeared to be a less distinct contrast in the urine production rate between the light phase and the dark phase compared to *M. namaquensis*. However, the rhythms still displayed one consistent feature, which was that in all of the ILCs the rate peaked

around dawn (Fig. 4.9). During the 1 lux-ILC and the 10 lux-ILC, the rhythm peaked at 07h00 (1 lux-ILC: 60.81 ± 20.70 μl/h; 10 lux-ILC: 83.60 ± 27.29 μl/h). Under the 100 lux-ILC, the rhythm peaked slightly earlier (04h00: 102.22 ± 45.34 μl/h), but during the 330 lux-ILC it once again peaked at 07h00 (93.97 ± 32.00 μl/h). In addition, the rate was relatively high in the late afternoon within the 1 lux-ILC (16h00: 53.63 ± 19.15 μl/h) and also the 10 lux-ILC (16h00: 80.11 ± 28.61 μl/h), but were lower at these time periods in the 100 lux-ILC (16h00: 52.51 ± 17.88 μl/h) and the 330 lux-ILC (39.66 ± 17.59 μl/h).

Urinary 6-sulfatoxymelatonin (6-SMT)

- **Namaqua rock mouse: *Micaelamys namaquensis***

When comparing the response of a low (10 lux) and a high (330 lux) photophase illuminance level on the urinary 6-SMT level, a non-significant effect was observed ($F_{1,54}$=2.317, P=0.134; Fig. 4.10). Nevertheless, the urinary 6-SMT level was higher under dim photophase light exposure (10 lux-ILC: 90.75 ± 11.41 ng/mg) than bright photophase light exposure (330 lux-ILC: 73.21 ± 9.01 ng/mg). The interactive effect of photophase illuminance with the phase (light/dark) of the day did not show any significant effects under either of the two ILCs. Still, nighttime values were consistently higher than daytime values. Under the 10 lux-ILC the nighttime 6-SMT value was 98.94 ± 15.52 ng/mg and the daytime value was 82.55 ± 14.25 ng/mg. Under the 330 lux-ILC the nighttime value was 74.65 ± 11.30 ng/mg and the daytime value 71.76 ± 10.81 ng/mg (Fig. 4.11).

The 24h 6-SMT profile for *M. namaquensis* is illustrated in Fig. 4.12. The interactive effect of photophase illuminance with the time of day significantly affected the urinary 6-SMT level during both ILCs (10 lux-ILC: $F_{7,54}$=6.505, P<0.001; 330 lux-ILC: $F_{7,54}$=6.039, P<0.001). A slight increase in the 6-SMT level followed the onset of the dark phase (19h00: 49.09 ± 11.28 ng/mg) and this was followed by a decrease to the lowest value of the rhythm, which was at 22h00 (28.80 ± 7.68 ng/mg). Subsequently, the level of 6-SMT increased significantly between 22h00 and 01h00 (55.47 ± 11.63 ng/mg, $F_{7,54}$=6.505, P=0.015) and displayed a further significant increase to the peak value at 04h00 (262.41 ± 55.28 ng/mg, $F_{7,54}$=6.505, P<0.001). The level of 6-SMT remained high at 07h00 (219.433 ± 41.78 ng/mg) and a significant decline was observed between 07h00 and 10h00 (35.80 ± 28.26 ng/mg, $F_{7,54}$=6.505, P=0.001). After this, the urinary 6-SMT level remained consistently low throughout the rest of the light phase. Exposure to the 330 lux-ILC yielded a 24h urinary 6-SMT rhythm similar to that of the 10 lux-ILC. The night rise in the 6-SMT level started earlier (from 22h00: 27.91 ± 7.85 ng/mg) yet the rhythm also peaked at 04h00 (152.17 ± 32.59 ng/mg) and this was also followed by a strong decline until 10h00 (36.52 ± 14.72 ng/mg). There was a smaller peak after midday, at 01h00 (80.39 ± 21.13 ng/mg) and the lowest 6-SMT value was observed at 22h00 (27.91 ± 7.85 ng/mg).

- **Four striped field mouse: *Rhabdomys pumilio***

A non-significant effect of photophase illuminance was observed when comparing the response in urinary 6-SMT production under a low (10 lux) and a high (330 lux) photophase illuminance level ($F_{1,39}$=0.008, P=0.930) with the values being 56.76 ± 10.29 ng/mg (10 lux-ILC) and 58.21 ± 12.77 ng/mg (330 lux-ILC; Fig. 4.10). A non-significant effect was obtained for the interactive

effect of photophase illuminance with the phase (light/dark) of the day in both ILCs. Nevertheless, nighttime 6-SMT values were consistently higher (10 lux-ILC: 67.49 ± 16.16 ng/mg; 330 lux-ILC: 64.87 ± 20.16 ng/mg) than daytime values (10 lux-ILC: 46.02 ± 12.74 ng/mg; 330 lux-ILC: 51.55 ± 15.70 ng/mg; Fig. 4.11).

The 24h 6-SMT profiles for *R. pumilio* are illustrated in Fig. 4.13. The interactive effect of photophase illuminance with the time of day had an overall strong, yet non-significant influence on the level of urinary 6-SMT under the 10 lux-ILC ($F_{7,39}$=1.887, P=0.098) and also a non-significant influence in the 330 lux-ILC ($F_{7,39}$=1.030, P=0.426). Subjection to the 10 lux-ILC produced a rhythm in which there was a distinct increase in the 6-SMT level at dusk, between 16h00 (21.87 ± 9.73 ng/mg) and 19h00 (84.47 ± 33.62 ng/mg), and a further increase to the first major peak in the rhythm that was at 22h00 (105.43 ± 46.91 ng/mg). The 6-SMT level then decreased consistently until 04h00 and this was followed by a second peak at dawn that was slightly larger than the first peak (07h00: 121.23 ± 48.25 ng/mg). Subsequently, the level of 6-SMT dropped dramatically and the lowest value was observed right after midday (13h00: 15.98 ± 7.11 ng/mg). Exposure to the 330 lux-ILC yielded a somewhat different 24h 6-SMT profile in which the peak of the rhythm was around dusk (19h00: 110.51 ± 56.78 ng/mg). A distinct decline in 6-SMT followed towards 22h00. From this point, the rhythm steadily increased towards 04h00 and then steadily decreased towards its lowest value, which was at 10h00 (17.51 ± 15.58 ng/mg). Interestingly, this was followed by a steady increase in the urinary 6-SMT right until the peak at dusk.

Discussion

Namaqua rock mice (*Micaelamys namaquensis*) are fundamentally nocturnally active whereas four striped field mice (*Rhabdomys pumilio*) are fundamentally diurnally active. Evidently, these two species are exposed to different levels of illumination in their natural habitats. The two species also possess different retinal photoreceptor arrangements that appear to be complementary to the temporal niches to which each of the species belongs (See Chapter 3). The present results suggest that the photophase illuminance level plays an important role in regulating locomotor activity, renal function and melatonin expression, but that it affects *M. namaquensis* and *R. pumilio* differently.

Daily rhythms in locomotor activity

Results of several studies suggest that species show unique thresholds to different qualities of lighting, which are reflective of the environments the species are adapted to, and that this feature enhances survival (Trent *et al.* 1977; Tast *et al.* 2001; Zubidat *et al.* 2009, 2010a, 2010b). The advantage of distinguishing between different intensities of lighting, within the boundaries of specific thresholds, is best demonstrated in nocturnal species that adjust their activity patterns according to the level of moonlight. Many nocturnal animals react for example, by either avoiding open areas or by reducing their locomotor activity altogether in an attempt to decrease predation risks when they are exposed to certain ranges of lighting that are equivalent to increasing moonlight (Alkon & Saltz 1988; Julien-Laferrière 1997; Topping *et al.* 1999). However, the timing of light exposure is another well-established facet that significantly

influences circadian timing (Pittendrigh & Daan 1976; Sharma *et al.* 1999). Although numerous studies report on the effects that light pulses of varying intensities have on locomotor activity patterns, relatively few studies have investigated the effects of different intensities of lighting throughout the photophase. The results of the present study indicate that *M. namaquensis* and *R. pumilio* possess unique locomotor activity responses to varying illuminance levels of the photophase and that the species' responses are related to their temporal niches under natural conditions. The level of photophase illuminance significantly influenced the mean amplitude of daily activity in both species, but had an overall greater effect in *M. namaquensis* than in *R. pumilo*. In addition, different levels of photophase illuminance did not seem to provoke changes in the pattern of daily activity expression in either of the two species, but this was again more prominent in *M. namaquensis* than in *R. pumilio*.

From the actograms, it was determined that under the range of ILCs used, even at a mere 1 lux of photophase lighting, all individuals of *M. namaquensis* and most individuals of *R. pumilio* possessed defined locomotor activity rhythms. *Micaelamys namaquensis* was predominantly and consistently nocturnal across the range of ILCs. In contrast, a considerable amount of inter-individual variation marked the temporal expression of activity in *R. pumilio*, yet activity was mostly pronounced around dusk and dawn. Nevertheless, each individual of *R. pumilio* generally retained its own characteristic locomotor activity rhythm across the range of ILCs. Therefore, photophase illuminance did not have a definitive influence on the expression of activity over the temporal axis, even though it did affect the amplitude of daily activity. Furthermore, although *R. pumilio* is described as being predominantly diurnal (Krug 2004; Schumann *et al.* 2005; Schradin 2006; Schradin *et al.* 2007), the species only displayed significantly more daytime activity

during the brightest ILC. This may suggest that a photophase illuminance brighter than 100 lux is required for the expression of a robust and predominantly diurnal locomotor activity rhythm in *R. pumilio*, such as is generally observed in the species. Ambient illuminance levels ranges considerably throughout the day and depends upon several factors such as the time of the day, the amount of cloud cover, latitude and season; during the brightest part of the day, sunlight reaches approximately 110 000 lux. It is thus evident that most small diurnal mammals avoid being active during the middle of the day and often make use of pathways that run underneath vegetation cover, not only to escape the heat but also the bright levels of lighting.

According to the effects that the level of photophase illuminance had on the mean amplitude of daily activity, *M. namaquensis* and *R. pumilio* appear to have responded in ways that reflect their temporal niches. Although *R. pumilio* is described as fundamentally diurnal, the species is mostly crepuscular (Krug 2004; Schumann *et al.* 2005; Schradin 2006; Schradin *et al.* 2007) and evidence also reveals that *R. pumilio* is visually adapted for crepuscular living; the species possesses a high density of both rods and cones (See Chapter 3). In its natural environment, *R. pumilio* is thus exposed to great fluctuations in the photoenvironment while it is active. Therefore, by being able to tolerate a wide range of illuminances, the stability and thus the adaptive capacity of the circadian timing of locomotor activity in *R. pumilio* is preserved. In contrast, the active phase of *M. namaquensis* corresponds to smaller variations in the photoenvironment under natural conditions; for example, the illuminance level during full moon nights only reaches approximately 2 lux (Vásquez 1994). This likely explains the greater sensitivity of *M. namaquensis* to the range of photophase illuminances used in the present study. It might also show that light exposure during the sleep phase could play an important role in

regulating the extent to which *M. namaquensis* is active at night. In humans, even low levels of light can be transmitted through closed eyelids. A recent study by Bierman *et al*. (2011) reported on the spectral transmittance of light through the human eyelid and found that there was a high attenuation at short-wavelengths, i.e. the spectral region to which the circadian system is most sensitive. It is reasonable to assume that the retinas of the animals used in the present study received light even while the animals were sleeping and it is possible that their eyelids exhibit similar light transmittance characteristics. Interestingly, *M. namaquensis* was overall significantly less active under the dimmest (1 lux) ILC compared to all other ILCs. It should be noted that a relatively small increase from 1 lux to 10 lux, which is also a relatively dim ILC, yielded an amount of daily locomotor activity comparable to that obtained under the 330 lux-ILC. Therefore, the species was able to distinguish day from night under 1 lux of photophase lighting, but at this level of illuminance stimulation of the pathway resulting in the expression of activity was attenuated. A different correlation has previously been reported in another nocturnal species, the social vole (*Microtus socialis*), whereby the mean daily energy expenditure rates, which is an index of locomotor activity, decreased with increased photophase intensity (Bennett & Ruben 1979; Zubidat *et al.* 2010a). In Macaque monkeys, distinct differences in activity onset time was observed in bright compared to dim light (Takasu *et al.* 2002). However, the bright light presented was an order of magnitude higher than in the current study (3500 lx), the mice in the current study may also require higher light intensities for clear-cut differences to be observed. However, in some cases changes as small as 1 or 2 lx can induce changes in locomotor activity patterns (Kramer & Birney 2001). Whether differences in the densities and distributions of visual and non-visual retinal photoreceptors could be attributed to these species-related differences remains to be elucidated.

Urine production rate

The daily fluctuation in the production of urine is not merely a function of changes in the eating and drinking patterns of an organism across the day, but is a physiological process that is timed by the circadian system (Negoro *et al.* 2012). Several processes that are related to urine production clearly exhibit daily or circadian variations and have been shown to be essential to the well-being of organisms (Kamperis *et al.* 2004; Noh *et al.* 2011). For example, the normal circadian timing of a bladder gap junction protein (connexin43), which regulates changes in bladder capacity, is fundamental to preventing micturition during sleep and thus improving sleep quality (Negoro *et al.* 2012). Another example is that of the relationship between atypical circadian rhythms of arginine vasopressin, a hormone renowned for regulating renal water excretion in mammals, and nocturnal polyuria syndrome (Asplund 1995; Rittig *et al.* 2008). The endogenous timing of urine production is thus expected to ensure that urine production rates are higher during the wake period than during the sleep period. Furthermore, evidence suggests that animals possess different thresholds, in terms of their urine production rhythms, to different photophase intensities (Zubidat *et al.* 2009). In the present study, the photophase illuminance and the time of the day did not show significant interaction effects on the urine production rhythm in either *M. namaquensis* or in *R. pumilio*. Despite this there were distinguishable 24 h urine production rhythms across all four ILCs in *M. namaquensis*. As expected, the rhythms were largely correlated to the species' nocturnal activity rhythm with urine voiding being consistently higher during the night. On the other hand, *R. pumilo* lacked an obvious 24 h urine production rhythm. Nevertheless, urine production rates consistently peaked around dawn and were interestingly only significantly higher during the daytime while subjected to the 10 lux-ILC. In

social voles (*Microtis socialis*), significant daily rhythms of urine excretion were observed at higher as opposed to dimmer photophase light intensities whereas, in blind mole rats (*Spalax ehrenbergi*), the rhythms were significant under both dim and bright photophase intensities (Zubidat *et al.* 2009).

Although the photophase illuminance did not have a significant effect on the mean daily urine production rates in *M. namaquensis*, brighter photophase illuminances seem to cause an increase in the overall daily urine production. A similar trend was also observed in *R. pumilio*; mean daily urine production rates were significantly higher during the two brightest ILCs than during the two dimmer ILCs. It is interesting to note that in both species the mean daily urine production and the mean daily locomotor activity were not correlated across the four ILCs. For example, whereas there was in *M. namaquensis* a significant increase in daily activity from the 1 lux-ILC to the 10 lux-ILC, the daily urine production rate remained unchanged in these two groups. Likewise, in *R. pumilio*, an increase in the photophase illuminance from 1 lux to 100 lux yielded a significant increase in urine production rate, but without any effect on the daily amount of activity. Together these results could indicate that the circadian regulation of locomotor activity and of urine production each possesses their own sensitivity threshold to the level of photophase illuminance. Knowing that daily urine production rhythms result from the integrative workings of several hormones (e.g. arginine vasopressin, aldosterone, plasma renin and natriuretic peptide), which are also regulated by the circadian timing system (Kamperis *et al.* 2004; Noh *et al.* 2011), it is possible that the regulatory pathways of each of these hormones respond differently to varying qualities of lighting and that this caused the dissociation between locomotor activity and urine production, quantitatively.

Urinary 6-sulfatoxymelatonin

Melatonin is produced by the pineal and has been shown to be primarily metabolized to 6-sulfatoxymelatonin in mammalian species (Bojkowski *et al.* 1987; Kennaway *et al*. 1989). Accordingly, 6-sulfatoxymelatonin (6-SMT) is known to be a reliable indicator of pineal melatonin production and rhythmicity (Nowak *et al.* 1987). In rats, light exposure of as low as 0.2 lux during the normal dark phase has been shown to reduce melatonin by 87%, compared to the 94% reduction in melatonin by constant lighting (Dauchy *et al.* 1997). The present results indicate that the photophase illuminance level is an important component in the regulation of melatonin expression in both of the studied species. Only *M. namaquensis* showed significant interactive effects between the photophase illuminance and the time of the day under both ILCs (10 lux and 330 lux). *Micaelamys namaquensis* expressed clear daily rhythms in 6-SMT that were generally low during the day and the early night with a peak at around two hours before the lights went on. It is likely that the period between pineal melatonin production and catabolism until 6-SMT detection in the urine caused a slight (1-2h) delay (Nowak *et al.* 1987). The peak in melatonin might thus have occurred slightly earlier and this would also imply that the contrast between the daytime and nighttime melatonin values is slightly larger in *M. namaquensis* than revealed here. Similar peaks in the melatonin content during the late night have also been observed in different strains of mice and in hamsters (Panke *et al.* 1978; Goto *et al.* 1989). In *M. namaquensis*, brighter photophase lighting actually attenuated the melatonin rhythm and lead to a slightly lower mean urinary melatonin value than observed during the dim ILC. A similar effect has been reported in the strictly fossorial 'blind' mole rat (*Spalax ehrenbergi*), whereby the melatonin rhythm was weakened by brighter photophase lighting conditions, presumably as a

result of an increased stress response in the animals under bright lighting (Zubidat *et al.* 2009). Although *M. namaquensis* is terrestrial and bright daytime lighting therefore less uncommon to the species than it is to *S. ehrenbergi*, the species sleeps and rests in sheltered spaces such as between rock crevices where they are protected from not only predators but also from intense daytime illumination. For this reason, the attenuated melatonin levels under bright lighting conditions may be stress related. Nevertheless, the statistically significant interactive effect between the photophase illuminance and the time of the day under the 330 lux-ILC suggests that the photoreception system of the mice were not yet saturated at this intensity. Also in contrast to what was observed in *M. namaquensis*, Afrotropical stonechats (*Saxicola torquota axillaris*) show higher melatonin levels (with activity peaking in the early and late night) when exposed to bright light, but the light presented to the birds was orders of magnitude higher than in the mice (Kumar *et al.* 2007).

In *R. pumilio*, the intensity of the photophase lighting did not affect the amplitude of the mean amount of melatonin produced across the 24 h day and the nighttime values were also slightly higher than daytime values under both lighting conditions. Interestingly, two relatively different daily rhythms in 6-SMT were observed, but both rhythms appeared to be ultradian. Subjection to the dim ILC resulted in consistently low daytime values, but an abrupt increase in 6-SMT was detected at the transition from day to night and a distinct peak was again observed at dawn. Other than during the dim ILC, the 6-SMT levels steadily increased throughout the day under the bright ILC until it reached the peak of the rhythm at dusk. Levels gradually increased towards the late night and gradually decreased until around 4 h into the light phase. Ultradian patterns of melatonin secretion have also previously been observed in humans and in mice and it has been

suggested that two separate oscillators are foundational to these patterns (Wehr *et al.* 1995; Nakahara *et al.* 2003). Evidence also suggests that daytime and nighttime melatonin is regulated by different processes. At night, neurological signals from the superior cervical ganglia stimulates the rise in pineal melatonin production *via* sympathetic nerves (Moore 1996; Reiter *et al.* 2011). In CBA mice, application of tetrodotoxin, a Na^+ channel blocker, effectively suppresses neurological stimulation of pineal melatonin production by night, but not by day (Nakahara *et al.* 2003). It is therefore suggested that daytime melatonin regulation primarily result from endogenous activation inside the pinealocyte (Li *et al.* 2000). The present results strongly indicate that daytime and nighttime melatonin production is also regulated separately in *R. pumilio*; this is best demonstrated by the prominent rise in daytime 6-SMT levels under the bright ILC, but not the dim ILC. It also reveals that the daytime illuminance level play an essential role in regulating melatonin production. Furthermore, the relatively high levels of 6-SMT during the day while subjected to the bright ILC was not unusual since a similar pattern has been observed in $B6D2F_1$ mice (Li *et al.* 2000). Tast *et al.* (2001) determined that photophase light intensity has a relatively low threshold light intensity (40 lux) in diurnal domestic pigs, whereafter further increases in light intensity does not affect melatonin levels any longer. It is concluded that pigs can differentiate between day and night if the photophase light intensity is 40 lux and the scotophase light intensity is less than 1 lux.

To conclude, the present results indicate that *R. pumilio* and *M. namaquensis* adjust their daily patterns in locomotor activity, urine production and melatonin excretion according to the light dark cycle. It is further demonstrated that the intensity of lighting during the photophase is an essential component in the process of photic entrainment of physiology and behavior,

irrespective of whether the species is active by day or by night. However, *M. namaquensis* and *R. pumilio* were affected differently by the varying photophase light intensities, likely because they are adapted to different temporal niches in their natural environments where they are exposed to very different photoenvironments.

Figures: Daily rhythms in locomotor activity

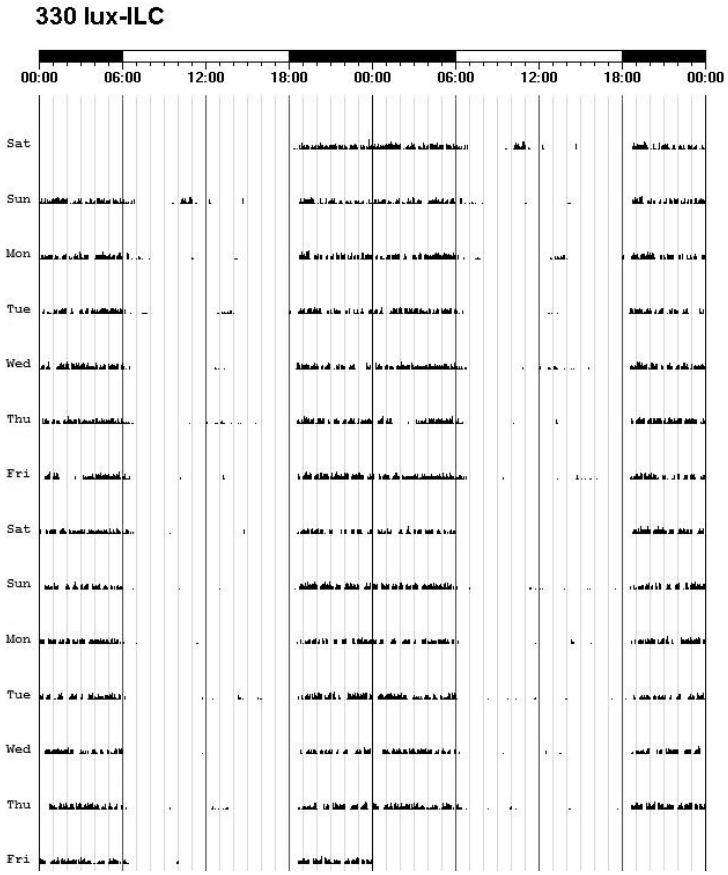

Figure 4.1: A representative actogram for the Namaqua rock mouse (*Micaelamys namaquensis*), showing a strong nocturnal locomotor activity rhythm under an illuminance light cycle (ILC) with a photophase that consisted of 330 lux lighting.

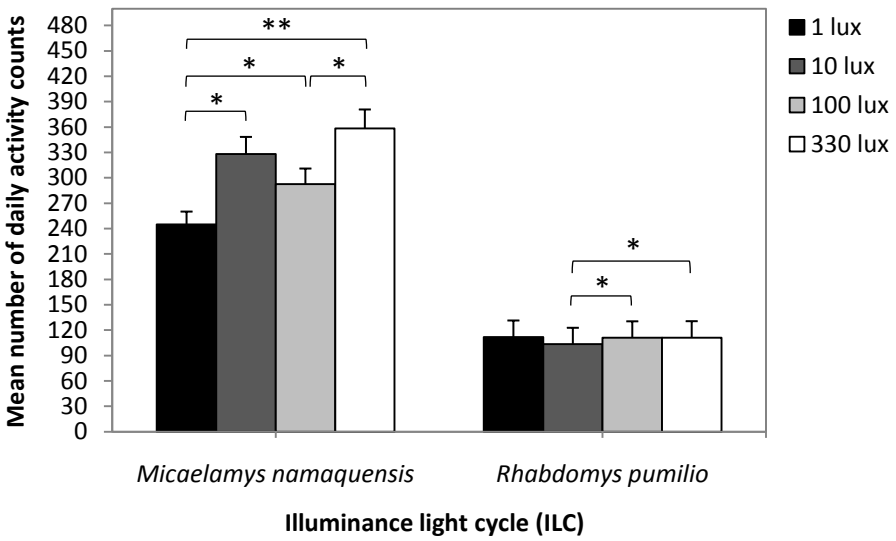

Figure 4.2: Mean number of activity counts in the Namaqua rock mouse (*Micaelamys namaquensis*) and the four striped field mouse (*Rhabdomys pumilio*) under exposure to four successive illuminance light cycles (ILCs). The photophase of each ILC was illuminated using different levels of illuminance (i.e. 1 lux, 10 lux, 100 lux and 330 lux), whereas the scotophase consisted of complete darkness (*=P<0.05; **=P<0.001).

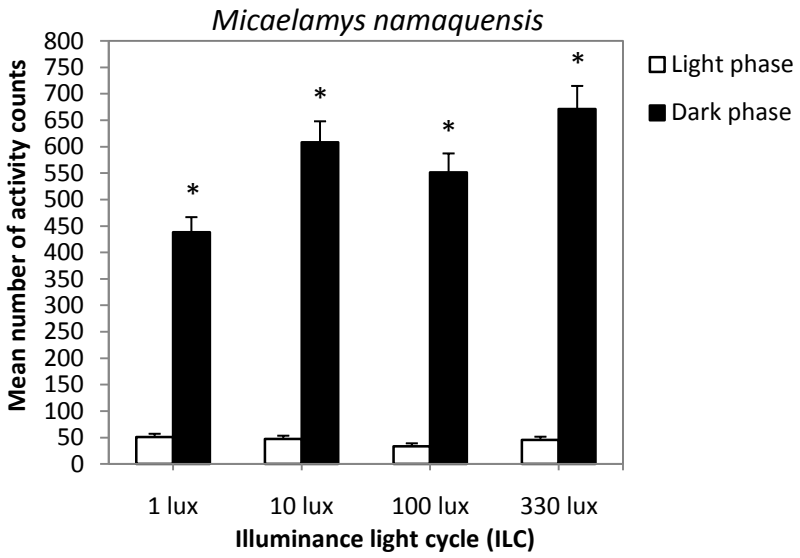

Figure 4.3: The mean number of activity counts, under different illuminance light cycles (ILCs) showing significantly higher nighttime values than daytime values in the Namaqua rock mouse (*Micaelamys namaquensis*; *P<0.001).

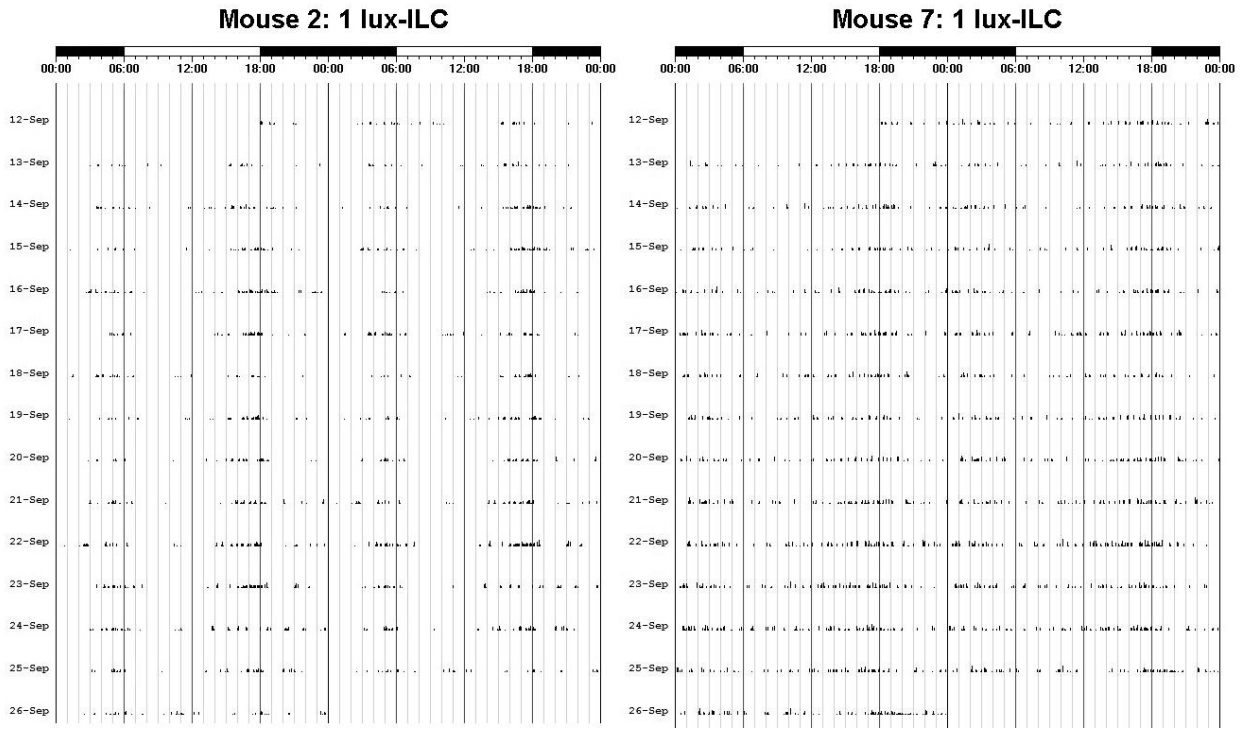

Figure 4.4: Representative actograms for the four striped field mouse (*Rhabdomys pumilio*) under an illuminance light cycle (ILC) with a photophase that consisted of 1 lux lighting. In mouse number 2 (on the left), activity was concentrated around dusk and dawn whereas in mouse number 7 (on the right), activity was expressed intermittently throughout the day but was elevated around dusk and during the period between midnight and dawn.

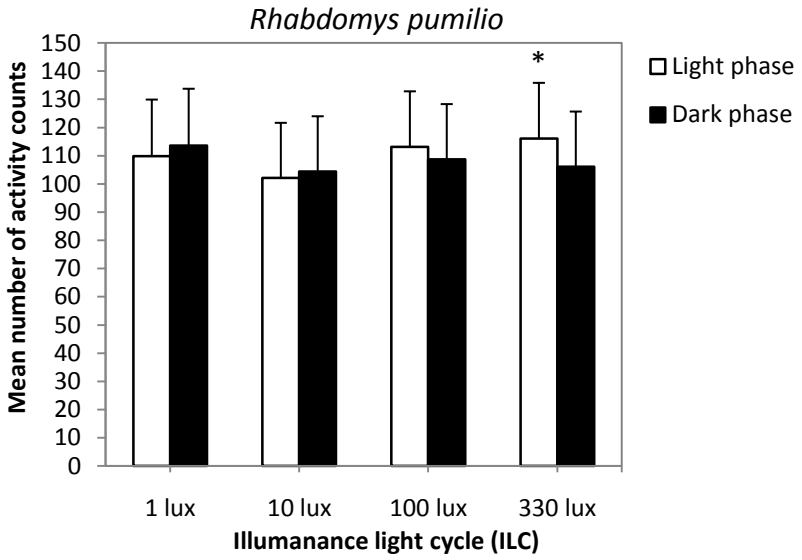

Figure 4.5: The mean number of activity counts, under different illuminance light cycles (ILCs). Daytime values were only significantly higher than nighttime values during the brightest photophase ILC (330 lux) in the four striped field mouse (*Rhabdomys pumilio*; *P<0.001).

Figures: Urine production rate

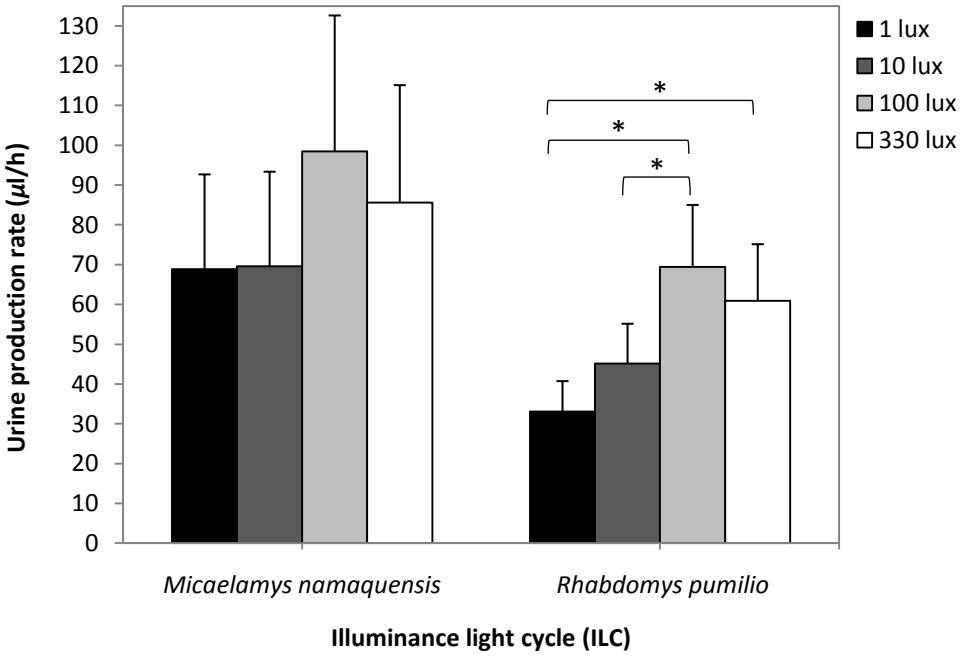

Figure 4.6: Mean urine production rate (μl/h) in the Namaqua rock mouse (*Micaelamys namaquensis*) and the four striped field mouse (*Rhabdomys pumilio*) after exposure to four successive illuminance light cycles (ILCs). The photophase of each ILC was illuminated using different levels of illuminance (i.e. 1 lux, 10 lux, 100 lux and 330 lux) whereas the scotophase consisted of complete darkness (*=P<0.05).

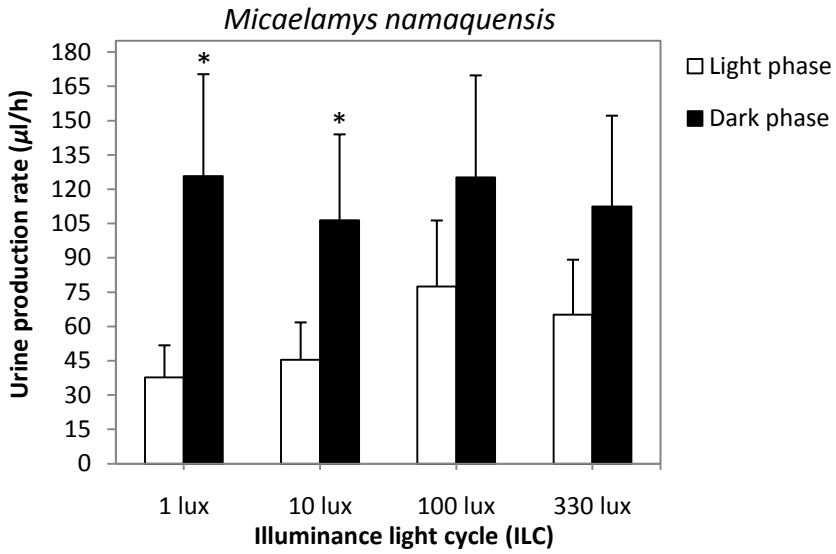

(a)

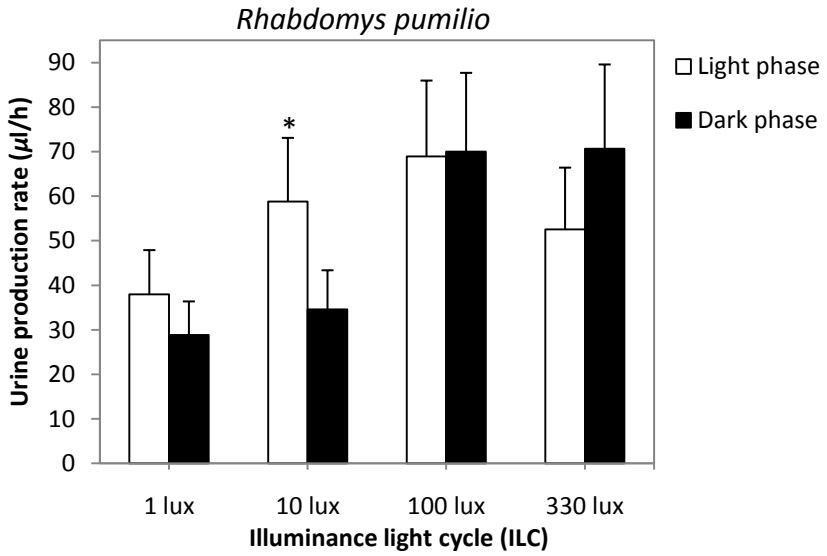

(b)

Figure 4.7: Mean urine production rate (μl/h) in (a); the Namaqua rock mouse (*Micaelamys namaquensis*) and (b); the four striped field mouse (*Rhabdomys pumilio*) after exposure to four successive illuminance light cycles (ILCs), showing daytime and nighttime values separately. In *M. namaquensis*, the rate was consistently higher during the night and in *R. pumilio*, the rate was higher during the day only under the 1 lux-ILC and 10 lux-ILC (*P<0.05).

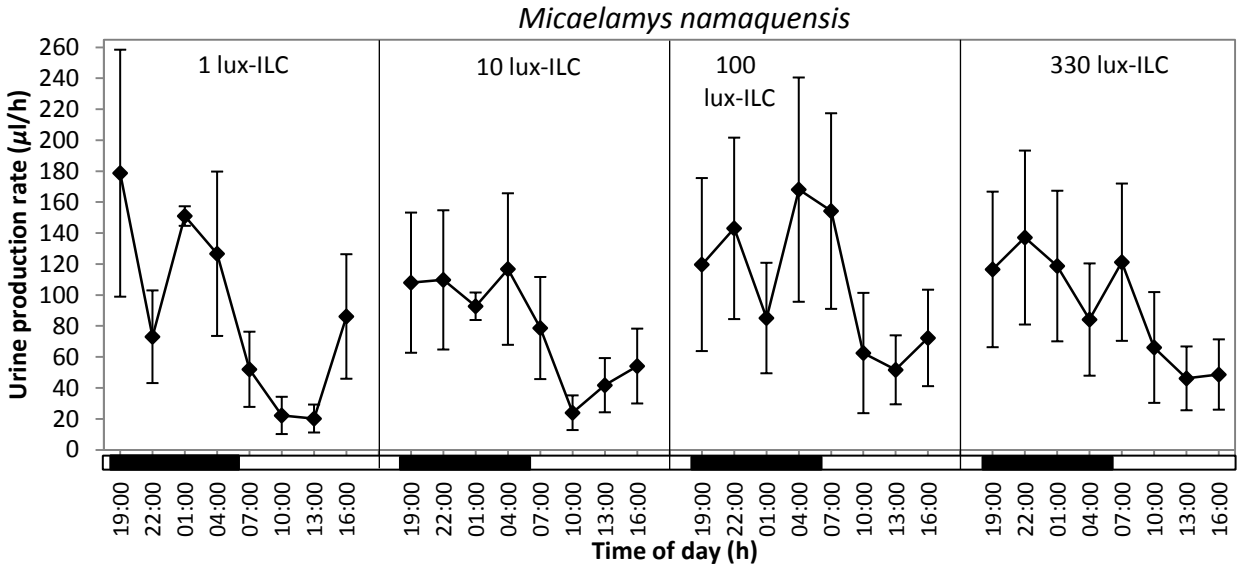

Figure 4.8: The 24h rhythms of urine production rate (μl/h) in the Namaqua rock mouse (*Micaelamys namaquensis*) for four illuminance light cycles (ILCs). The black and white bars at the bottom of each graph indicate the dark- and light phases of each ILC, separately

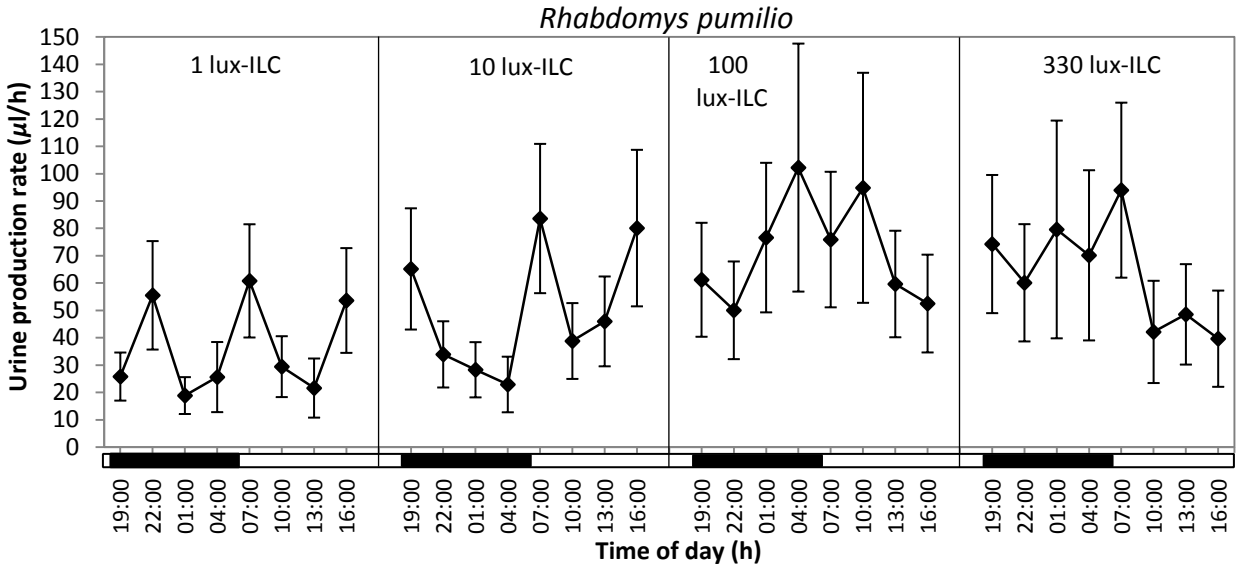

Figure 4.9: The 24h rhythms of urine production rate (μl/h) in four the striped field mouse (*Rhabdomys pumilio*) for four illuminance light cycles (ILCs). The black and white bars at the bottom of each graph indicate the dark- and light phases of each ILC, separately.

Figures – Urinary 6-sulfatoxymelatonin (ng/mg):

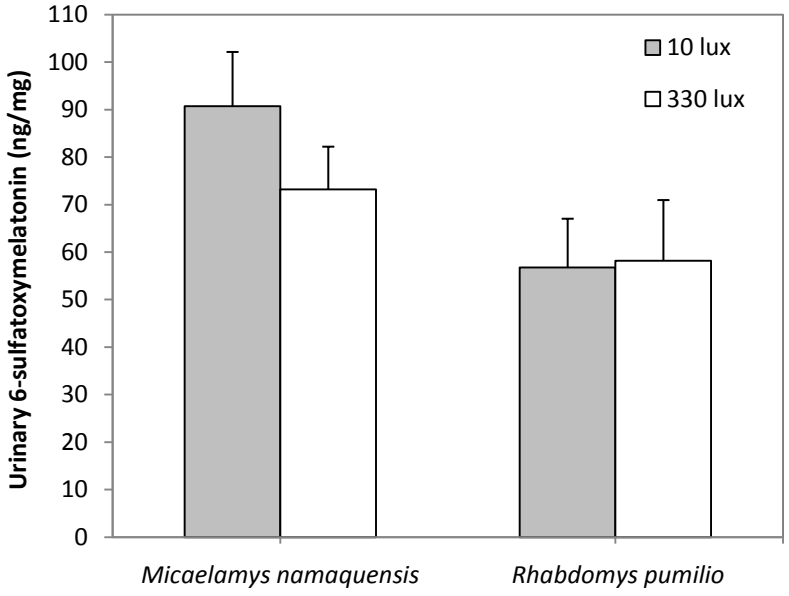

Figure 4.10: Mean urinary 6-sulfatoxymelatonin values (6-SMT; ng/mg) in the Namaqua rock mouse (*Micaelamys namaquensis*) and in the four striped field mouse (*Rhabdomys pumilio*) after exposure to a dim illuminance light cycle (10 lux-ILC) and a bright illuminance light cycle (330 lux-ILC).

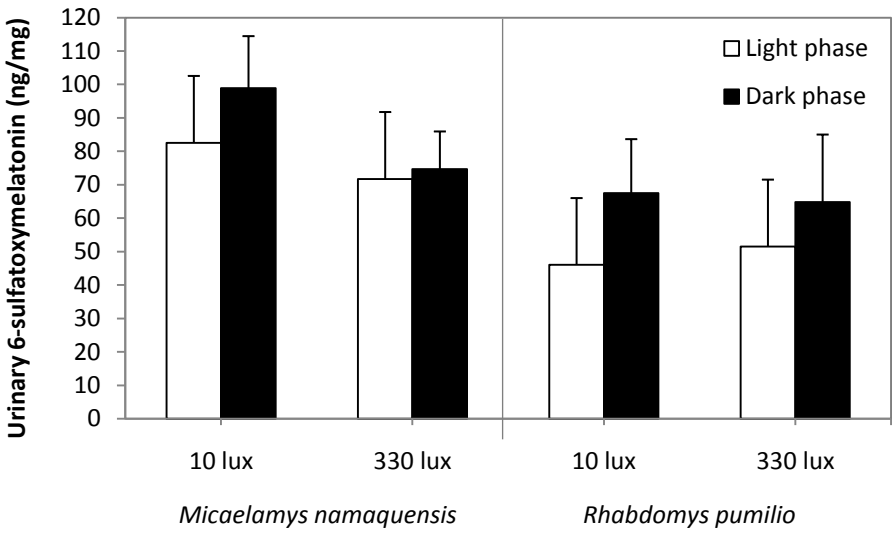

Figure 4.11: Mean urinary 6-sulfatoxymelatonin values (6-SMT; ng/mg) during the daytime and nighttime in the Namaqua rock mouse (*Micaelamys namaquensis*) and the four striped field mouse (*Rhabdomys pumilio*) after exposure to a dim illuminance light cycle (10 lux-ILC) and a bright illuminance light cycle (330 lux-ILC).

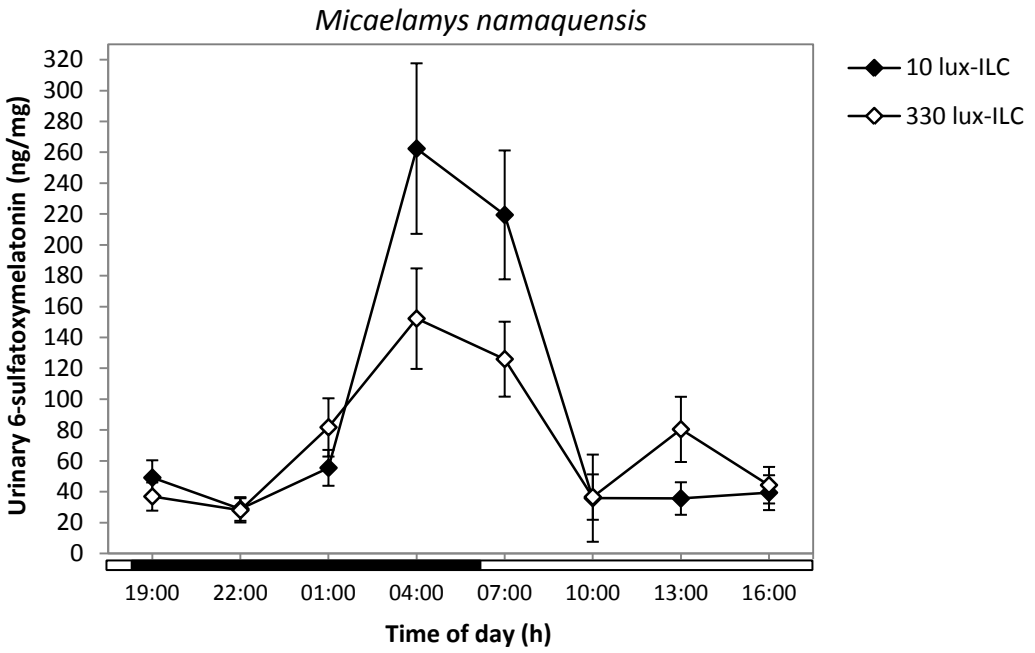

Figure 4.12: The 24h rhythms of urinary 6-sulfatoxymelatonin (6-SMT; ng/mg) in the Namaqua rock mouse (*Micaelamys namaquensis*) under a dim illuminance light cycle (10 lux-ILC) and a bright illuminance light cycle (330 lux-ILC). The black and white bars at the bottom of each graph indicate the dark- and light phases of each ILC, separately.

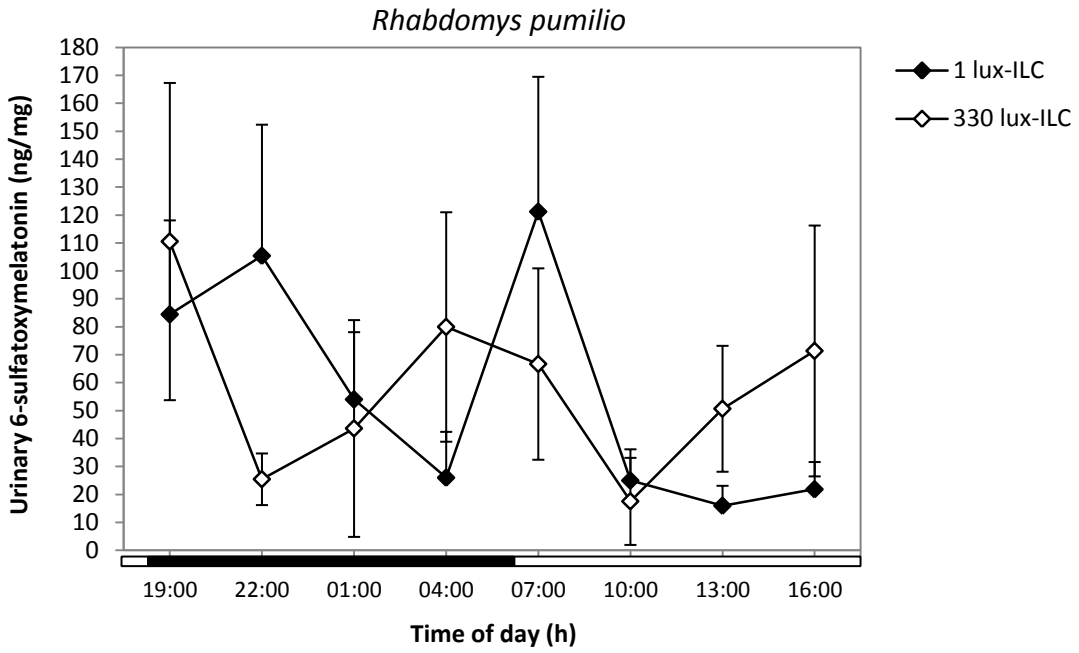

Figure 4.13: The 24h rhythms of urinary 6-sulfatoxymelatonin (6-SMT; ng/mg) in the four striped field mouse (*Rhabdomys pumilio*) under (a): a dim illuminance light cycle (10 lux-ILC) and under (b): a bright illuminance light cycle (330 lux-ILC). The black and white bars at the bottom of each graph indicate the dark- and light phases of each ILC, separately.

CHAPTER 5:

EFFECTS OF PHOTOPHASE WAVELENGTH LIGHTING ON LOCOMOTOR ACTIVITY, URINE PRODUCTION, URINARY 6-SULFATOXYMELATONIN AND CORTICOSTERONE IN A NOCTURNAL AND A DIURNAL SOUTH AFRICAN RODENT

Abstract

The effects of near-monochromatic short- (blue: 465 – 470 nm), medium- (green: 515 - 520 nm) and long wavelength (red: 625 – 630 nm) photophase lighting on daily rhythms of locomotor activity, urine production, urinary 6-sulfatoxymelatonin (6-SMT) and corticosterone were investigated and compared between the nocturnally active rodent, the Namaqua rock mouse (*Micaelamys namaquensis*) and the diurnally active four striped field mouse (*Rhabdomys pumilio*). *Micaelamys namaquensis* expressed between ~85-97% nocturnal activity while *R. pumilio* expressed between ~31-51% nocturnal activity; photophase light spectra significantly affected the amplitude of the overall daily activity only in *R. pumilio*. Both species exhibited ~10% more diurnal activity under the long wavelength photophase. In *M. namaquensis*, the reason for this appears to be related to the visual capabilities of the species whereas in *R. pumilo*, higher stress levels under the short- and medium wavelengths appears to have restricted daytime activity. Irrespective of the temporal niches of the species, short wavelength photophase lighting significantly attenuated the overall mean daily urine production rates while values under medium and long wavelengths were similar. In *M. namaquensis*, significant daily 6-SMT rhythms were only detected under short- and medium wavelengths and in *R. pumilio*, only under short wavelengths. In both species, wavelength was inversely correlated to the level of 6-SMT and corticosterone. Significant daily corticosterone rhythms were observed across all light schedules except under the long wavelength photophase for *R. pumilio*. Although near-monochromatic blue photophase lighting greatly increased overall daily 6-SMT levels, it also produced the highest stress responses in the two species. Together, these results illustrate that photophase wavelength

is a fundamental component in the photo-entrainment of daily rhythms in diurnal as well as in nocturnal rodent species.

Introduction

Most organisms respond and adjust cellular, physiological and behavioral functions to the light-dark cycle by means of an endogenous time-keeping system (Navara & Nelson 2007; Paul *et al.* 2008). The importance of the circadian timing system and its entrainment by light-dark cycles is best demonstrated by the prevalence of increased health risks and in some cases disturbances within ecological systems, which emerges from disruptions of the circadian clock network and desynchronization in timing of the different biological rhythms (Bird *et al*. 2004; Navara & Nelson 2007; Haim *et al*. 2010; Rotics *et al*. 2011; Haim & Portnov 2013). Variations within several components of the light-dark cycle, such as intensity, spectral wavelength, duration and timing of the light exposure, are able to affect the circadian timing system (Gorman *et al.* 2003; Duffy & Wright 2005; Aral *et al*. 2006; Zubidat *et al.* 2009, 2010b). Moreover, species exhibit specific sensitivity thresholds in their circadian or daily rhythms to different qualities of lighting, which most likely reflects the ecological niches that the species is adapted to (Kumar & Rani 1999; Peichl 2005; Zubidat *et al.* 2009, 2010a, 2010b). Accordingly, animals may actually exhibit stress responses when they are subjected to certain qualities of lighting that differs substantially from their natural photoenvironments. Although artificial light at night (ALAN) is one of the most effective ways to disrupt the balance of the circadian timing system and to induce stress, evidence suggests that certain qualities of light during the photophase can also act as a stressor (Zubidat *et al.* 2007; 2009).

In mammals, the photic information reaches the central clock mechanism (i.e. the suprachiasmatic nucleus; SCN) via the retinohypothalimc-tract (RHT), after being absorbed in the retina by classical photoreceptors (rods and cones) and by melanopsin-expressing intrinsically photosensitive retinal ganglion cells (ipRGCs; Cassone *et al*. 1988; Ralph *et al.* 1990). Although the ipRGCs are independently light sensitive (Freedman *et al*. 1999; Lucas *et al*. 1999, 2001), an increasing amount of evidence suggests that rods and cones contribute to non-visual processes that are related to the SCN (Aggelopoulos & Meissl 2002; Dkhissi-Benyahya 2007; Altimus *et al.* 2010; Gooley *et al.* 2010; van Diepen *et al.* 2013; Weng *et al.* 2013). This raises the possibility that different photoreceptor compositions between species may at least partly explain different circadian responses to photic stimuli between species. Circadian cues are subsequently projected from the SCN to the pineal through efferent connections, which leads to the synthesis or suppression of melatonin (Moore 1996; Reiter *et al.* 2011). Melatonin production is mostly induced by darkness and the circulating melatonin plays a central role in regulating daily adjustments and also seasonal adjustments in photoperiodic species (Reiter 1993; Challet 2007). One of its metabolites, 6-sulphatoxymelatonin (6-SMT), can easily be measured from urine and accurately represents the concentration of pineal secreted melatonin (Bojkowski *et al.* 1987). In terms of the spectral composition of the light source, short wavelengths (~420-500nm, blue light) are deemed to be the most potent spectra for suppressing melatonin in both humans and animals (Brainard *et al.* 2001, Thapan *et al.* 2001; Rahman *et al.* 2008). However, at sufficient intensities, light with longer wavelengths are also able to suppress melatonin (Hanifin *et al.* 2006).

The Namaqua rock mouse (*Micaelamys namaquensis*) and the four striped field mouse (*Rhabdomys pumilio*) occupy different temporal niches and also possess different retinal photoreceptor arrangements, which seem to reflect the temporal niche of the species (See Chapter 3 of the present thesis). In Chapter 2 of the present study, *M. namaquensis* is described as a strongly nocturnal species (~99% nocturnal activity under a 12L: 12D photoperiod), with an activity rhythm that is entrained by light-dark cycles and a free running period length of 23.89 h under constant darkness. Likewise, in *R. pumilio*, locomotor activity is also robustly entrained by light-dark cycles and the species has been described both in the laboratory and in the field as being fundamentally diurnal, but with marked activity at dusk and dawn (Schumann *et al.* 2005; Skinner & Chimimba 2005). Under constant darkness, *R. pumilio* expresses a cycle length of between 23.10 h to 24.80 h and under constant light, between 24.30 h to 24.79 h (Schumann *et al*. 2005).

The aim of the present study was to evaluate and compare the expression of different photoperiod-mediated processes in *M. namaquensis* and *R. pumilo* after subjecting them to three near-monochromatic lights (short-, medium-, and long wavelength) of the same irradiance, during the photophase. Locomotor activity, urine production and urinary 6-sulfatoxymelatonin (6-SMT) expression were selected as variables for measuring rhythmicity because it is well recognized that these processes are regulated by light-dark cycles and the SCN (Negoro *et al.* 2012). Furthermore, urinary corticosterone levels were also measured in order to evaluate stress responses of the study species under the designated light schedules.

Materials and methods

Animal housing

Nine wild male *M. namaquensis* (mean body mass = 41.1 g) and nine wild male *R. pumilio* (mean body mass = 38 g) were used in this experiment. *Rhabdomys pumilio* was live-trapped in June at Birha farms near Birha in the Eastern Cape Province (33°22'S, 27°19'E), while *Micaelamys namaquensis* was captured in the rocky outcrops of the Soutpansberg region at Goro Game Reserve, Limpopo Province, South Africa (22°58'S, 29°25'E). The animals were kept individually in semi-transparent plastic cages (58 x 38 x 36 cm) in a light (12L: 12D; ~400 lux) and temperature controlled animal room at an ambient temperature of 25 °C (± 1°C) and approximately 60% relative humidity. Each animal was given a small plastic shelter and tissue paper for nesting material. The mice had *ad libitum* access to food and water and were replaced or added at random times every second or third day to avoid activity entrainment to the feeding schedule. Water and food (parrot seed mix) were topped up and fresh food was replaced. The project was approved by the Animal Ethics Committee of the University of Pretoria, Pretoria, South Africa (EC063-11).

Experimental protocol

Double sets of LED strip lights (RGB, DC12V, 14.4 W/m, IP55, SMD 5050, 30 LED/m) were installed over the adjoining animal cages approximately 50 cm above the cage floor level. Four 5 meter LED strips were used for this purpose, each with an RGB controller and remote that

allowed selection of the specific color of light to be used. The strip lights were connected to a timer and were automatically switched on at 06:00h (start of photophase) and switched off at 18:00h (start of scotophase) each day. The animals were exposed for a period of three weeks to each of three wavelength light cycles (WLCs) at nearly the same irradiance levels (~0.2-0.3 W/m^2), during which different near-monochromatic colors of light illuminated the photophase; starting with the short-WLC (blue: 465 – 470 nm), followed by the medium-WLC (green: 515 - 520 nm) and ending with the long-WLC (red: 625 – 630 nm). Animals were given one week to acclimatize to the light conditions and locomotor activity was recorded throughout the second and third week whilst urine samples were collected at day 21 of each ILC. Urine samples were used to evaluate the rate of urine production and for measuring urinary 6-SMT levels and urinary corticosterone levels.

Locomotor activity: Recording and data analysis

Activity was recorded using infra-red motion captors (Quest PIR internal passive infrared detector; Elite Security Products (ESP), Electronic Lines, London, UK) that were attached to the top of each cage and detected movement over the whole cage floor area. The number of locomotory movements (activity counts) detected during each minute was stored on a computer using VitalView software (VitalView™, Minimitter Co., Sunriver, OR, USA; http://www.minimitter.com).

The recorded activity data were analyzed and the daily activity rhythms visually presented as double-plotted actograms using the computer program ActiView (ActiView™, Minimitter Co.,

Sunriver, OR, USA; http://www.minimitter.com). Activity counts and percentages of activity were compared between the four ILCs as well as within each ILC (light phase vs. dark phase) for all of the mice within a species. The sums of the activity counts per light phase and per dark phase of each day were calculated for each individual across all three testing light cycles at the end of each experimental period to a desired wavelength. These values were then used to estimate the mean number of activity counts (of all individuals combined) for each entire ILC as well as for the light phase and dark phase of each ILC separately. The number of activity counts during either the light or dark phase of each day was further expressed as a percentage against the total number of activity counts for each day and was calculated for all animals individually. The mean of these values within each of the ILCs were then presented as percentages of activity.

Urine production rate: Collection and analysis

During the last day of each ILC (day 21), urine samples were collected from *M. namaquensis* and *R. pumilio* at 3h intervals over a 24h period. For this, the animals were transferred to specially constructed 'urine cages' that were then placed at the animals' original positions in the experimental room. These 'urine cages' matched the regular cages (semi-transparent, 58 x 38 x 36 cm) but had stainless steel wire mesh floors that were fixed 2 cm above the cage bottoms. Each cage also had an open slit at one of its short sides, right below the stainless steel mesh, through which a plastic plate was slid to cover the cage floor and that could be removed whenever the screened urine had to be collected. Urine was transferred to Eppendorf tubes using disposable glass Pasteur pipettes, weighed immediately after collection using a Mettler digital scale (Mettler, Zurich, Switzerland) and stored at -30ºC until further analysis. When calculating

urine volume (sample mass divided by urine specific gravity), urine specific gravity was assumed to be 1 g/ml (Schoorlemmer *et al.* 2001; Tendron-Franzin *et al.* 2004). Urine volume was converted to indicate the hourly urine production rates (μl/h) and the collective means are presented per species for each ILC as well as for the dark phase and light phase of each ILC respectively. In addition, the mean values for all of the animals within a species were calculated at each 3h point to present the 24h daily rhythms in urine production rate.

Urinary 6-sulfatoxymelatonin (6-SMT) levels: Hormone analysis

Urinary 6-SMT concentrations were determined using enzyme-linked immunosorbent assay kits (ELISA, IBL, Hamburg, Germany, cat. no. RE54031). All of the samples were analyzed in duplicate and a standard curve was drawn from seven standard samples of known 6-SMT concentrations (0.0-, 1.7-, 5.2-, 15.6-, 46.7-, 140.0- and 420.0 μl). A volume of 10 μl of each urine sample, containing an unknown amount of antigen, was diluted with 500 μl Assay Buffer. 50 μl of the diluted solution was subsequently incubated for 2h with a known amount of enzyme labelled antigen (50 μl Enzyme Conjugate and 50 μl Melatonin Sulfate rabbit-Antiserum) in a well of the Microtiter Plate. During incubation, the unknown amount of antigen in the urine sample and the known amount of enzyme labelled antigen competed for the binding sites of the antibodies that coated the Microtiter Plates. The competition reaction was stopped by rinsing the wells with a wash buffer. Further incubation (30 min.) with a TMB (tetramethylbenzidine) Substrate Solution (100 μl) revealed the bound enzymatic activity. 100 μl TMB Stop Solution ended the substrate reaction and the intensity of the developed colour was indicative of the sample antigen concentration. The absorbance of the immunoreaction was measured

spectrophotometrically at a wavelength of 450 nm with a universal plate reader and the 6-SMT concentration values determined using the standard curve. The intra- and inter-assay coefficients of variation were 5.2-12.2% and 4.0-6.0%, respectively.

Urinary corticosterone levels: Hormone analysis

Urinary corticosterone concentrations were determined by enzyme immunoassay. The wells of microtiter plates were coated with 150 μl coating solution that comprised of 66 μl Protein A solution (3.47 mg), 1.59 g Na_2CO_3 and 1 L H_2O. Subsequently, each of the wells was saturated with 250 μl bovine serum albumin (BSA) solution (2.42 g Trihydroxyaminomethane, 17.923 g NaCl, 10 g BSA, 1 g NaN_3 and 1 L H_2O; pH 7.5). Aliquots (50 μl) of the diluted samples (1:20), standard samples and quality controls were pipetted in duplicates into each of the microtiter plate wells. 50 μl of biotin-label solution (Corticosterone-3-CMO:BSA) and 50 μl antibody solution were added and the plates incubated overnight at 4ºC. The wells were then washed four times with a wash buffer (300 μl). Subsequently, a solution of 150 μl of a streptavidin-peroxidase solution in assay buffer was added to each of the wells and the samples were left to incubate for 45 minutes on a plate shaker. Again, this was followed by four washes in a wash buffer (300 μl). 150 μl tetramethylbenzidine peroxide substrate solution was then added to each well and the samples left to incubate for 30 to 60 minutes on a plate shaker. A stop solution (50μl H_2SO_4, 2 mol/L) was added to stop the enzyme reaction. Optical density was measured at a dual wavelength (450 nm and 620 nm). The intra assay coefficient of variation was 6.4-7.1% and the inter assay coefficient of variation was 14.2-16.4%. Parallelism was also tested and yielded a slope of <1%.

Creatinine

The urinary 6-SMT and corticosterone concentrations were furthermore corrected for urine concentration, which was indicated by the level of creatinine in the samples. Creatinine determination was also carried out in microplates, samples analyzed in duplicate and a standard curve drawn using eight standard samples of known createnine concentration (0.0-, 0.05-, 0.1-, 0.5-, 1.0-, 1.5-, 2.0- and 2.5 μl). A volume of 7 μl of a urine sample was incubated in 210 μl of freshly prepared Picric reagent for 2 h in the dark. The latter comprised of one volume of saturated picric acid solution, one volume of alkaline triton solution and 10 volumes of distilled water. In turn, the alkaline triton solution comprised of 4.2 ml triton and 12.5 ml NaOH 1N dissolved in 66.0 ml distilled water. After incubation, the absorbancy of the samples were measured at 492 nm with a universal plate reader and the creatinine concentration values determined using the standard curve.

Statistical analysis

Data and statistical analyses were performed using Microsoft Excel (Microsoft Corp., Redmond, WA, USA) and IBM SPSS Statistics version 21.0 (SPSS Inc., Chicago, IL, USA). Data were not normally distributed and hence were analyzed for statistical significance by generalized linear mixed models; the *post hoc* least significant difference test was used where significant differences were detected. $P<0.05$ were considered significantly different and all values are expressed as means ± standard error (SE). Generalized linear mixed models tested for mean effects of spectral wavelength on the different variables and also tested for the interaction effects

of spectral wavelength with the phase of the day, as well as the interaction effects of spectral wavelength with the time of the day (h) on the different variables.

Results

Daily rhythms in locomotor activity

- **Namaqua rock mouse: *Micaelamys namaquensis***

Micaelamys namaquensis displayed a robust daily locomotor activity rhythm in accordance with the alternation of light and dark and was primarily nocturnal (See Fig. 5.1a for a representative actogram). Under the short-WLC and under the medium-WLC, the mice were invariably nocturnal, except in one of the mice, in which activity was at times spread out to the photophase under the medium-WLC (Fig. 5.1a). The locomotor activity patterns were less robust under the long-WLC. Although all of the mice were mostly nocturnal under the long-WLC, five of the mice displayed intermittent activity during the light phase as well (Fig. 5.1b). Locomotor activity did not show significant photophase wavelength variations ($F_{2,665}$=0.287, P=0.751); the mean amount of daily activity counts was highest under the short-WLC, shortest under the medium-WLC and at an intermediate under the long-WLC (Fig. 5.2). *Micaelamys namaquensis* exhibited nocturnal activity during all WLCs. Nocturnality was the strongest under the short-WLC (96.62%) and comparably strong under the medium-WLC (95.46%), while the percentage of nocturnal activity was nearly 10% lower under the long-WLC (85.38 ± 15.84%; Fig. 5.3). Nighttime activity counts were significantly higher than daytime activity counts during all WLCs (Fig. 5.3).

- **Four striped field mouse: *Rhabdomys pumilio***

Compared with *M. namaquensis*, *R. pumilio* was less active and hence displayed a less robust locomotor activity pattern. A large inter-individual variation in the daily activity rhythms of *R. pumilio* was observed. Nevertheless, activity was mostly elevated around dusk and dawn (Fig. 5.4). In general, three of the mice expressed activity only around dusk and dawn. In four other mice, activity peak around dusk and dawn, but was then also expressed to various extents throughout the daytime or nighttime. The remaining individual expressed activity intermittently throughout the light phase, but without any observable peaks at dusk or dawn. Interestingly, in two of the mice, there was a clear decrease in activity as the photophase wavelength increased and in a third mouse the opposite pattern was observed. In *R. pumilio*, light spectra had a significant effect on locomotor activity, with the mice being most active during the light schedule with the short wavelength photophase and least active during the light schedule with the medium wavelength photophase (Fig. 5.2). The mice displayed significantly more activity counts during exposure to the short-WLC (120.37 ± 19.51) than during exposure to the medium-WLC (77.56 ± 19.00; $F_{2,622}$=25.818, P<0.001) and the long-WLC (89.32 ± 19.20; $F_{2,622}$=25.818, P<0.001). The difference between the mean activity counts of the medium-WLC and the long-WLC was also significant ($F_{2,622}$=25.818, P<0.05). *Rhabdomys pumilio* was consistently more active during the daytime and similar to *M. namaquensis*, the percentage of nocturnal activity did not differ much between the short- (41.04%) and the medium-WLC (41.96%), while exposure to the long-WLC caused a nearly 10% decrease in nocturnal activity (31.11%; Fig. 5.5). Significantly higher activity counts were obtained during daytime than during nighttime in all three of the light cycles (Fig. 5.5).

Urine production rate

- **Namaqua rock mouse: *Micaelamys namaquensis***

The spectral exposure of photophase light had an overall significant effect on the rate of urine produced by *M. namaquensis* ($F_{2,139}$=6.488, P=0.002). The rate was lowest in response to the short-WLC (228.54 ± 48.50 μl/h) and in comparison to this, the rate was significantly higher in response to the medium-WLC (302.53 ± 50.71 μl/h, $F_{2,139}$=6.448, P=0.004; Fig. 5.6). Exposure to the long-WLC resulted in a production rate of 295.49 ± 49.81 μl/h, which did not differ significantly from the production rate in response to the medium-WLC ($F_{2,139}$=6.448, P=0.800), but was significantly higher than under the short-WLC ($F_{2,139}$=6.448, P=0.004; Fig. 5.6). The interactive effect between spectral wavelength and the phase of the day (light/dark) yielded significant differences in urine production rates, which were consistently higher during nighttime than daytime. Differences between night and day values were significant in the short-WLC and the medium-WLC, but not under the long-WLC (Fig. 5.7a).

The daily rhythms of urine production rate in *M. namaquensis* are depicted in Fig. 5.8. The interactive effect of photophase wavelength with the time of the day showed significant effects under the short-WLC ($F_{7,139}$=6.121, P<0.001) and the medium-WLC ($F_{7,139}$=3.067, P=0.005), but not under the long-WLC ($F7_{,139}$=1.771, P=0.0.98). Under the short-WLC there was a significant increase in the rate during the dusk period (19:00h: 231.57 ± 50.00 μl/h, $F_{7,139}$=6.121, P<0.001) and this was followed by a further rate increase until 22:00h. At this point during the nighttime the rate remained roughly constant until it reached its maximum peak at 04:00h (338.29 ± 87.38 μl/h) from where it declined consistently. Values were comparatively low during

daytime. The urine production rate showed a relative peak at 13:00h after which it declined significantly to the lowest point of the rhythm, which was in the late afternoon (16:00h: 82.07 ± 52.58 μl/h, $F_{7,139}$=6.121, P<0.001). Under exposure to the medium-WLC, a significant increase in the rate occurred between 19:00h (232.30 ± 50.09 μl/h) and 22:00h (462.62 ± 115.02 μl/h, $F_{7,139}$=3.067, P=0.034), at which point the rhythm peaked. A moderate decrease in the rate followed the peak and the rate remained consistent until 04:00h. Subsequently, the rate decreased consistently towards the lowest point, which was in the earlier afternoon (13:00h: 173.43 ± 52.68 μl/h). Under the long-WLC, urine production was always relatively high compared to the 24-h rhythms obtained under the short- and medium-WLCs. The rate was similarly low in the earlier afternoon (13:00h: 231.69 ± 80.23 μl/h) and in the early night (22:00h: 229.27 ± 49.99 μl/h). The largest increased was during the night, between 22:00h and 01:00h (357.96 ± 76.71 μl/h) and the peak of the rhythm was at 04:00h (383.69 ± 82.62 μl/h), and this was followed by a consistent decline towards the low point at 13:00h.

- **Four striped field mouse: *Rhabdomys pumilio***

The spectral exposure of photophase light had an overall significant effect on the rate of urine production ($F_{2,104}$=3.931, P=0.023). Even though compared to *M. namaquensis*, urine production rate of *R. pumilio* (the smaller of the two species) was consistently lower, the spectral wavelength affected urine production similarly in both species (Fig. 5.6). The urine production rate was lowest under exposure to the short-WLC (84.38 ± 26.21 μl/h) and in comparison it was significantly higher under exposure to the medium-WLC (121.92 ± 26.42 μl/h, $F_{2,104}$=3.931, P=0.024). Long-WLC exposure resulted in a rate of 121.24 ± 26.18 μl/h, which was not significantly different to the rate under the medium-WLC ($F_{2,104}$=3.931, P=0.966), but which

was significantly higher than under the short-WLC ($F_{2,104}$=3.931, P=0.014; Fig. 5.6). Daytime urine production rates were higher than nighttime rates under all WLCs. The interactive effect between spectral wavelength and the phase of the day (light/dark) revealed a significant difference between nighttime and daytime urine production rates only under the short-WLC (light phase: 105.42 ± 28.43 μl/h; dark phase: 63.33 ± 26.61 μl/h, $F_{1,104}$=6.159, P=0.015; Fig. 5.7b).

The urine production daily rhythm of *R. pumilio* is depicted in Fig. 5.9. In *R. pumilio*, the interactive effect of photophase wavelength with the time of the day did not significantly affect the urine production rate in any of the WLCs. Under the short-WLC there were two periods during which the urine production rate showed a pronounced rise; once at dawn, between 04:00h and 07:00h (07:00h: 99.21 ± 33.51 μl/h) and again in the afternoon between 13:00h and 16:00h (16:00h: 162.84 ± 52.09 μl/h). The rate was consistently low throughout the night (19:00h to 04:00h) with the lowest point at 04:00h (47.89 ± 44.21 μl/h). Then, it slightly increased between 10:00h and 13:00h. Under the medium-WLC, the urine production rate was highest after dusk (19:00h: 156.59 ± 43.19 μl/h). A sharp decline followed in the early night to the lowest point of the rhythm at 22:00h (61.73 ± 46.30 μl/h). Through the rest of the night, the rate was slightly higher and at dawn, between 04:00h and 07:00h, the rate increased again. Exposure to the long-WLC produced an interesting 24h urine production rhythm. The lowest point of the rhythm was in the early night at 22:00h (79.28 ± 28.59 μl/h). From this time point, the rate steadily increased over the next 12h until 10:00h (117.97 ± 32.68 μl/h). Subsequently, the largest increase in the rate occurred at midday, between 10:00h and 13:00h, with the latter time point also being the acrophase (13:00h: 190.72 ± 55.45 μl/h).

Urinary 6-sulfatoxymelatonin (6-SMT)

- **Namaqua rock mouse: *Micaelamys namaquensis***

Significant effects of the photophase exposure to different spectral wavelengths on urinary 6-SMT levels in *M. namaquensis* ($F_{2,66}$=8.489, P=0.001) were noted. An increase in the wavelength of the light cycle induced a decrease in the mean 6-SMT levels from 108.69 ± 18.52 ng/mg (short-WLC), to 81.81 ± 13.97 ng/mg (medium-WLC) and to 41.18 ± 12.19 ng/mg (long-WLC; Fig. 5.10). The latter value differed significantly from the valued obtained under the short-WLC ($F_{2,66}$=8.489, P=0.001) as well as from the medium-WLC value ($F_{2,66}$=8.489, P=0.005) and no significant differences were obtained between the short- and medium-WLCs ($F_{2,66}$=8.489, P=0.181). Exposure to the short-WLC yielded 6-SMT levels that were significantly higher at night (145.09 ± 30.36 ng/mg) than during the day (72.28 ± 17.52 ng/mg; $F_{2,66}$=4.882, P=0.031; Fig. 5.11a). Under medium-WLC exposure, daytime values were slightly higher compared to nighttime values, and as a result to long-WLC exposure, nighttime values were slightly higher compared to daytime values (Fig. 5.11a).

The 24h urinary 6-SMT rhythm for *M. namaquensis* is depicted in Fig. 5.12. The interactive effect of photophase wavelength with the time of the day significantly affected the 6-SMT level under exposure to the short-WLC ($F_{7,66}$=2.691, P=0.016) and medium-WLC ($F_{7,66}$=2.460, P=0.026), but not to the long-WLC ($F_{7,66}$=0.549, P=0.794). There was a decrease in the 6-SMT levels in the early night between 19:00h and 22:00h and this was followed by a significant surge in the 6-SMT level towards the maximum value, which was at 01:00h (236.36 ± 88.95 ng/mg, $F_{7,66}$=2.691, P=0.029). From this point there was a moderate decline in the 6-SMT level until

07:00h and a further significant decline until 10:00h ($F_{7,66}$=2.691, P=0.022). After this, the 6-SMT levels remained low between the lowest point of the rhythm, which was at 10:00h (38.11 ± 13.82 ng/mg), and 16:00h (40.09 ± 18.22 ng/mg) and finally, a small peak followed the onset of the dark phase (19:00h: 114.72 ± 39.14 ng/mg). Subjection to the medium-WLC produced a 6-SMT rhythm in which there was also one smaller peak and one larger peak. The 6-SMT levels were low during the early night (19:00h) but increased towards 04:00h and remained high until its peak value at 07:00h (161.53 ± 55.06 ng/mg). Subsequently, a large decrease in the level occurred between 07:00h and 10:00h and there was a smaller peak at 16:00h (87.02 ± 20.76 ng/mg). Under the long-WLC, the 6-SMT rhythm was not pronounced, yet as in the preceding two WLCs the largest increase in the level of 6-SMT occurred between 22:00h (23.53 ± 12.36 ng/mg) and 04:00h (70.42 ± 36.82 ng/mg), with the latter being the maximum value. The level remained comparatively high until 07:00h (65.79 ± 34.31 ng/mg) from where it decreased.

- **Four striped field mouse: *Rhabdomys pumilio***

Statistical analyses detected significant effects of photophase exposure to spectral wavelength, on urinary 6-SMT levels ($F_{2,73}$=10.064, P<0.001). Similar to *M. namaquensis*, an increase of the photophase wavelength was also associated with a decrease in the mean 6-SMT levels in *R. pumilio* (Fig. 5.10). The 6-SMT value decreased significantly from the short-WLC (69.59 ± 14.02 ng/mg) to the medium-WLC (31.45 ± 5.29 ng/mg, $F_{2,73}$=10.064, P=0.012) and again significantly from the medium to the long-WLC (16.23 ± 2.68 ng/mg, $F_{2,66}$=8.489, P=0.009). The latter value was also significantly different from the value obtained under the short-WLC ($F_{2,73}$=10.064, P<0.001; Fig. 5.10). Nighttime 6-SMT values were much higher than daytime values under the short-WLC, yet the difference was not significant. The the same was true for the

medium-WLC, while under the long-WLC nighttime and daytime values were the same (Fig. 5.11b).

The 24h urinary 6-SMT rhythm in *R. pumilio* is depicted in Fig. 5.13. Only under the short-WLC did the interactive effect between the photophase wavelength exposure and the time of the day, significantly affect the 6-SMT levels ($F_{7,73}$=5.260, P<0.001). Under the medium-WLC, the interactive effect was not significant ($F_{7,73}$=1.828, P=0.095) and under the long-WLC there was a strong yet non-significant effect ($F_{7,73}$=2.110, P=0.053). During the short-WLC, the 6-SMT level was 37.58 ± 11.56 ng/mg in the early night (19:00h), it decreased slightly towards 22:00h and then increased again until 01:00h. There was a significant increase in 6-SMT between 01:00h and 04:00h (265.95 ± 105.03 ng/mg, $F_{7,73}$=5.260, P=0.043), with the latter value also being the peak (acrophase) value of the rhythm. After this, the 6-SMT level declined sharply until the onset of the light phase at 07:00h and showed a further significant decrease towards the lowest point in the rhythm, which was at 10:00h (9.19 ± 2.94 ng/mg, $F_{7,73}$=5.260, P=0.005). Finally, the 6-SMT level gradually increased over the next six hours. After exposure to the medium-WLC, 6-SMT levels remained roughly uniform throughout the 24h day but with the exception of a significant increase between 01:00h (14.71 ± 22.87 ng/mg) and 04:00h (105.03 ± 89.71 ng/mg, $F_{7,73}$=1.828, P=0.039). The 6-SMT level was also relatively high at 07:00h (63.27 ± 21.49 ng/mg). Under the long-WLC, the 6-SMT rhythm was relatively level compared to that of the preceding two WLCs. Nighttime values were overall slightly higher and the strongest increase in the 6-SMT level was between 04:00h (22.35 ± 7.63 ng/mg) and the peak of the rhythm, which was at 07:00h (42.55 ± 14.39 ng/mg).

Urinary corticosterone

- **Namaqua rock mouse: *Micaelamys namaquensis***

Significant effects of photophase exposure to wavelength spectrum on urinary corticosterone levels were detected in *M. namaquensis* ($F_{2,86}$=13.984, P<0.001). Overall, urinary corticosterone levels decreased as the spectral wavelength increased (Fig. 5.14**)**. There was a significant decrease from the short-WLC (6.31 ± 0.98 μg/mg, $F_{2,86}$=13.984, P=0.012) to the medium-WLC (3.83 ± 0.65 μg/mg, $F_{2,86}$=13.984, P=0.002) and again a significant decrease to the long-WLC (2.26 ± 0.54 μg/mg, $F_{2,86}$=13.984, P=0.002). In addition, urinary corticosterone level differed significantly between the short- and long-WLCs ($F_{2,86}$=13.984, P<0.001; Fig. 5.14). Phase-related variation in urinary corticosterone had a significant effect under the short-WLC ($F_{1,86}$=17.029, P<0.001) and long-WLC ($F_{1,86}$=0.006, P=0.936), but not the medium-WLC ($F_{1,86}$=5.980, P=0.017). Under the short-WLC, the mean nighttime corticosterone value was significantly higher than the daytime value, under the medium-WLC night and day values were similar and under the long-WLC, the nighttime value was once again significantly higher (Fig. 5.15a).

The 24h corticosterone rhythm for *M. namaquensis* is illustrated in Fig. 5.16. Significant effects were observed for the time of day within all three WLCs (short-WLC: $F_{7,86}$=4.677, P<0.001; medium-WLC: $F_{7,86}$=3.558, P=0.002; long-WLC: $F_{7,86}$=2.922, P=0.009). During the short-WLC, urinary corticosterone levels peaked after the onset of the dark phase (19:00h: 18.23 ± 5.01 μg/mg). Subsequently, corticosterone levels decreased significantly until 22:00h (6.76 ± 2.09 μg/mg, $F_{7,86}$=4.677, P=0.036), showed a relative increase at 01:00h and then it decreased

significantly until 04:00h (2.87 ± 0.84 μg/mg, $F_{7,86}$=4.677, P=0.019). Corticosterone levels remained low at 07:00 and rose significantly between 07:00h and 10:00h to a value of 2.87 ± 0.84 μg/mg ($F_{7,86}$=4.677, P=0.020) after which, levels remained low. Subjection to the medium-WLC produced a rhythm during which the urinary corticosterone level was moderately high in the early night (19:00h: 3.94 ± 1.12 μg/mg; 22:00h: 3.56 ± 1.02 μg/mg). There was a moderate peak after midnight, from where the level then decreased significantly until 04:00h (2.11 ± 0.67 μg/mg, $F_{7,86}$=3.558, P=0.027) and continued to decrease until right after the start of the light phase at 07:00h. The rhythm had its maximum corticosterone value at 10:00h (8.94 ± 2.71 μg/mg), which was followed by a significant decrease towards 13:00h (1.78 ± 0.60 μg/mg, $F_{7,86}$=3.558, P=0.009). Exposure to the long-WLC produced an even 24h urinary corticosterone rhythm. Levels were highest during the early night (19:00h: 3.56 ± 1.27 μg/mg; 22:00h: 3.41 ± 0.98 μg/mg) and subsequently decreased gradually over the next twelve hours to the lowest point (10:00h: 1.19 ± 0.51 μg/mg) from where it increased again until nighttime.

- **Four striped field mouse: *Rhabdomys pumilio***

Exposure to photophase wavelength spectrum had a significant effect on urinary corticosterone levels in *R. pumilio* ($F_{2,65}$=13.666, P<0.001). It is interesting to note that the levels were higher for *R. pumilio* than the ones obtained for *M. namaquensis* and as in *M. namaquensis*, an increase in the spectral wavelength caused *R. pumilio* urinary corticosterone levels to decrease (Fig. 5.14). Corticosterone levels decreased significantly from the short-WLC (15.97 ± 2.03 μg/mg) to the medium-WLC (7.33 ± 0.89 μg/mg, $F_{2,65}$=13.666, P<0.001) and displayed a further decrease under the long-WLC (5.31 ± 0.62 μg/mg) but this was not significant ($F_{2,65}$=13.666, P=0.054). There was also a significant difference in urinary corticosterone level between the short- and

long-WLCs ($F_{2,65}$=13.666, P<0.001; Fig. 5.14). There was no significant phase-related variation in urinary corticosterone for any of the spectral groups. Under the short-WLC, urinary corticosterone was slightly higher during the dark phase than the light phase (Fig. 5.15b). In contrast, daytime values were highest under the medium-WLC and also under the long-WLC (Fig. 5.15b).

The 24h corticosterone rhythm for *R. pumilio* is illustrated in Fig. 5.17. Significant effects were observed for the time of day under the short-WLC ($F_{7,65}$=2.745, P=0.015), but not under the medium-WLC ($F_{7,65}$=0.672, P=0.695) or long-WLC ($F_{7,65}$=0.773, P=0.612). Exposure to the short-WLC produced a relatively high corticosterone level during the early night (19:00h: 13.05 ± 4.36 μg/mg), which was followed by a decrease in the level at 22:00h. Urinary corticosterone then increased until the first distinct peak in the rhythm, which was at 04:00h (33.79 ± 11.28 μg/mg). A sharp decreased in the level followed and this lead to the lowest point of the rhythm that was at 10:00h (6.14 ± 1.60 μg/mg). There was a significant increase in the urinary corticosterone level between 13:00h and 16:00h (31.58 ± 8.18 μg/mg; $F_{7,65}$=2.745, P=0.010) that resulted in a second major peak. Under the medium-WLC, the urinary corticosterone level was again relatively high right after dusk and again this was followed by a decrease in the level until 01:00h. After this point, there was a consistent increase over the next six hours until right after the onset of the light phase where a second peak was observed (07:00h: 9.27 ± 3.10 μg/mg). The urinary corticosterone level was again low at 10:00h a third peak could be observed right after midday (13:00h: 9.69 ± 2.52 μg/mg). Exposure to the long-WLC produced a 24h urinary corticosterone rhythm that was similar to the rhythm obtained under the medium-WLC, yet more even. Levels were once again moderately high during the early night and subsequently decreased

gradually until its lowest point at 01:00h (3.26 ± 0.97 μg/mg) from where it increased again until right after the onset of daytime (07:00h: 6.10 ± 1.77 μg/mg). Finally, the highest value was observed after midday (13:00h: 7.92 ± 2.65 μg/mg).

Discussion

Daily rhythms in locomotor activity

The nocturnally active *M. namaquensis* and the diurnally active *R. pumilio* are two terrestrial species that possess different retinal photoreceptor arrangements, which are complementary to the particular temporal niche of each respective species (Chapter 3 of this thesis). The present study indicated that short-, medium- and long wavelengths of near-monochromatic photophase lighting exposure effectively entrained locomotor activity in the two species. It was further observed that the spectral composition had a significant impact on the mean amplitude of daily activity in *R. pumilio*, but not in *M. namaquensis*. In contrast to *M. namaquensis*, the social vole (*Microtus socialis*), which is also a nocturnal species, displayed mean daily energy expenditure rates (an index of locomotor activity) that were significantly lower during short wavelength (479 nm) than during long wavelength (697 nm) photophase lighting (Bennett & Ruben 1979; Zubidat *et al.* 2010b). Furthermore, both short and long wavelengths LAN (light at night) exposure dramatically decreased the daily energy expenditure in *M. socialis* (Zubidat *et al.* 2011). Thompson *et al*. (2008) suggests that the combined input of cones with ipRGCs contributes to negative masking, such as that observed in *M. socialis*. Therefore, a study of the photoreceptor composition of *M. socialis* and a comparison with *M. namaquensis* may potentially be insightful.

In nocturnal field mice (*Mus booduga*), light pulses of different wavelengths (480, 548 and 649 nm) produced phase shifts with similar directions, but not similar magnitudes; phase shifts were maximal at 548 nm (Geetha & Subbaraj 1996). Interestingly, *M. namaquensis* was distinctly nocturnal under all three WLCs, but expressed around 10% more daytime activity during the long-WLC (~85% nocturnal activity), than during the preceding two WLCs (~95% nocturnal activity). The reason for this appears to be related to the visual capabilities of the species. Although humans possess trichromatic vision, most mammals are typically dichromatic, i.e. they possess one retinal cone type (S-cones), which is sensitive to short wavelengths of light (maximally sensitive to either blue, violet, or near-ultraviolet light) and a second retinal cone type (generally denoted as M/L-cones) that is sensitive to medium and long wavelengths (maximal sensitivity ranging from green to red depending on the species; Jacobs 1993; Peichl 2005). In Chapter 3 of the present thesis, *M. namaquensis* is reported as being dichromatic; immunocytochemistry revealed the presence of S-cones as well as M/L-cones, but as expected for a nocturnal species, the densities of both cone types were low. For example in *M. namaquensis*, the M/L-cone density peak was ~5066/mm^2 whereas in *R. pumilio*, the average M/L-cone density was over five times more (~28302/mm^2). For this reason, *M. namaquensis* might not have perceived the long wavelength lighting as clearly and therefore became slightly more active during the photophase of the long-WLC. In agreement with this, a similar increase in daytime activity has been observed in *M. namaquensis* under a lighting regime consisting of constant darkness (See Chapter 2 of the present thesis).

Rhabdomys pumilio was significantly more active during the day than at night and was consequently more affected by the different photophase light spectra than *M. namaquensis*.

Short-wavelength and medium-wavelength exposure produced the highest and the lowest mean amounts of daily activity, respectively, but with the percentages of diurnal activity being similar (~58%) during both of these WLCs. In rodents, peak sensitivities are mostly reported as falling in the blue-green range (480-530 nm; McGuire *et al.* 1973; Boulos 1994). Interestingly, in many species, ultraviolet radiation is capable of phase shifting circadian rhythms (Brainard *et al.* 1994; Amir & Robinson 1995). Since melanopsin, the photopigment of the ipRGCs, is maximally sensitive to short wavelengths of light (~420nm-500nm, blue light), it has the most dramatic influence on the circadian timing system (Brainard *et al.* 2001, Thapan *et al.* 2001; Rahman *et al.* 2008). For this reason, exposure to LAN, particularly at short wavelengths, is considered profoundly adverse to health (Bird *et al.* 2004; Navara & Nelson 2007; Haim *et al.* 2010; Rotics *et al*. 2011; Haim & Portnov 2013). Conversely, short wavelength photophase lighting, or even light rich in short wavelengths, have been shown to increase sympathetic nervous activity, alertness and cognitive functions in humans (Noguchi & Sakaguchi 1999; Beaven & Ekström 2013). In agreement with this, the present results revealed that near-monochromatic blue light exposure during the photophase caused a distinct stimulation of the SCN pathway that leads to mobile activity. Unlike LAN exposure, it would appear that exposure to short wave light during the photophase enhanced the locomotor activity rhythm in *R. pumilio*. However, it is interesting to note that at the same time, the short-WLC caused a pronounced stress response in *R. pumilio* (See the section entitled *Urinary corticosterone* below) and in essence the stimulator that induced activity (near-monochromatic short wavelength light) was also the stressor. Furthermore, as in *M. namaquensis*, *R. pumilio* also expressed around 10% more diurnal activity during the long-WLC (~69% diurnal activity) than during the preceding WLCs. However, the relative increase in nocturnal activity under the short- and medium-WLCs seems to be stress

related as *R. pumilio* was dramatically less stressed while being subjected to short wavelength lighting during the photophase (See the section entitled *Urinary corticosterone* below).

Urine production rate

Urine production is regulated by the circadian timing system and consequently expresses clear daily rhythms (Negoro *et al.* 2012). Evidently, several processes that are related to urine production also express distinct daily or circadian variations (Kamperis *et al.* 2004; Noh *et al.* 2011). Unsurprisingly, the cyclical nature of these processes is essential to the well-being of organisms (Asplund 1995; Rittig *et al.* 2008; Negoro *et al.* 2012). The endogenous timing of urine production is thus expected to ensure that urine production rates are attenuated during the sleep phases of organisms as a means to improve sleep quality. The present results revealed significant interaction effects of photophase wavelength and the time of the day, on the urine production rhythm in *M. namaquensis* only under short- and medium wavelength photophase exposure. This agrees with previous data in another nocturnal species (*M. socialis*) where a distinct rhythm was observed in urine production under short wavelength, but not long wavelength monochromatic photophase lighting (Zubidat *et al.* 2010b). The production of urine largely correlated with the nocturnal activity rhythm of *M. namaquensis* and was consistently higher during the night than during the day. However, the difference between the day rate and night rate was not significant under the long-WLC and most likely reflected the ~10% increase in diurnal activity that was observed under this lighting regime. In contrast to *M. namaquensis*, *R. pumilo* did not display an obvious 24 h urine production rhythm under any of the WLCs, but under the short-WLC and the medium-WLC urine production peaked before dusk and after dusk,

respectively. Under the long-WLC the peak was observed right after midday. As in *M. namaquensis*, the contrast between the day and night values reflected the activity rhythm of the species and was higher by day than by night but the difference was only significant under the short-WLC.

The effect of light spectra on the overall mean daily urine production rates showed very similar responses in *M. namaquensis* and *R. pumilio*. Near-monochromatic blue photophase lighting significantly attenuated the overall amount of urine produced across the day, irrespective of the temporal niche of the species. It suggests the involvement of the short wavelength sensitive ipRGCs and further confirms the idea that urine production is physiologically timed by the circadian system, which in turn is regulated by the quantity and quality of light (Negoro *et al.* 2012).

Urinary 6-sulfatoxymelatonin

Several qualities of light including intensity, spectral wavelength, duration and timing of the light exposure, affect the circadian rhythm of melatonin synthesis (Gorman *et al.* 2003; Duffy & Wright 2005; Aral *et al*. 2006; Zubidat *et al.* 2009, 2010b). There is also a large variation in the capacity of light to suppress melatonin rhythms among different species. From the present results, it is clear that the spectral wavelength of the photophase is an important component in the regulation of melatonin production in both of the studied species. Nighttime melatonin production is not only altered by light exposure during darkness, but also by the quality of daytime lighting (Hashimoto *et al.* 1997; Griffith & Minton 1992; Park & Tokura 1999).

Although numerous studies have investigated the effects of light exposure during the night on melatonin production, few studies have looked at the effects of different qualities of photophase lighting on melatonin production. Light exposure consisting of short wavelengths (~420-500nm, blue light) are deemed to be the most potent spectra for suppressing melatonin in both humans and animals (Brainard *et al.* 2001, Thapan *et al.* 2001; Rahman *et al.* 2008). However, at very high intensities, light with longer wavelengths (>600 nm) are also able to suppress pineal nighttime melatonin production (Hanifin *et al.* 2006). In the present study we reported that in *M. namaquensis*, significant manifested interactive effects between the photophase wavelength and the time of the day under exposure to the short-WLC and the medium-WLC, but not under exposure to the long-WLC. The shape of the 6-SMT rhythms of *M. namaquensis* is comparable when the photophase lighting is of a white incandescent source (See Chapter 4 of the present thesis) and reflects that of other rodents (Panke *et al*. 1978; Goto *et al*. 1989). Howbeit short wavelength lighting appears to have caused an advance in the melatonin rhythm. It is probable that the period between pineal melatonin production and catabolism until 6-SMT detection in the urine caused a slight (1-2h) delay (Nowak *et al*. 1987). The peak in melatonin might thus have occurred slightly earlier and this would also imply that the contrast between the daytime and nighttime melatonin values is slightly larger in *M. namaquensis* than revealed here. Interestingly, in a study by Dauchy *et al.* (2013), it was shown that light, transmitted through translucent cages with a blue tint as opposed to a clear or amber tint, caused a dramatic increase in the amplitude of the melatonin rhythm in rats. In accordance to the rhythms observed in the present study, the mean daily production values in melatonin showed an inverse relationship with the wavelength of the photophase lighting and with the value being significantly lower under long-WLC than during the preceding wavelengths. Zubidat *et al.* 2010b obtained a similar trend in *M. socialis*

where mean daily melatonin values were lower under long wavelength photophase exposure. This is consistent with data for action spectra of ipRGCs, according to which short wavelengths (~420nm-500nm, blue light) of light most effectively suppresses melatonin in both humans and animals when exposure is during the normal dark phase (Brainard *et al.* 2001, Thapan *et al.* 2001; Rahman *et al.* 2008). Interestingly, Zubidat *et al* (2010b) also reported that in the blind mole rat (*Spalax ehrenbergi*), long wavelength exposure amplified daily melatonin output and that this was most likely due to the species being adapted to an underground environment where spectral power is weak.

In *R. pumilio,* significant interactive effects between the photophase wavelength and the time of the day were detected only under the short-WLC. A similar daily melatonin rhythm was observed in *R. pumili*o under white incandescent photophase lighting of 330 lux (See Chapter 4 of the previous thesis). According to these daily patterns nighttime values were significantly higher than daytime values only after short wavelength exposure. Interestingly, as in *M. namaquensis*, the mean daily production values in melatonin showed an inverse relationship with the wavelength of the photophase lighting and the values differed significantly between all groups. Irrespective of differences in the retinal photoreceptor topographies and densities between *R. pumilio* and *M. namaquensis*, both species showed similar melatonin responses to the wavelegnths of photophase lighting presented to them. This confirms the fundamental involvement of the ipRGC's, with maximal sensitivity to short wavelength exposure, in conveying photoperiodic information for melatonin regulation (Thapan *et al.* 2001). In both species, ipRGCs share similar densities (*R. pumilio*: total number=1012 ipRGCs/mm^2; *M. namaquensis*: total number=862 ipRGCs), but different distributions; in *R. pumilio*, ipRGCs

were densest in the dorso-nasal quadrant whereas in *M. namaquensis*, ipRGCs were uniformly distributed. It is not yet clear how different distributional patterns of photoreceptors facilitate vision and photic entrainment. Here it is shown that the wavelength of daytime lighting plays a crucial role in regulating the daily melatonin rhythm in both nocturnal and diurnal species and the importance of daytime exposure to sunlight, which is rich in short wavelengths (blue light), is also reflected.

Urinary corticosterone

Animals tolerate a wide range of stressors in their natural environments. Glucocorticoids are widely used as agents to counteract stress; in rats and mice corticosterone is the primary glucocorticoid (Möstl & Palme 2002; Palme *et al.* 2005). It has previously been demonstrated that the intensity and the timing of light exposure affects cortisol production in humans (Jung *et al.* 2010). It has also previously been reported, not only that LAN induces stress responses in animals, but also that the quality of lighting during the photophase can act as a stressor (Ishida *et al.* 2005; Zubidat *et al.* 2007, 2010a, 2010b).

The results of the present study show that the spectral wavelength of the photophase is an important component in the regulation of corticosterone expression in both of the studied species. In *M. namaquensis*, there were significant interactive effects between the photophase wavelength and the time of the day during all three WLCs. Mean daily corticosterone values were significantly and inversely related to the wavelength of the photophase lighting. With the exception of the daytime peaks observed under short- and long wavelength exposure, the present

rhythms generally reflect those of nocturnal rodents, in which peak values are observed approximately around the onset of the dark phase (Atkinson & Waddell 1997). In mice, peak concentrations of corticosterone metabolites are visible in the urine within 2 hours following intraperitoneal corticosterone injection (Touma *et al.* 2002). This might suggest that the actual activation of the stress response in *M. namaquensis* occurred slightly earlier than it is represented by the corticosterone. Therefore, the daytime peaks observed under the short-and medium-WLCs most likely portray activation of the stress response system in *M. namaquensis* right after the onset of the photophase. Likewise, the dramatic peak at the onset of the dark phase probably reflected activation of the stress response during the last one or two photophase hours. In *R. pumilio*, overall daily corticosterone values were also inversely correlated to the photophase wavelength, but significant differences existed only between the short-WLC and medium-WLC, as well as between the short-WLC and long-WLC. Moreover, mean values were consistently higher for *R. pumilio* than for *M. namaquensis* and it is evident that the diurnal activity rhythm of *R. pumilio* increased its susceptibility to the stress inducing effects of the photophase lighting. A similar relationship between the photophase wavelength and stress response exists in *M. socialis* but interestingly, *S. ehrenbergi* exhibited an opposite pattern (Zubidat *et al.* 2010b). Furthermore, in *R. pumilio*, significant interaction effects between the time of the day and the photophase wavelength were only observed under the short-WLC. Short wavelength exposure provoked dramatic stress responses at two hours prior to the onset of the light phase and again twelve hours later, at around two hours prior to the onset of the dark phase. Different sensitivities to light stimulation at different times of the day, such as is represented by phase responsive curves, are characteristic to circadian rhythms (Golombek & Rosenstein 2010). Finally, the

increased sensitivity to short wavelength lighting that was observed in both species indicates the involvement of the ipRGCs in mediating daily corticosterone rhythms.

In conclusion, the results of the present study indicate that the light-dark cycle plays a central role in the entrainment of circadian or daily rhythms in *R. pumilio* and in *M. namaquensis*. Furthermore, it is shown that the light spectra of the photophase exposure is an important aspect in the process of physiological and behavioural adjustment, irrespective of whether the species is active by day or by night. Although the locomotor activity rhythm was less affected by the light spectra in *M. namaquensis* compared to in *R. pumilio*, responses in urine production, 6-SMT and corticosterone were largely similar.

Figures - Daily rhythms in locomotor activity:

(a)

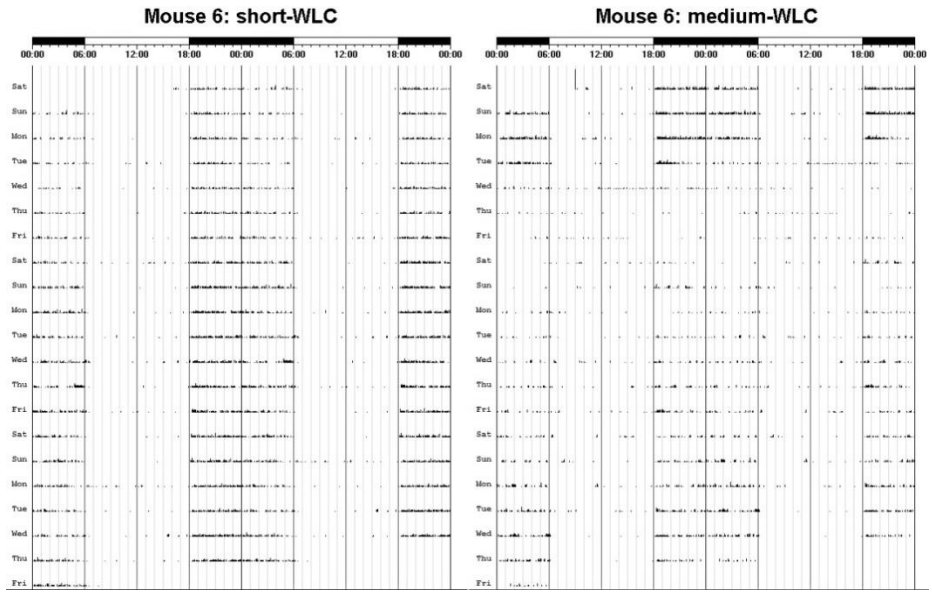

(b)

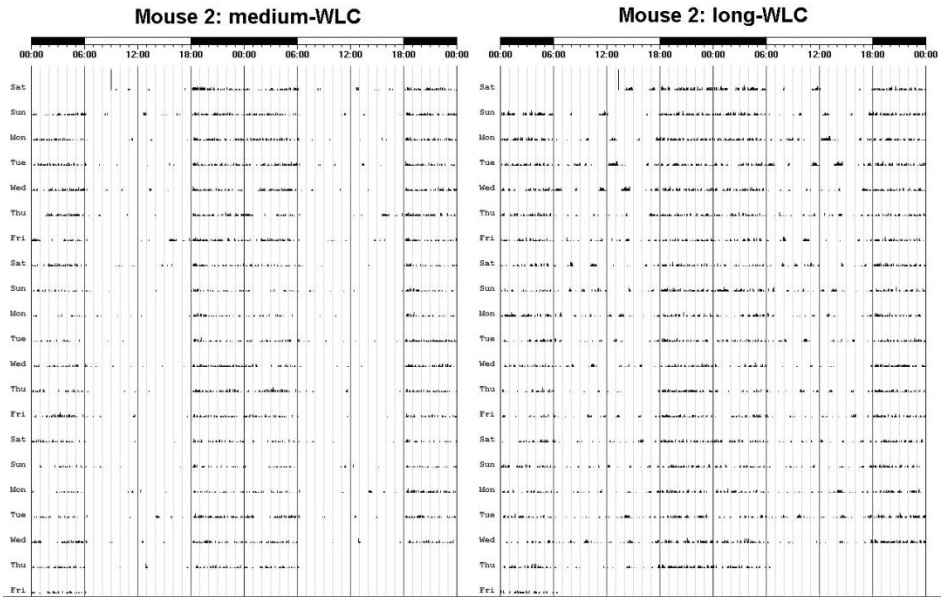

Figure 5.1: (a) On the left: a representative actogram for the Namaqua rock mouse (*Micaelamys namaquensis*), showing a strong nocturnal locomotor activity rhythm. On the right: actogram for mouse 6, the only animal to display a less robust activity rhythm under the medium wavelength light cycle (WLC). (b) Representative actograms showing an increase in the daytime activity, when the wavelength of the photophase is increased (medium-WLC to long-WLC).

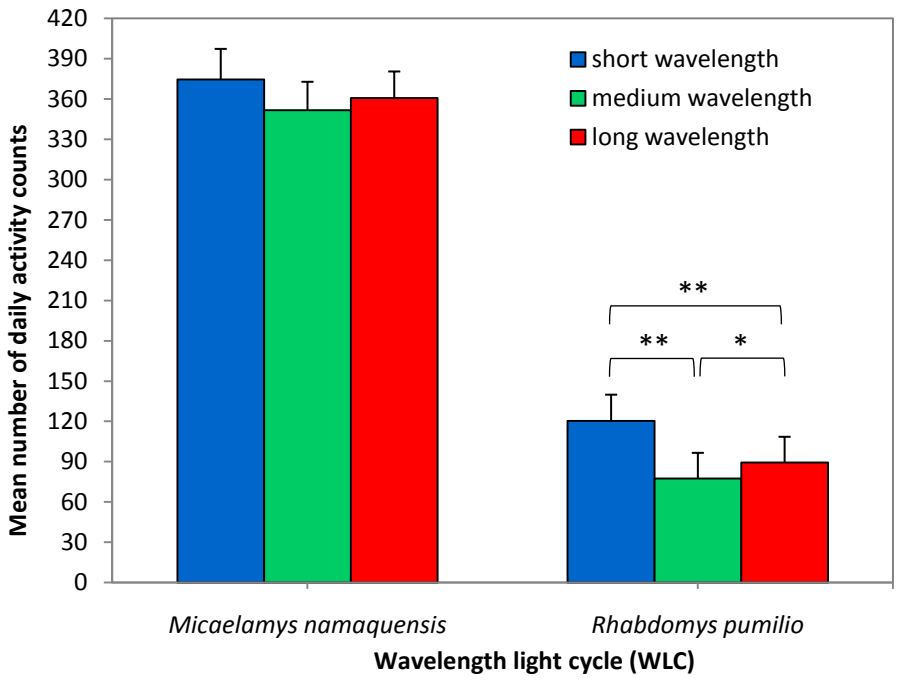

Figure 5.2: Mean number of activity counts in the Namaqua rock mouse (*Micaelamys namaquensis*) and the four striped field mouse (*Rhabdomys pumilio*) after exposure to three successive wavelength light cycles (WLCs). The photophase of each WLC was illuminated using near-monochromatic lighting (i.e. short-, medium-, or long wavelength of light) whereas the scotophase consisted of complete darkness (*=P<0.05; **=P<0.001).

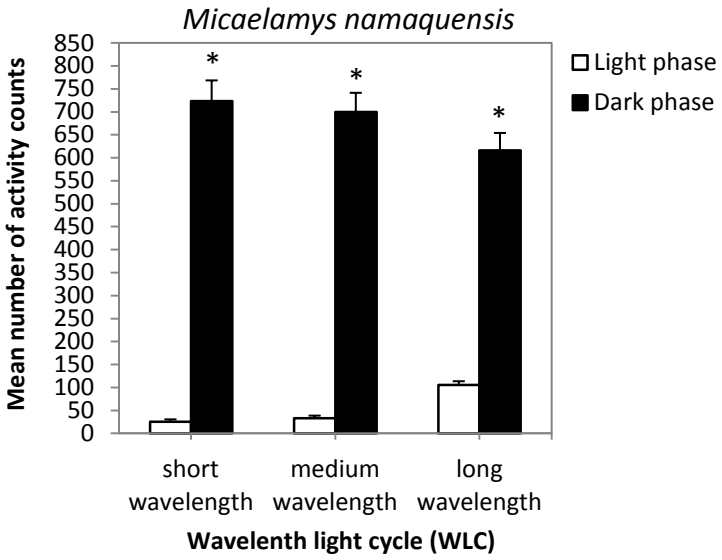

Figure 5.3: The mean number of activity counts, under different wavelength light cycles (WLCs) showing significantly higher nighttime values than daytime values in the Namaqua rock mouse (*Micaelamys namaquensis*; *P<0.001).

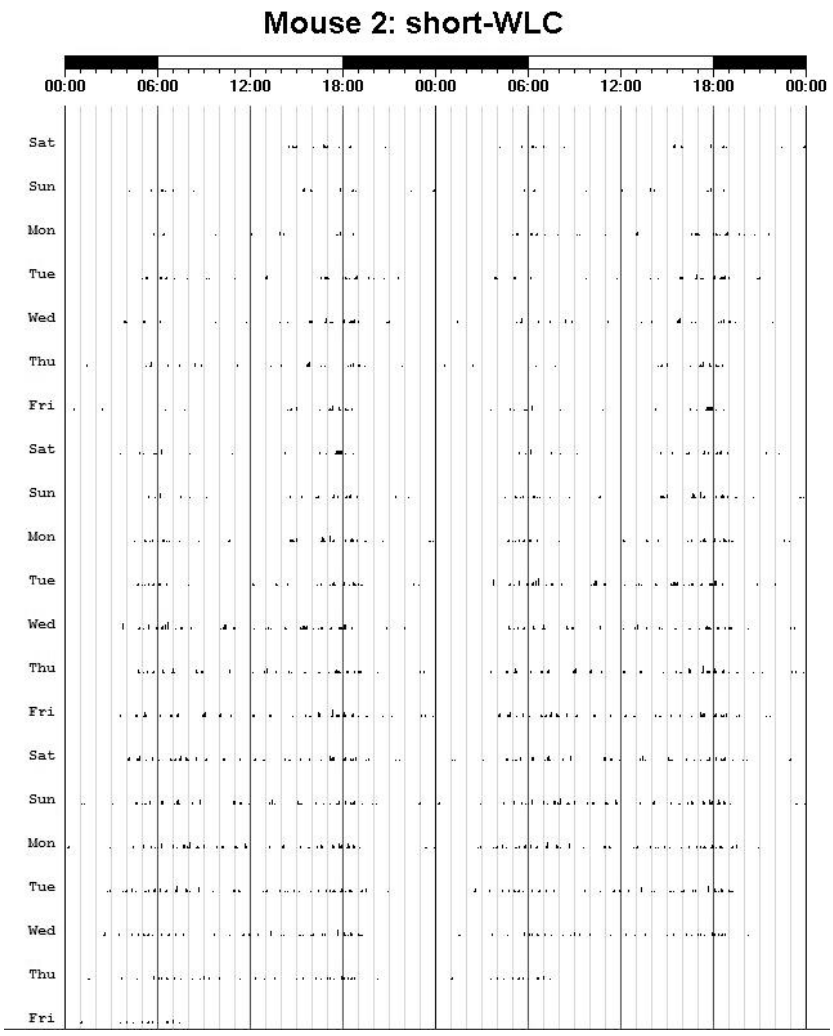

Figure 5.4: A representative actogram for the four striped field mouse (*Rhabdomys pumilio*) under the short wavelength light cycle (WLC), showing elevated activity around dusk and dawn with activity extending across the diurnal phase.

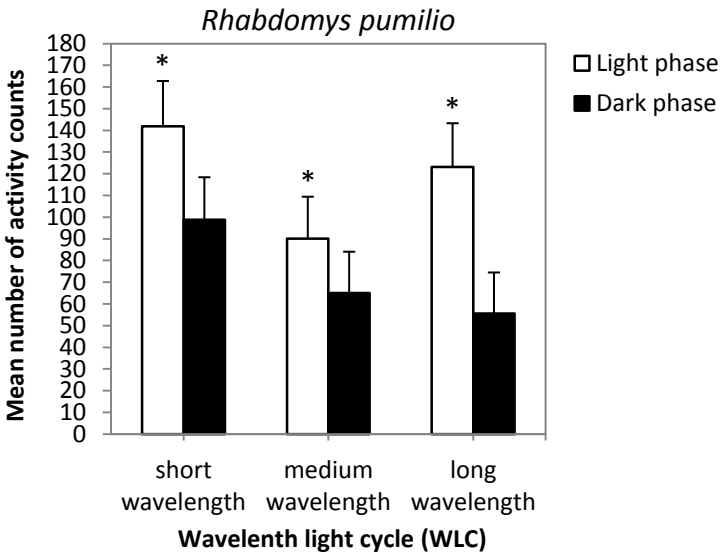

Figure 5.5: The mean number of activity counts, under different wavelength light cycles (WLCs) showing significantly higher daytime values than nighttime values in the four striped field mouse (*Rhabdomys pumilio*; *P<0.001).

Figures – Urine production rate:

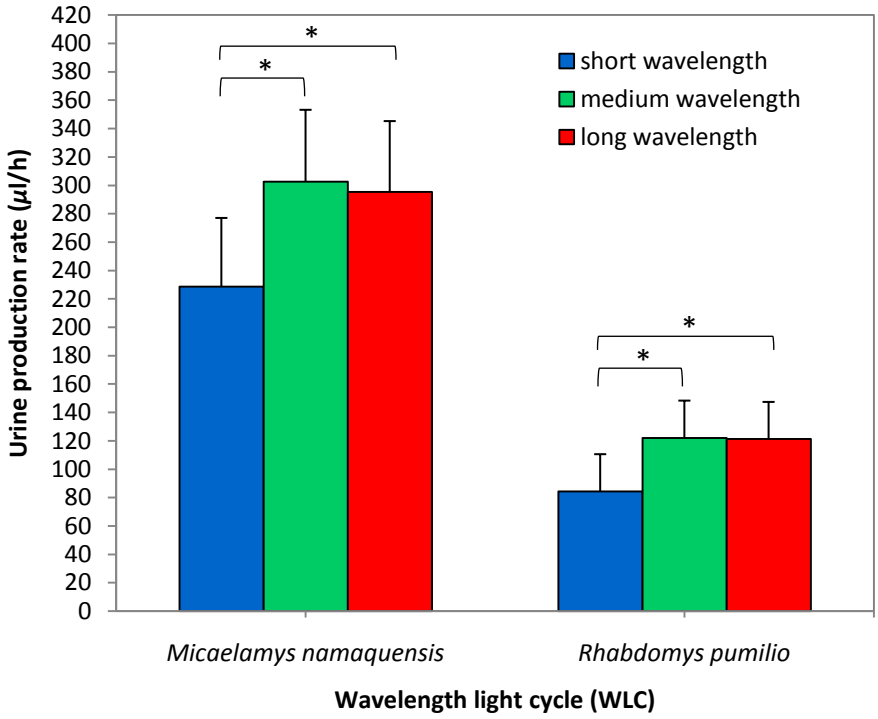

Figure 5.6: Mean urine production rate (μl/h) in the Namaqua rock mouse (*Micaelamys namaquensis*) and the four striped field mouse (*Rhabdomys pumilio*) after exposure to three successive wavelength light cycles (WLCs). The photophase of each WLC was illuminated using near-monochromatic lighting (i.e. short-, medium-, or long wavelength of light) whereas the scotophase consisted of complete darkness (*=P<0.05).

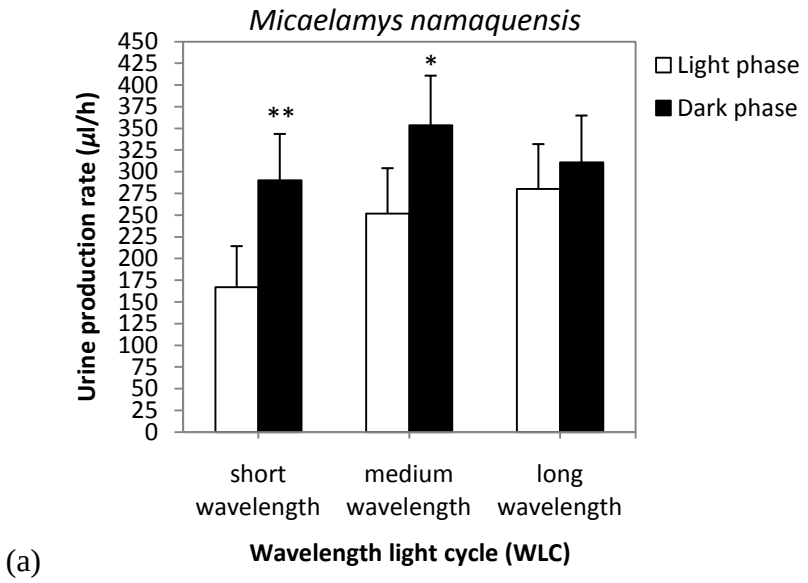

(a)

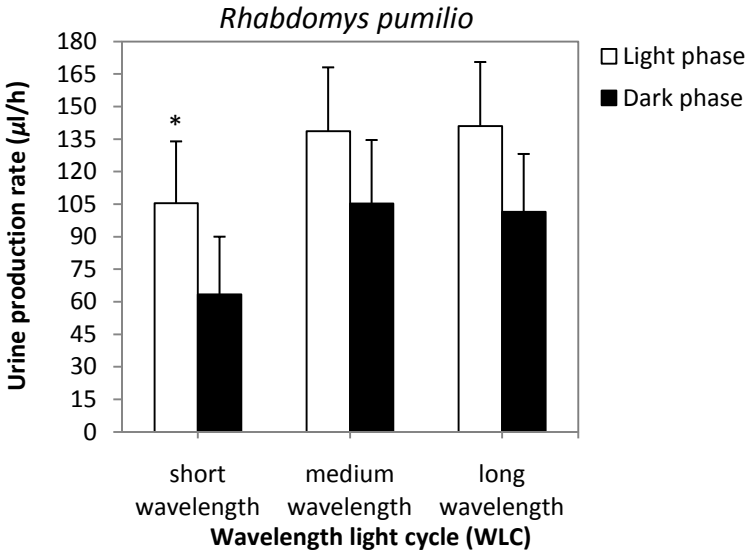

(b)

Figure 5.7: Mean urine production rate (μl/h) in (a); the Namaqua rock mouse (*Micaelamys namaquensis*) and (b); the four striped field mouse (*Rhabdomys pumilio*) after exposure to three successive wavelength light cycles (WLCs), showing daytime and nighttime values separately. In *M. namaquensis*, the rate was consistently higher during the night and in *R. pumilio*, the rate was consistently higher during the day (*P<0.05; **=P<0.001).

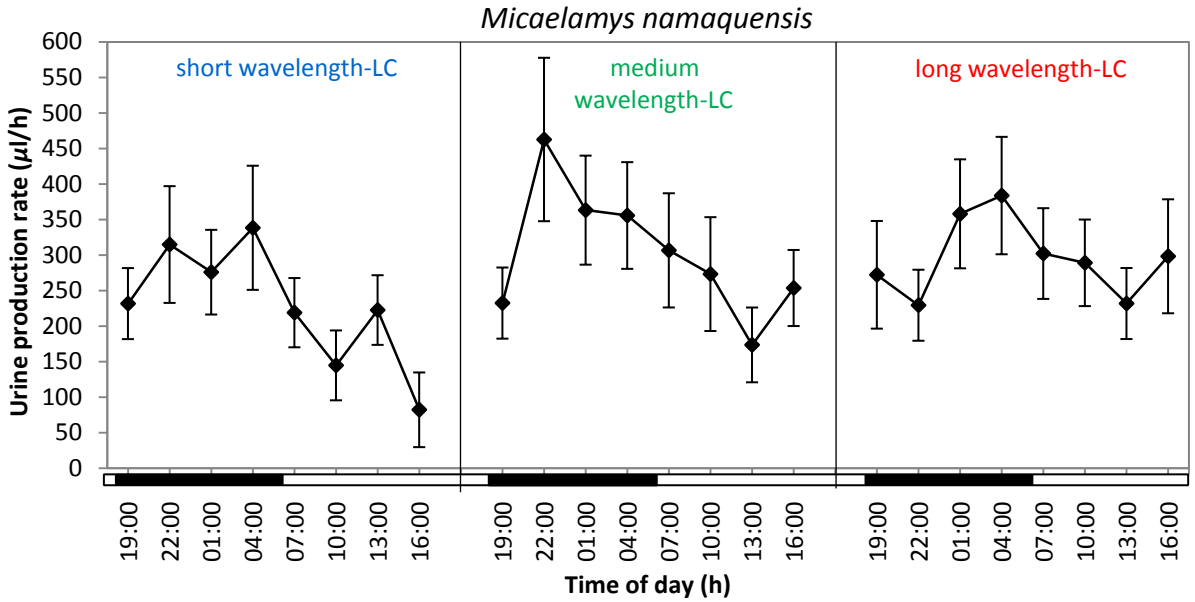

Figure 5.8: The 24h rhythms of urine production rate (μl/h) in the Namaqua rock mouse (*Micaelamys namaquensis*) under three wavelength light cycles (WLCs). The black and white bars at the bottom of each graph indicate the dark- and light phases of each WLC, separately.

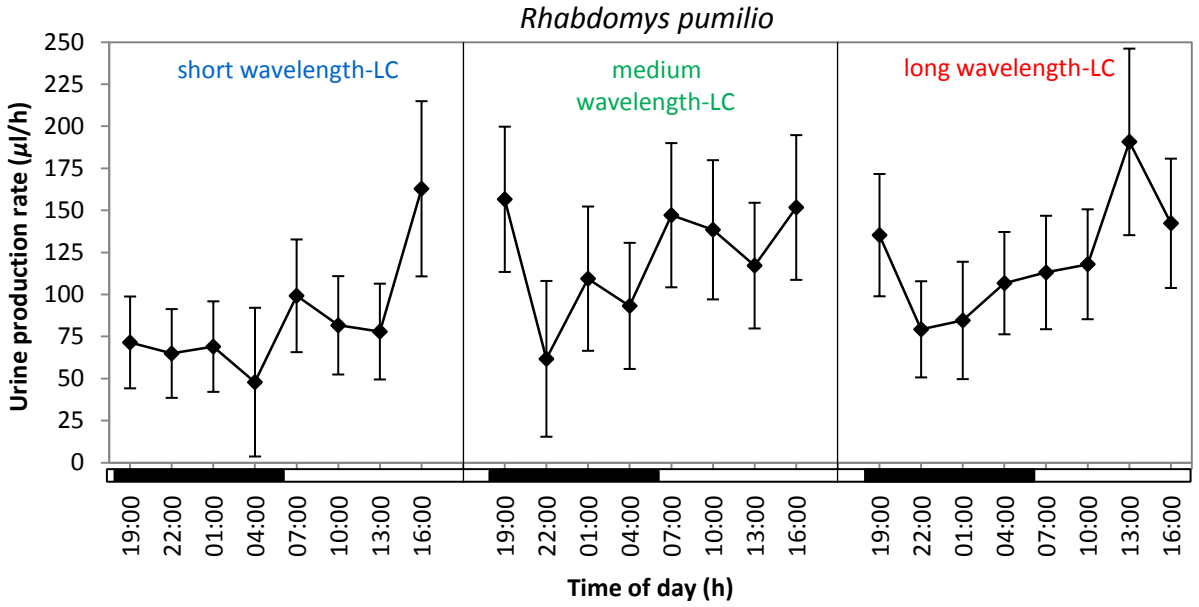

Figure 5.9: The 24h rhythms of urine production rate (μl/h) in four the striped field mouse (*Rhabdomys pumilio*) under three wavelength light cycles (WLCs). The black and white bars at the bottom of each graph indicate the dark- and light phases of each WLC, separately.

Figures – Urinary 6-sulfatoxymelatonin (ng/mg):

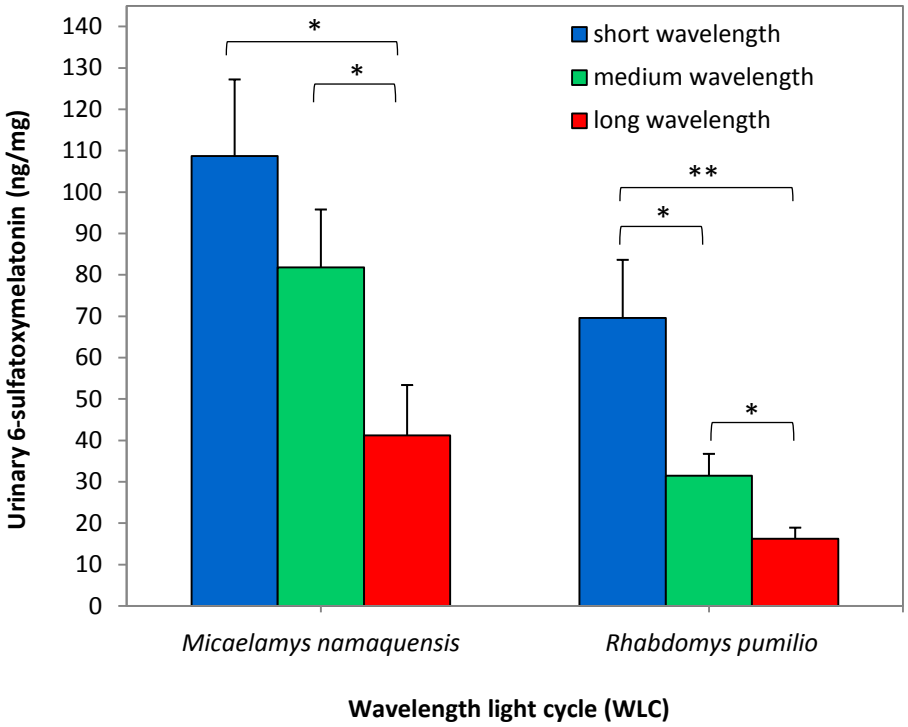

Figure 5.10: Mean urinary 6-sulfatoxymelatonin values (6-SMT; ng/mg) in the Namaqua rock mouse (*Micaelamys namaquensis*) and in the four striped field mouse (*Rhabdomys pumilio*) after exposure to three successive wavelength light cycles (WLCs). The photophase of each WLC was illuminated using near-monochromatic lighting (i.e. short-, medium-, or long wavelength of light) whereas the scotophase consisted of complete darkness (*=P<0.05; **=P<0.001).

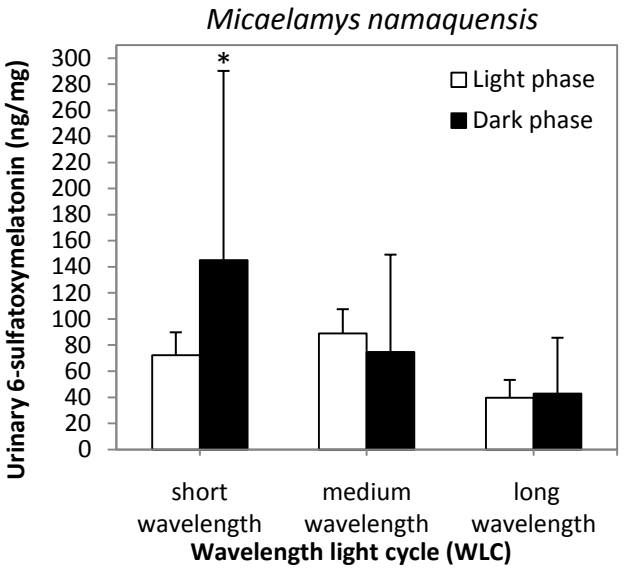

(a)

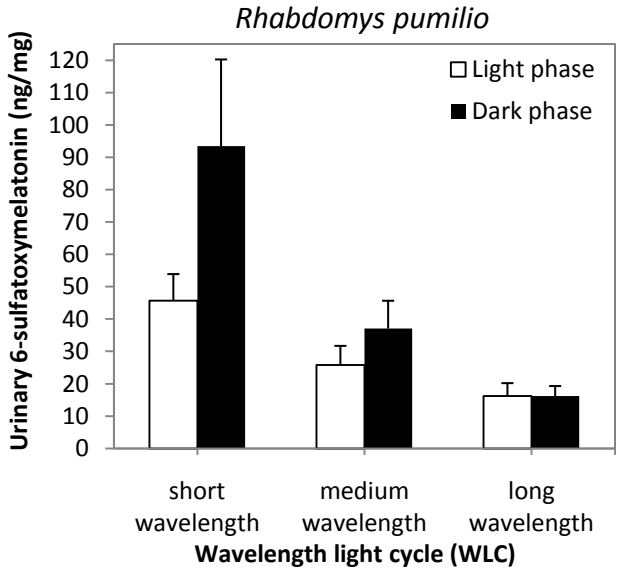

(b)

Figure 5.11: Mean urinary 6-sulfatoxymelatonin values (6-SMT; ng/mg) in (a); the Namaqua rock mouse (*Micaelamys namaquensis*) and (b); the four striped field mouse (*Rhabdomys pumilio*) after exposure to three successive wavelength light cycles (WLCs), showing daytime and nighttime values separately ($P<0.05$).

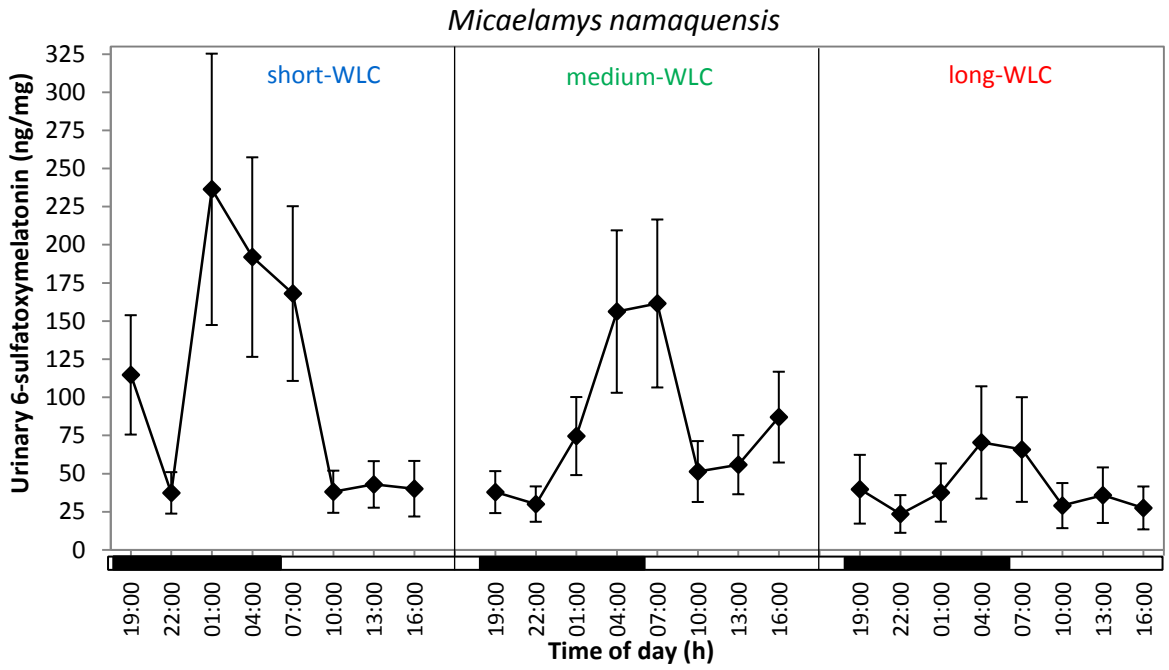

Figure 5.12: The 24h rhythms of urinary 6-sulfatoxymelatonin (6-SMT; ng/mg) in the Namaqua rock mouse (*Micaelamys namaquensis*) under three wavelength light cycles (WLCs). The black and white bars at the bottom of each graph indicate the dark- and light phases of each WLC, separately.

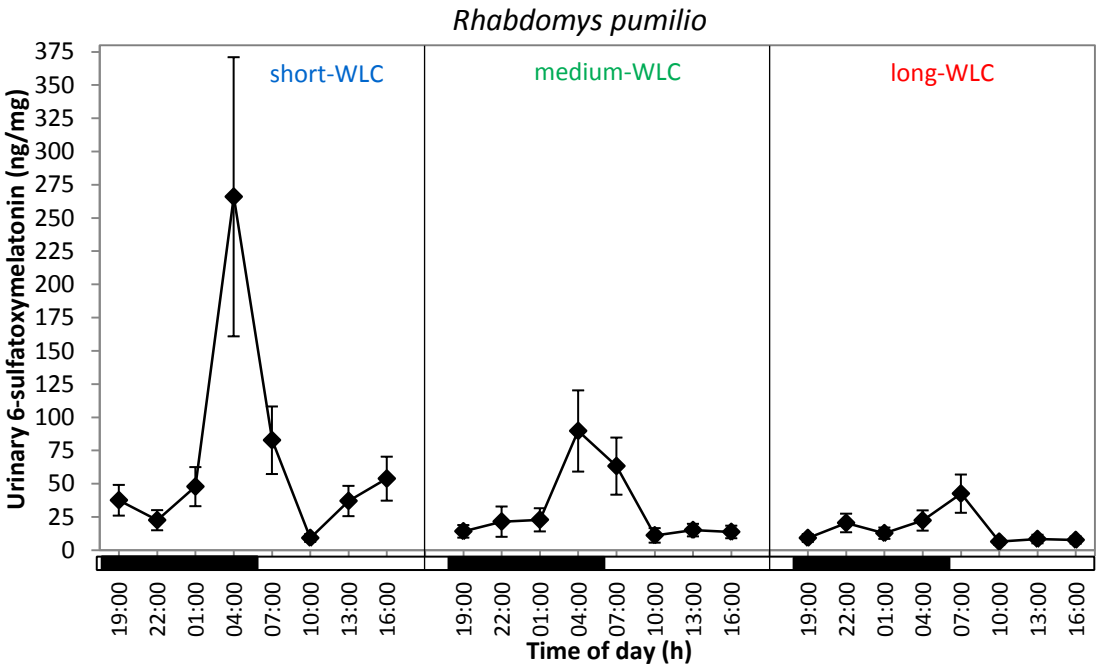

Figure 5.13: The 24h rhythms of urinary 6-sulfatoxymelatonin (6-SMT; ng/mg) in the four striped field mouse (*Rhabdomys pumilio*) under three wavelength light cycles (WLCs). The black and white bars at the bottom of each graph indicate the dark- and light phases of each WLC, separately.

Figures – Urinary Corticosterone (μg/mg):

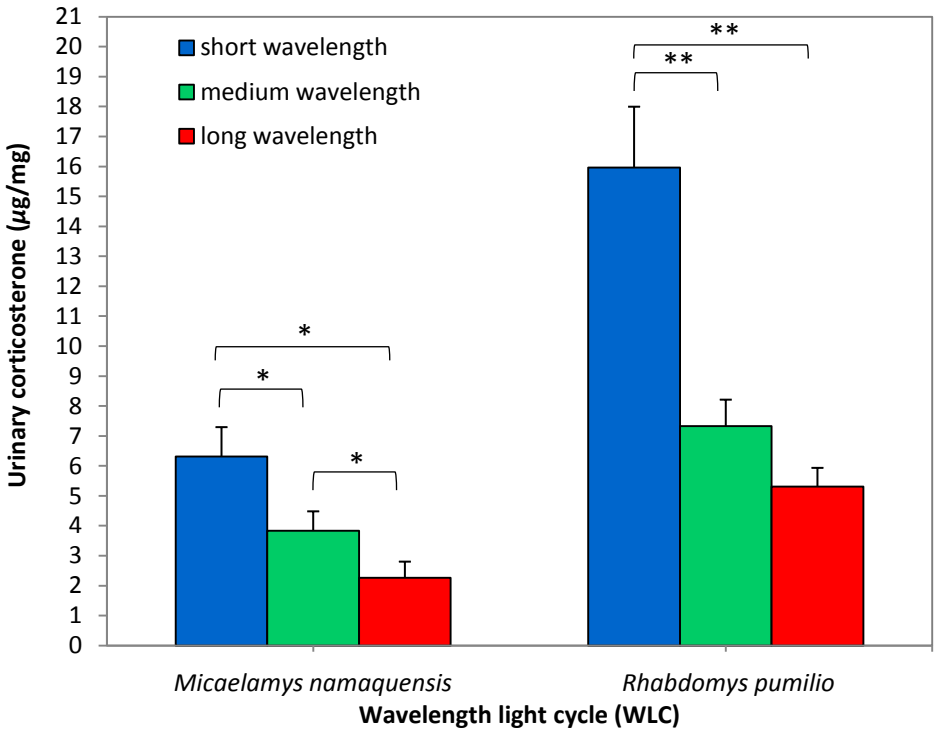

Figure 5.14: Mean urinary corticosterone values (μg/mg) in the Namaqua rock mouse (*Micaelamys namaquensis*) and the four striped field mouse (*Rhabdomys pumilio*) after exposure to three successive wavelength light cycles (WLCs). The photophase of each WLC was illuminated using near-monochromatic lighting (i.e. short-, medium-, or long wavelength of light) whereas the scotophase consisted of complete darkness (*=P<0.05; **=P<0.001).

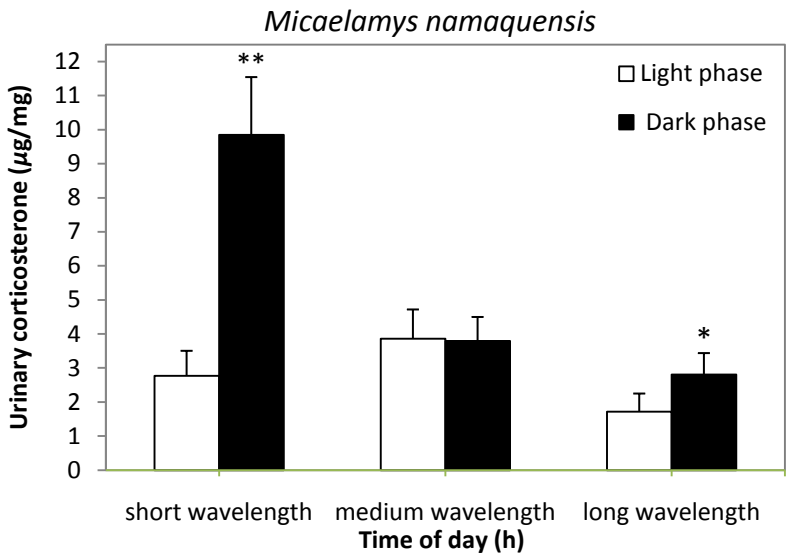

(a)

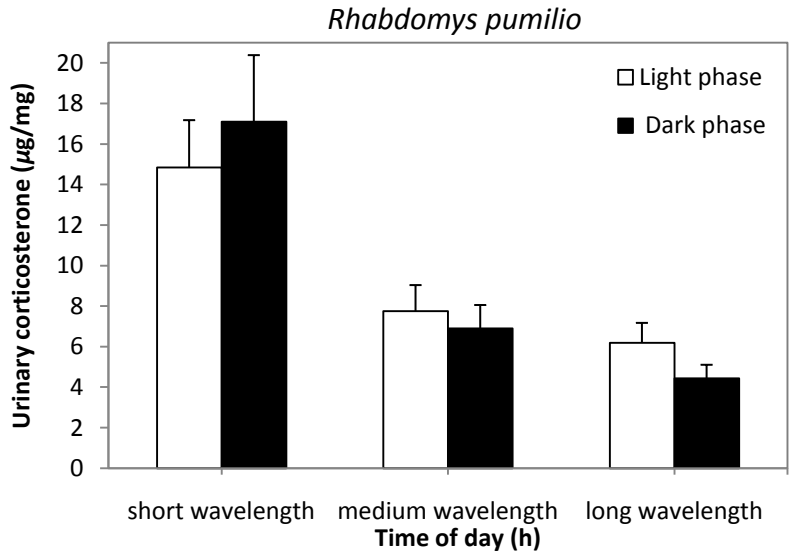

(b)

Figure 5.15: Mean urinary corticosterone values ((µg/mg) in (a); the Namaqua rock mouse (*Micaelamys namaquensis*) and (b); the four striped field mouse (*Rhabdomys pumilio*) after exposure to three successive wavelength light cycles (WLCs), showing daytime and nighttime values separately.

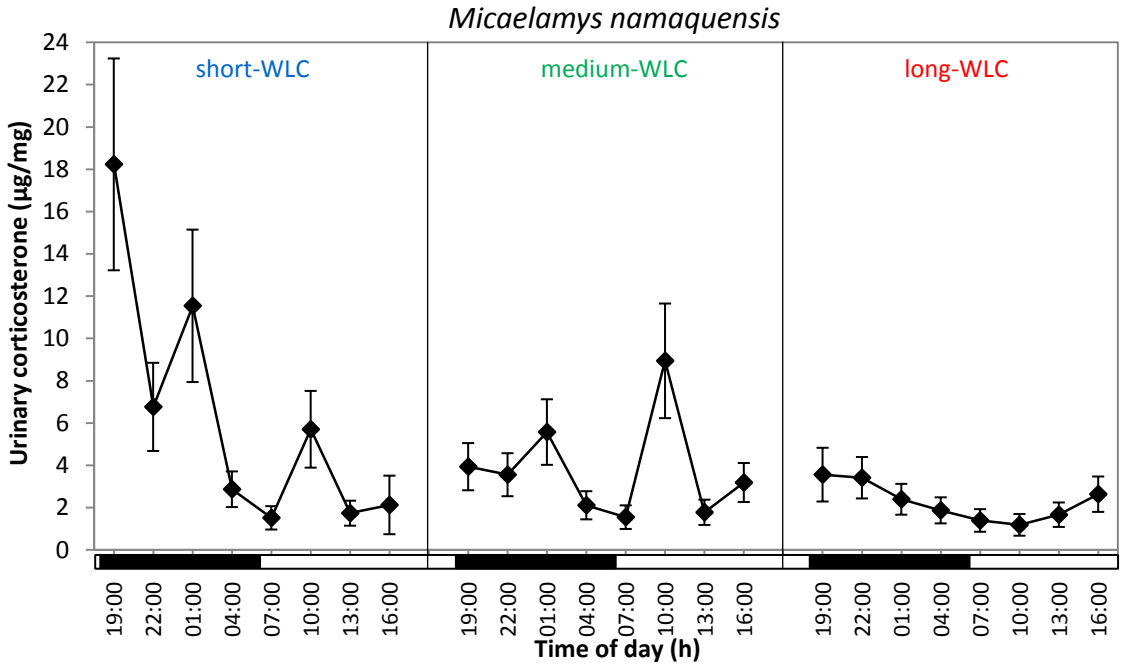

Figure 5.16: The 24h rhythms of urinary corticosterone level (*µg*/mg) in the Namaqua rock mouse (*Micaelamys namaquensis*) under three wavelength light cycles (WLCs). The black and white bars at the bottom of each graph indicate the dark- and light phases of each WLC, separately.

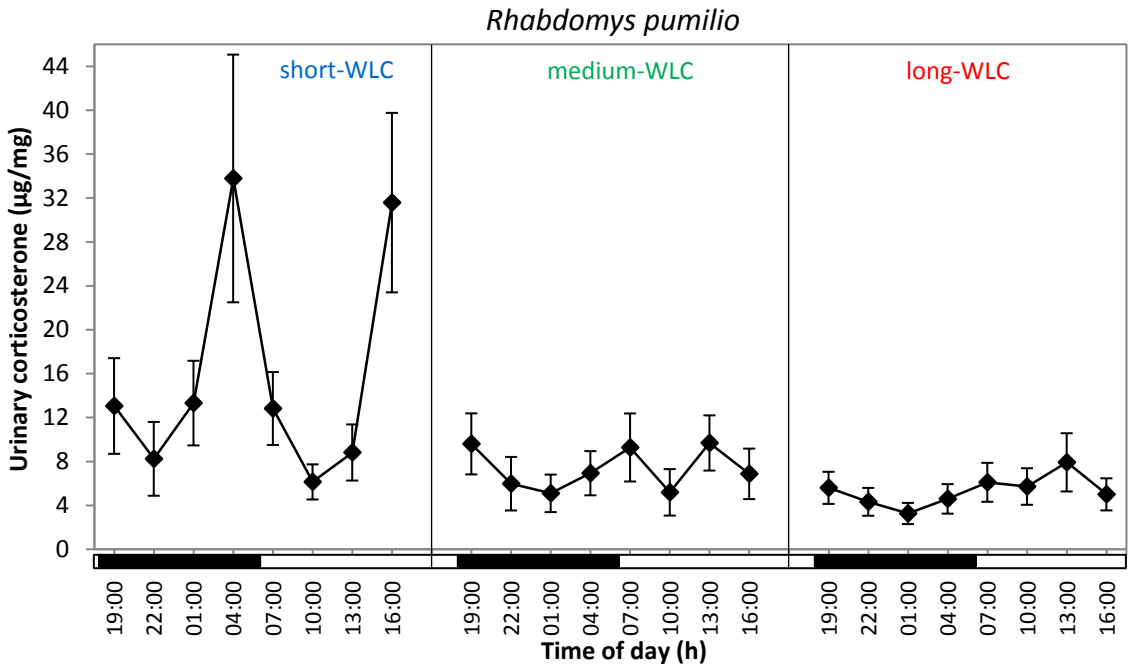

Figure 5.17: The 24h rhythms of urine production rate (μl/h) in the four striped field mouse (*Rhabdomys pumilio*) under three wavelength light cycles (WLCs). The black and white bars at the bottom of each graph indicate the dark- and light phases of each WLC, separately.

CHAPTER 6:

SYNTHESIS

In their natural environments, nearly all organisms are exposed to the perpetual cycling of the light-dark cycle, which in conjunction with the length of day, provides a reliable framework of daily and seasonal time, according to which myriads of physiological, pathological, behavioral and biochemical processes transpire (Pittendrigh & Minis 1964; Gachon *et al.* 2004; Mohawk *et al.* 2012). Such rhythmicity is achieved through biological clock mechanisms that allow organisms to adjust to the temporal environment and evidently ensures survival in many species (Navara & Nelson 2007; Paul *et al.* 2008). The most familiar and widespread rhythm is the circadian rhythm; rhythms that oscillate at a near 24h cycle (Reppert & Weaver 2002; Holzberg & Albrecht 2003). Ultimately, circadian timing ensures that multiple processes emerge orderly and at optimal times of the day. It is therefore not surprising that disruption and desynchronization of internal timing, most notably through exposure to artificial light at night, is associated with various health risks (see Navara & Nelson 2007 for a review). There are in fact studies that provide clear evidence of the negative consequences of light exposure during the normal dark phase (Haim *et al*. 2010). Untimely and/or unnatural light exposure may further greatly alter normal animal behavior and over time cause disturbances in ecological systems (Bird *et al.* 2004; Deda *et al.* 2007). In the present study, a number of direct or related aspects of the internal timing system were investigated in the Namaqua rock mouse (*M. namaquensis*) and the four striped field mouse (*Rhabdomys pumilio*).

Firstly, nocturnality of locomotor activity rhythms was tested and confirmed in *M. namaquensis*. Findings of the present study provide evidence that *M. namaquensis* possesses a distinct and fundamentally nocturnal locomotor activity rhythm that is entrained by the light-dark cycle. The study further revealed that locomotor activity has a circadian rhythm, with period length of close

to 24h and that females tended to be more active than males, presumably due to having higher levels of estrogen (Lightfoot 2008).

Secondly, the topographical density arrangements of visual (rods/cones) and non-visual photoreceptors (intrinsically photosensitive retinal ganglion cells; ipRGCs) were studied in *M. namaquensis* and in *R. pumilio*. According to the findings of the present study, *M. namaquensis* and *R. pumilio* possess duplex retinas that are dominated by rods. Despite similar density peak values, *M. namaquensis* possesses on average more rods than *R. pumilio* and rods are differently distributed in the two species. In agreement with the original predictions, the cone to rod ratios of the species generally reflects their temporal niches. Accordingly, whereas *M. namaquensis* possesses far more rods than cones, *R. pumilio* possesses a high amount of both rods and cones. Furthermore, the present results suggest dichromatic colour vision in both species, but the S- and the M/L-cone populations are homogenously distributed only in *M. namaquensis*. Finally, as expected, ipRGCs are sparsely distributed across the retinas of both species and in *R. pumilio* ipRGCs are distinctly concentrated in the dorso-nasal quadrant. Although the cone to rod ratios reflect the temporal niches of the species, the adaptive values of the specific topographical photoreceptor distributions remain unclear and should be investigated in future studies.

Thirdly, the effects of different photophase illuminance levels on the photoentrainment of various daily rhythms in *M. namaquensis* and in *R. pumilio* were tested. Across the various lighting regimes, both species expressed activity patterns that were in general typical to the species. However, brighter illuminances might be needed to increase the amount of daytime activity in *R. pumilio* to levels that reflect its activity under natural conditions. In both species, the photophase illuminance level does not affect the temporal expression of daily activity but the

amplitude of daily activity and *M. namaquensis* seems to be more susceptible to it than *R. pumilio*. These responses seem to reflect the photoenvironments of the species under natural conditions, whereby *R. pumilio* is expected to tolerate a wider range of illuminances than *M. namaquensis*. Furthermore, studies have shown that conventional rod and cone pathways contribute to non-visual pathways (van Diepen *et al.* 2013). Therefore, it is possible that the observed differences could be related to variations in the retinal photoreceptor densities of the two species. In contrast to what was expected, dim photophase lighting actually reduces daily activity in *M. namaquensis*. Furthermore, the mean daily urine production values were related to the photophase illuminance level in both species and day/night urine production values seem to reflect the activity patterns of the species. Interestingly, the melatonin rhythm was attenuated by the brighter photophase cycle (330 lux); this indicates that the sensitivity threshold of the melatonin rhythm in *M. namaquensis* lies below 330 lux. *Rhabdomys pumilio* seems to express ultradian melatonin rhythms under both dim (10 lux) and bright (330 lux) photophase lighting regimes and although the mean daily 6-SMT values were comparable under the present illuminance levels, the temporal expression of the rhythms seem to have differed.

Lastly, the present study tested the effects of different photophase wavelengths on the photo-entrainment of various daily rhythms of *M. namaquensis* and of *R. pumilio*. In the case of *M. namaquensis*, long wavelength photophase lighting slightly increased daytime activity, presumably as a result of the visual capabilities of the species. Although a similar trend was observed in *R. pumilio*, it seems to have resulted from high stress levels under the short- and medium wavelengths, which evoked a restriction in daytime activity under these light schedules. Irrespective of the temporal niches of the species, short wavelength photophase lighting

attenuates the overall daily urine production, while medium and long wavelengths exert similar effects. Furthermore, the photophase wavelength seems to be inversely correlated to the level of daily 6-SMT in both species and the same trend exists between the photophase wavelength and corticosterone in both species. These results clearly suggest that the ipRGCs, which are maximally sensitive to shorter wavelengths, mediate urine-, melatonin- and corticosterone production in both species.

Collectively, the results indicate that the intensity and the spectral composition of daytime lighting are a fundamental components in the photoentrainment of daily rhythms, not only in diurnal species that are evidently awake during the photophase, but also in nocturnal species that are resting or sleeping during the photophase. Furthermore, the resulsts suggest that the visual capabilities of the species play a role in mediating the daily activity response to photophase light quality. In the nocturnally active *M. namaquensis*, different photophase intensities seem to have a greater effect on activity than different photophase wavelengths; this reflects the rod-rich retina of the species, which effectively allows discrimination between objects, light and dark, but not between colors. In contrast, photophase spectra has a distinct effect on the amplitude of daily activity in *R. pumilio* and evidently, this is because the species is primarily active by day, but it also reflects the high density of both rods and cones of the species. It is also evident from these results that the ipRGCs play a central role in mediating daily urine-, melatonin- and corticosterone rhythms in the two species. The different responses to the quality of the photophase lighting between *M. namaquensis* and *R. pumilio* are most likely related to the specific photoenvironments the species are adapted to. It is clear that light plays an integral role

in both photic and non-photic processes in animals and a wide range of anatomical and physiological features reflect different adaptations according to their respective temporal niches.

REFERENCES

Aggelopoulos NC & Meissl H (2000). Responses of neurons of the rat suprachiasmatic nucleus to retinal illumination under photopic and scotopic conditions. *The Journal of Physiology* **523**: 211-222.

Ahnelt PK & Kolb H (2000). The mammalian photoreceptor mosaic-adaptive design. *Progress in Retinal and Eye Research* **19**: 711-777.

Alkon PU & Saltz D (1988). Influence of season and moonlight on temporal activity patterns of Indian crested porcupines (*Hystrix indica*). *Journal of Mammalogy* **69**: 71-80.

Altimus CM, Güler AD, Alam NM, Arman AC, Prusky GT, Sampath AP & Hattar S (2010). Rod photoreceptors drive circadian photoentrainment across a wide range of light intensities. *Nature Neuroscience* **13**: 1107-1112.

Amir S & Robinson B (1995). Ultraviolet light entrains rodent suprachiasmatic nucleus pacemaker. *Neuroscience* **69**: 1005-1011.

Applebury ML, Antoch MP, Baxter LC, Chun LLY, Falk JD, Farhangfar F, Kage K, Krzystolik MG, Lyass LA & Robbins JT (2000). The murine cone photoreceptor: a single cone type expresses both S and M opsins with retinal spatial patterning. *Neuron* **27**: 513-523.

Aral E, Uslu S, Sunal E, Sariboyaci AE, Okar İ & Aral E (2006). Response of the pineal gland in the rats exposed to three different light spectra of short periods. *Turkish Journal of Veterinary and Animal Sciences* **30**: 29-34.

Arrese CA, Rodger J, Beazley LD & Shand J (2003). Topographies of retinal cone photoreceptors in two Australian marsupials. *Visual Neuroscience* **20**: 307-311.

Aschoff J. (1981). Free running and entrained circadian rhythms. *In* Handbook of behavioral neurobiology: biological rhythms. *Edited by* Aschoff J. Plenum Press, New York. pp. 81- 93.

Asenjo AB, Rim J & Oprian DD (1994). Molecular determinants of human red/green color discrimination. *Neuron* **12**: 1131-1138.

Asplund R (1995). The nocturnal polyuria syndrome (NPS). *General Pharmacology: The Vascular System* **26**: 1203-1209.

Atkinson HC & Waddell BJ (1997). Circadian Variation in Basal Plasma Corticosterone and Adrenocorticotropin in the Rat: Sexual Dimorphism and Changes across the Estrous Cycle 1. *Endocrinology* **138**: 3842-3848.

Baker MAA & Brown JS (2011). Patch use behavior of *Elephantulus myurus* and *Micaelamys namaquensis*: the role of diet, foraging substrates and escape substrates. *African Journal of Ecology* **50**: 167-175.

Bandyopadhyay D, Biswas K, Bhattacharyya M, Reiter RJ & Banerjee RK (2001). Gastric toxicity and mucosal ulceration induced by oxygen-derived reactive species: protection by melatonin. *Current Molecular Medicine* **1**: 501–513.

Baylor DA, Lamb TD & Yau KW (1979). Responses of retinal rods to single photons. *The Journal of Physiology* **288**: 613-634.

Beaven CM & Ekström J (2013). A comparison of blue light and caffeine effects on cognitive function and alertness in humans. *PloS One* **8**: e76707.

Begall S, Daan S, Burda H & Overkamp GJF (2002). Activity patterns in a subterranean social rodent, *Spalacopus cyanus* (Octodontidae). *Journal of Mammalogy* **83:** 153-158.

Bennett AF & Ruben JA (1979). Endothermy and activity in vertebrates. *Science* **206**: 649-654.

Benstaali C, Mailloux A, Bogdan A, Auzéby A & Touitou Y (2001). Circadian rhythms of body temperature and motor activity in rodents. Their relationships with the light-dark cycle. *Life Sciences* **68**: 2645-2656.

Berson DM (2003). Strange vision: ganglion cells as circadian photoreceptors. *TRENDS in Neurosciences* **26**: 314-320.

Berson DM, Castrucci AM & Provencio I (2010). Morphology and mosaics of melanopsin-expressing retinal ganglion cell types in mice. *Journal of Comparative Neurology* **518**: 2405-2422.

Berson DM, Dunn FA & Takao 2002. Phototransduction by retinal ganglion cells that set the circadian clock. *Science* **295**: 1070-1073.

Biccard A & Midgley JJ (2009). Rodent pollination in *Protea nana*. *South African Journal of Botany* **75**: 720-725.

Bierman A, Figueiro MG & Rea MS (2011). Measuring and predicting eyelid spectral transmittance. *Journal of Biomedical Optics* **16**: 067011-067011.

Bird BL, Branch LC & Miller DL (2004). Effects of coastal lighting on foraging behavior of beach mice. *Conservation Biology* **18**: 1435-1439.

Bobu C, Craft CM, Masson-Pevet M & Hicks D (2006). Photoreceptor organization and rhythmic phagocytosis in the nile rat *Arvicanthis ansorgei*: A novel diurnal rodent model for the study of cone pathophysiology. *Investigative Ophtalmology and Visual Science* **47**: 3109–3118.

Bojkowski CJ, Aldhous ME, English J, Franey C, Poulton AL, Skene DJ & Arendt J (1987). Suppression of nocturnal plasma melatonin and 6-sulfatoxymelatonin by bright and dim light in man. *Hormone and Metabolic Research* **19**: 437-440.

Bomholt SF, Harbuz MS, Blackburnmunro G & Blackburn-Munro RE (2004). Involvement and role of the hypothalamo-pituitaryadrenal (HPA) stress axis in animal models of chronic pain and inflammation. *Stress* **7**: 1–14.

Boulos Z (1995). Wavelength dependence of light-induced phase shifts and period changes in hamsters. *Physiology & Behavior* **57**: 1025-1033.

Brainard GC, Sliney D, Hanifin JP, Glickman G, Byrne B, Greeson JM, Jasser S, Gerner E & Rollag MD (2008). Sensitivity of the human circadian system to short-wavelength (420-nm) light. *Journal of Biological Rhythms* **23**: 379-386.

Brown JS, Kotler BP, Smith RJ & Wirtz II WO (1988). The effects of owl predation on the foraging behavior of heteromyid rodents. Oecologia **76**: 408-415.

Buffenstein R (1984). The importance of microhabitat in thermoregulation and thermal conductance in two Namib rodents - a crevice dweller, *Aethomys namaquensis*, and a burrow dweller, *Gerbillurus paeba*. *Journal of Thermal Biology* **9**: 235-241.

Caldelas I, Poirel VJ, Sicard B, Pevet P & Challet E (2003). Circadian profile and photic regulation of clock genes in the suprachiasmatic nucleus of a diurnal mammal *Arvicanthis ansorgei*. *Neuroscience* **116**: 583–91.

Carrillo-Vico A, Guerrero JM, Lardone PJ & Reiter R (2005). A review of the multiple actions of melatonin on the immune system. *Endocrine* **27**: 189-200.

Carter-Dawson LD & La Vail MM (1979). Rods and cones in the mouse retina. I. Structural analysis using light and electron microscopy. *Journal of Comparative Neurology* **188**: 245-262.

Cassone VM, Speh JC, Card JP & Moore RY (1988). Comparative anatomy of mammalian suprachiasmatic nucleus. *Journal of Biological Rhythms* **3**: 71-91.

Cermakian N, Monaco L, Pando MP, Dierich A & Sassone-Corsi P (2001). Altered behavioral rhythms and clock gene expression in mice with a targeted mutation in the *Period1* gene. *The EMBO Journal* **20**: 3967-3974.

Challet E (2007). Minireview: entrainment of the suprachiasmatic clockwork in diurnal and nocturnal mammals. *Endocrinology* **148**: 5648-5655.

Chepesiuk R (2009). Missing the dark: Health effects of light pollution. *Environmental Health Perspectives* **1**: 20-27.

Chrousos GP (2009). Stress and disorders of the stress system. *Nature Reviews Endocrinology* 5**:** 374-381.

Cohen R & Kronfeld-Schor N (2006). Individual variability and photic entrainment of circadian rhythms in golden spiny mice. *Physiology & Behavior* **87**: 563-574.

Cornish EE, Xiao M, Yang Z, Provis JM & Hendrickson AE (2004). The role of opsin expression and apoptosis in determination of cone types in human retina. *Experimental Eye Research* **78**: 1143–1154.

Dardente H, Menet JS, Challet E, Tournier BB, Pévet P & Masson-Pévet M (2004). Daily and circadian expression of neuropeptides in the suprachiasmatic nuclei of nocturnal and diurnal rodents. *Molecular Brain Research* **124**: 143-151.

Dauchy RT, Sauer LA, Blask DE & Vaughan GM (1997). Light contamination during the dark phase in "photoperiodically controlled" animal rooms: effect on tumor growth and metabolism in rats. *Laboratory Animal Science* **47**: 511-518.

Davidson AJ, Yamazaki S, Arble DM, Menaker M & Block GD (2008). Resetting of central and peripheral circadian oscillators in aged rats. *Neurobiology of Aging* **29**: 471– 477.

De Boer SF, Van der Gugten J & Slangen JL (1989). Plasma catecholamine and corticosterone responses to predictable and unpredictable noise stress in rats. *Physiology & Behavior* **45**: 789-795.

De Kloet ER, Joëls M & Holsboer F (2005). Stress and the brain: from adaptation to disease. *Nature Reviews Neuroscience* **6**: 463-475.

Deveson AL, Arendt J & Forsyth IA (1990). Sensitivity of goats to a light pulse during the night as assessed by suppression of melatonin concentration in the plasma. *Journal of Pineal Research* **8**: 169-177.

Dkhissi-Benyahya O, Gronfier C, De Vanssay W, Flamant F & Cooper HM (2007). Modeling the role of mid-wavelength cones in circadian responses to light. *Neuron* **53**: 677-687.

Doyle SE, Yoshikawa T, Hillson H & Menaker M (2008). Retinal pathways influence temporal niche. *Proceedings of the National Academy of Sciences* **105**: 13133-13138.

Duffy JF & Wright KP (2005). Entrainment of the human circadian system by light. *Journal of Biological Rhythms* **20**: 326-338.

Ecker JL, Dumitrescu ON, Wong KY, Alam NM, Chen SK, LeGates T, Renna JM, Prusky GT, Berson DM & Hattar S (2010). Melanopsin-expressing retinal ganglion-cellphotoreceptors: Cellular diversity and role in pattern vision. *Neuron* **67**: 49-60.

Edmonds SC & Adler NT (1977). Food and light as entrainers of circadian running activity in the rat. *Physiology & Behavior* **18**: 915-919.

Edwards E, King JA & Fray JC (1999). Increased basal activity of the HPA axis and renin angiotensin system in congenital learned helpless rats exposed to stress early in development. *International Journal of Developmental Neuroscience* **17**: 805–812.

Estevez ME, Fogerson PM, Ilardi MC, Borghuis BG, Chan E, Weng S, Auferkorte ON, Demb JB & Berson DM (2012). Form and function of the M4 cell, an intrinsically photosensitive retinal ganglion cell type contributing to geniculocortical vision. *The Journal of Neuroscience* **32**: 13608-13620.

Feldman JL & Phillips CJ (1984). Comparative retinal pigment epithelium and photoreceptor ultrastructure in nocturnal and fossorial rodents: the eastern woodrat, *Neotoma floridana*, and the plains pocket gopher, *Geomys bursarius*. *Journal of Mammalogy* 231-245.

Fleming PA & Nicolson SW (2004). Sex differences in space use, body condition and survivorship during the breeding season in the Namaqua rock mouse, *Aethomys namaquensis*. *African Zoology* **39**: 123-132.

Fonken LK, Workman JL, Walton JC, Weil ZM, Morris JS, Haim A & Nelson RJ (2010). Light at night increases body mass by shifting the time of food intake. *Proceedings of the National Academy of Sciences* **107**: 18664-18669.

Foster RG & Helfrich-Förster C (2001). The regulation of circadian clocks by light in fruitflies and mice. *Philosophical Transactions of the Royal Society of London. Series B, Biological Sciences* **356**: 1779-1790.

Foster RG, Argamaso S, Coleman S, Colwell CS, Lederman A & Provencio I (1993). Photoreceptors regulating circadian behavior: a mouse model. *Journal of Biological Rhythms* **8**: S17-23.

Foster RG, Provencio I, Hudson D, Fiske S, De Grip W & Menaker M (1991). Circadian photoreception in the retinally degenerate mouse (rd/rd). *Journal of Comparative Physiology A* **169**: 39-50.

Francis AJP & Coleman GJ (1988). The effect of ambient temperature cycles upon circadian running and drinking activity in male and female laboratory rats. *Physiology & Behavior* **43**: 471-477.

Freedman MS, Lucas RJ, Soni B, von Schantz M, Muñoz M, David-Gray Z & Foster R (1999). Regulation of mammalian circadian behavior by non-rod, non-cone, ocular photoreceptors. *Science* **284**: 502-504.

Gachon F, Nagoshi E, Brown SA, Ripperger J & Schibler U (2004). The mammalian circadian timing system: from gene expression to physiology. *Chromosoma* **113**: 103-112.

Gaillard F, Bonfield S, Gilmour GS, Kuny S, Mema SC, Martin BT, Smale L, Crowder N, Stell WK & Sauvé Y (2008). Retinal anatomy and visual performance in a diurnal cone-rich laboratory rodent, the Nile grass rat (*Arvicanthis niloticus*). *Journal of Comparative Neurology* **510**: 525-538.

Gattermann R, Johnston RE, Yigit N, Fritzsche P, Larimer S, Özkurt S, Neumann K, Song Z, Colak E, Johnston J & McPhee ME (2008). Golden hamsters are nocturnal in captivity but diurnal in nature. *Biology Letters* **4**: 253-255.

Geetha L & Subbaraj R (1996). Green light evokes maximum phase shifts in the locomotor activity rhythm of the field mouse *Mus booduga*. *Journal of Photochemistry and Photobiology B: Biology* **33**: 79-82.

Golombek DA & Rosenstein RE (2010). Physiology of circadian entrainment. *Physiological Reviews* **90**: 1063-1102.

Gonzalez MMC & Aston-Jones G (2008). Light deprivation damages monoamine neurons and produces a depressive behavioral phenotype in rats. *Proceedings of the National Academy of Sciences* **105**: 4898-4903.

Gooley JJ, Lu J, Chou TC, Scammell TE & Saper CB (2001) Melanopsin in cells of origin of the retinohypothalamic tract. *Nature Neuroscience* **4**: 1165.

Gooley JJ, Rajaratnam SM, Brainard GC, Kronauer RE, Czeisler CA & Lockley SW (2010). Spectral responses of the human circadian system depend on the irradiance and duration of exposure to light. *Science Translational Medicine* **2**: 31ra33.

Gorman MR, Elliott JA & Evans JA (2003). Plasticity of hamster circadian entrainment patterns depends on light intensity. *Chronobiology International* **20**: 233-248.

Goto M, Oshima I, Tomita T & Ebihara S (1989). Melatonin content of the pineal gland in different mouse strains. *Journal of Pineal Research* **7**: 195-204.

Govardovskii VI, Röhlich P, Szél Á & Khokhlova TV (1992). Cones in the retina of the mongolian gerbil, *Meriones unguiculatus*: an immunocytochemical and electophysiological study. *Vision Research* **32**: 19–27.

Griffith MK & Minton JE (1992). Effect of light intensity on circadian profiles of melatonin, prolactin, ACTH, and cortisol in pigs. *Journal of Animal Science* **70**: 492-498.

Habib KE, Gold PW & Chrousos GP (2001). Neuroendocrinology of stress. *Endocrinology Metabolism Clinics of North America* **30**: 695-728.

Haddock SHD, Moline MA & Case JF (2010). Bioluminescence in the Sea. *Annual Review of Marine Science* **2**: 443–493.

Haim A, van Aarde RJ & Zisapel N (1998). Body temperature daily rhythms in the striped mouse *Rhabdomys pumilio*: The effects of and blockade. *Physiology & Behavior* **63**: 889-893.

Haim A, Yukler A, Harel O, Schwimmer H & Fares F (2010). Effects of chronobiology on prostate cancer cells growth in vivo. *Sleep Science* **3**: 32-35.

Haim A & Portnov BA (2013). Light pollution as a new risk factor for human breast and prostate cancers. Springer, Dordrechet Heidelberg New York London.

Hall MI & Ross CF (2007). Eye shape and activity pattern in birds. *Journal of Zoology* **271**: 437-444.

Hanifin JP, Stewart KT, Smith P, Tanner R, Rollag M, Brainard GC 2006. High-intensity red light suppresses melatonin. *Chronobiology International* **23**: 251–268.

Hardeland R, Cardinali DP, Srinivasan V, Spence DW, Brown GM & Pandi-Perumal SR (2011). Melatonin - A pleiotropic, orchestrating regulator molecule. *Progress in Neurobiology* **93**: 350-384.

Hashimoto S, Kohsaka M, Nakamura K, Honma H, Honma S & Honma KI (1997). Midday exposure to bright light changes the circadian organization of plasma melatonin rhythm in humans. *Neuroscience Letters* **221**: 89-92.

Hattar S, Liao HW, Takao M, Berson DM & Yau KW (2002). Melanopsin-containing retinal ganglion cells: architecture, projections, and intrinsic photosensitivity. *Science* **295**: 1065-1070.

Hattar S, Lucas RJ, Mrosovsky N, Thompson S, Douglas RH, Hankins MW, Lem J, Biel M, Hofmann F, Foster RG & Yau KW (2003). Melanopsin and rod-cone photoreceptive systems account for all major accessory visual functions in mice. *Nature* **424**: 75-81.

Haverkamp S & Wässle H (2000). Immunocytochemical analysis of the mouse retina. *Journal of Comparative Neurology* **424**: 1-23.

Hemmi JM & Grünert U (1999). Distribution of photoreceptor types in the retina of a marsupial, the tammar wallaby (*Macropus eugenii*). *Visual Neuroscience* **16:** 291-302.

Hicks D & Molday RS (1986). Differential immunogold-dextran labeling of bovine and frog rod and cone cells using monoclonal antibodies against bovine rhodopsin. *Experimental Eye Research* **42**: 55-71.

Holsboer F & Ising M (2010). Stress hormone regulation: biological role and translation into therapy. *Annual Review of Psychology* **61**: 81-109.

Holzberg D & Albrecht U (2003). The circadian clock: a manager of biochemical processes within the organism. *Journal of Neuroendocrinology* **15**: 339-343.

Hoole C, Oosthuizen MK, Chimimba CT & Bennett NC (2012). The locomotory activity rhythm of the spiny mouse, *Acomys spinosissimus* from southern Africa: light entrainment and endogenous circadian rhythms. *Journal of Zoology (London)* **288**: 93-102.

Hut RA, Mrosovsky N and Daan S (1999). Nonphotic entrainment in a diurnal mammal, the European ground squirrel (*Spermophilus citellus*). *Journal of Biological Rhythms* **14**: 409-419.

Imai H, Kojima D, Oura T, Tachibanaki S, Terakita A & Shichida Y (1997). Single amino acid residue as a functional determinant of rod and cone visual pigments. *Proceedings of the National Academy of Sciences* **94**: 2322-2326.

Ishida A, Mutoh T, Ueyama T, Bando H, Masubuchi S, Nakahara D, Tsujimoto G & Okamura H (2005). Light activates the adrenal gland: timing of gene expression and glucocorticoid release. *Cell Metabolism* **2**: 297-307.

Jackson C & Bernard RTF (1999). Short day length alone does not inhibit spermatogenesis in the seasonally breeding four-striped field mouse (*Rhabdomys pumilio*). *Biology of Reproduction* **60**: 1320-1323.

Jacobs GH (1993). The distribution and nature of colour vision among the mammals. *Biological Reviews* **68**: 413-471.

Jasser SM, Hanifin JP, Rollag MD & Brainard GC (2006). Dim light adaptation attenuates acute melatonin suppression in humans. *Journal of Biological Rhythms* **21**: 394-404.

Jeon CJ, Strettoi E & Masland RH (1998). The major cell populations of the mouse retina. *Journal of Neuroscience* **18**: 8936–8946.

Johnson AG **(**1980). The Social Organisation and Behaviour of the Striped Fieldmouse *Rhabdomys Pumilio* (Sparrman 1784): Studies in Captivity and in the Field. MSc Thesis, University of Cape Town.

Johnson SD, Pauw A & Midgley J (2001). Rodent pollination in the African lily *Massonia depressa* (Hyacinthaceae). *American Journal of Botany* **88**: 1768-1773.

Julien-Laferrière D (1997). The influence of moonlight on activity of woolly opossums (*Caluromys philander*). *Journal of Mammalogy* **78**: 251–255.

Jung CM, Khalsa SBS, Scheer FA, Cajochen C, Lockley SW, Czeisler CA & Wright KP (2010). Acute effects of bright light exposure on cortisol levels. *Journal of Biological Rhythms* **25**: 208-216.

Kamperis K, Hansen MN, Hagstroem S, Hvistendahl G, Djurhuus JC & Rittig S (2004). The circadian rhythm of urine production, and urinary vasopressin and prostaglandin E2 excretion in healthy children. *The Journal of Urology* **171**: 2571-2575.

Kappers JA (1995). Survey of the innervation of the epiphysis cerebri and the accessory pineal organs of vertebrates. *Progress in Brain Research* **10**: 87-153.

Karnas D, Hicks D, Mordel J, Pévet P & Meissl H (2013). Intrinsic photosensitive retinal ganglion cells in the diurnal rodent, *Arvicanthis ansorgei*. *PloS One* **8**: e73343.

Kas MJ & Edgar DM (1999). A nonphotic stimulus inverts the diurnal–nocturnal phase preference in *Octodon degus*. *The Journal of Neuroscience* **19**: 328-333.

Keeney A, Jessop DS, Harbuz MS, Marsden CA, Hogg S & Blackburn-Munro RE (2006). Differential effects of acute and chronic social defeat stress on hypothalamic-pituitary-adrenal axis function and hippocampal serotonin release in mice. *Journal of Neuroendocrinology* **18**: 330-338.

Kennaway DJ, Blake P & Webb HA (1989). A melatonin agonist and *N*-acetyl-N^2-formyl-5-methoxykynurenamine accelerate the reentrainment of the melatonin rhythm following a phase advance of the light-dark cycle. *Brain Research* **495**: 349-354.

Klein DC & Moore RY (1979). Pineal *N*-acetyltransferase and hydroxyindole-*O*-methyltransferase: control by the retinohypothalamictract and the suprachiasmatic nucleus. *Brain Research* **174**: 245–262.

Kloog I, Haim A, Stevens RG & Portnov BA (2009). Global co-distribution of light at night (LAN) and cancers of prostate, colon, and lung in men. *Chronobiology International* **26**: 108–125.

Kloog I, Stevens RG, Haim A & Portnov BA (2010). Nighttime light level co-distributes with breast cancer incidence worldwide. *Cancer Causes Control* **21**: 2059-2068.

Koolhaas JM, Bartolomucci A, Buwalda B, De Boer SF, Flügge G, Korte SM, Meerlo P, Murison R, Olivier B, Palanza P, Richter-Levin G, Sgoifo A, Steimer T, Stiedl O, van Dijk G, Wöhr M & Fuchs E. (2011). Stress revisited: a critical evaluation of the stress concept. *Neuroscience & Biobehavioral Reviews* **35**: 1291-1301.

Kotler BP, Brown JS, Oldfield A, Thorson J & Cohen D (2001). Foraging substrate and escape substrate: patch use by three species of gerbils. *Ecology* **82**: 1781–1790.

Kotler BP, Brown JS, Dall SRX, Gresser S, Ganeym D & Bouskila A (2002). Foraging games between gerbils and their predators: temporal dynamics of resource depletion and apprehension in gerbils. *Evolutionary Ecology Research* **4**: 495-518.

Kramer KM & Birney EC (2001). Effect of light intensity on activity patterns of Patagonian leaf-eared mice, *Phyllotis xanthopygus*. *Journal of Mammalogy* **82**: 535-544.

Kronfeld-Schor N & Dayan T (2008). Activity patterns of rodents: the physiological ecology of biological rhythms. *Biological Rhythm Research* **39**: 193-211.

Krug CB (2004). Survival in the Namib: adaptations of the striped mouse to an arid environment. *Transactions of the Royal Society of South Africa* **59**: 93-98.

Kryger Z, Galli-Resta L, Jacobs GH & Reese BE (1998). The topography of rod and cone photoreceptors in the retina of the ground squirrel. *Visual Neuroscience* **15**: 685-691.

Kumar V & Rani S (1999). Light sensitivity of the photoperiodic response system in higher vertebrates: wavelength and intensity effects. *Indian Journal of Experimental Biology* **37**: 1053-1064.

Kumar V, Rani S, Malik S, Trivedi AK, Schwabl I, Helm B & Gwinner E (2007). Daytime light intensity affects seasonal timing via changes in the nocturnal melatonin levels. *Naturwissenschaften* **94**: 693-696.

Kuwayama S, Imai H, Hirano T, Terakita A & Shichida Y (2002). Conserved proline residue at position 189 in cone visual pigments as a determinant of molecular properties different from rhodopsins. *Biochemistry* **41**: 15245–15252.

Landgraf R & Wigger A (2003). Born to be anxious: neuroendocrine and genetic correlates of trait anxiety in HAB rats. *Stress* **6**: 111–119.

Li XM, Liu XH, Filipski E, Metzger G, Delagrange P, Jeanniot JP & Lévi F (2000). Relationship of atypical melatonin rhythm with two circadian clock outputs in B6D2F$_1$ mice. *American Journal of Physiology – Regulatory, Integrative and Comparative Physiology* **278**: R924-R930.

Lightfoot, J.T. (2008). Sex hormones' regulation of rodent physical activity: a review. *International Journal of Biological Sciences* **4**: 126-132.

Lockley SW & Gooley JJ (2006). Circadian photoreception: spotlight on the brain. *Current Biology* **16**: R795-R797.

Longcore T & Rich C (2004). Ecological light pollution. *Frontiers in Ecology and the Environment* **2**: 191-198.

Lovegrove BG & Papenfus M E (1995). Circadian activity rhythms in the solitary Cape molerat (*Georychus capensis*: Bathyergidae) with some evidence of splitting. *Physiology & Behavior* **58**: 679-685.

Lovegrove BG, Heldmaier G & Ruf T (1991). Perspectives of endothermy revisited: the endothermic temperature range. *Journal of Thermal Biology* **16**: 185-197.

Lovegrove BG & Heldmaier G (1994). The amplitude of circadian body temperature rhythms in three rodents (*Aethomys namaquensis*, *Thallomys paedulcus* and *Cryptomys damarensis*) along an arboreal-subterranean gradient. *Australian Journal of Zoology* **42**: 65-78.

Lucas RJ, Douglas RH & Foster RG (2001). Characterization of an ocular photopigment capable of driving pupillary constriction in mice. *Nature Neuroscience* **4**: 621-626.

Lucas RJ, Freedman MS, Muñoz M, Garcia-Fernández JM & Foster RG (1999). Regulation of the mammalian pineal by non-rod, non-cone, ocular photoreceptors. *Science* **284**: 505-507.

Lukáts Á (2004). Photopigment coexpression in mammals: comparative and developmental aspects. Ph. D. thesis, Department of Human Morphology and Developmental Biology, Semmelweis University, Hungary.

Lukáts Á, Dkhissi-Benyahya O, Szepessy Z, Röhlich P, Vígh B, Bennett NC, Cooper HM & Szél Á (2002). Visual pigment coexpression in all cones of two rodents, the Siberian hamster and the pouched mouse. *Investigative Ophthalmology and Visual Science* **43**: 2468-2473.

Lukáts Á, Szabó A, Röhlich P, Vigh B & Szél A (2005). Photopigment coexpression in mammals: comparative and developmental aspects. *Histology and Histopathology* **20**: 551-574.

Mahoney M, Bult A & Smale L (2001) Phase response curve and light-induced Fos expression in the suprachiasmatic nucleus and adjacent hypothalamus of *Arvicanthis niloticus*. Journal of Biological Rhythms **16**: 149-162

Martin GR (2007). Visual fields and their functions in birds. *Journal of Ornithology* **148**: 547-562.

Masland RH (2001). Neuronal diversity in the retina. *Current Opinion in Neurobiology* **11**: 431-436.

Matsuo T, Yamaguchi S, Mitsui S, Emi A, Shimoda F & Okamura H (2003). Control mechanism of the circadian clock for timing of cell division in vivo. *Science* **302**: 255-259.

McGuire RA, Rand WM & Wurtman RJ (1973). Entrainment of the body temperature rhythm in rats: effect of color and intensity of environmental light. *Science* **181**: 956-957.

Mohawk JA, Green CB & Takahashi JS (2012). Central and peripheral circadian clocks in mammals. *Annual Review of Neuroscience* **35**: 445-462.

Mohawk JA & Lee TM (2005). Restraint stress delays reentrainment in male and female diurnal and nocturnal rodents. *Journal of Biological Rhythms* **20**: 245-256.

Moore RY (1996). Neural control of the pineal gland. *Behavioural Brain Research* **73**: 125-130.

Moore RY & Eichler VB (1972). Loss of a circadian adrenal corticosterone rhythm following suprachiasmatic lesions in the rat. *Brain Research* **42**: 201-206.

Möstl E & Palme R (2002). Hormones as indicators of stress. *Domestic Animal Endocrinology* **23**: 67-74.

Mrosovsky N (1999). Masking: history, definitions, and measurement. *Chronobiology International* **16**: 415-429.

Mrosovsky N, Edelstein K, Hastings MH & Maywood ES (2001). Cycle of period gene expression in a diurnal mammal (*Spermophilus tridecemlineatus*): implications for nonphotic phase shifting. *Journal of Biological Rhythms* **16**: 471–78.

Mrosovsky N, Foster RG & Salmon PA (1999). Thresholds for masking responses to light in three strains of retinally degenerate mice. *Journal of Comparative Physiology A* **184**: 423-428.

Mrosovsky, N (1999). Masking: history, definitions, and measurement. *Chronobiology International* **16**: 415-429.

Muteka SP, Chimimba CT & Bennett NC (2006). Reproductive seasonality in *Aethomys namaquensis* (Rodentia: Muridae) from southern Africa. *Journal of Mammalogy* **87**: 67-74.

Muteka SP, Chimimba CT & Bennett NC (2006). Reproductive photoresponsiveness in *Aethomys ineptus* and *A. namaquensis* (Rodentia: Muridae) from southern Africa. *Journal of Zoology (London)* **268**: 225-231.

Nakahara D, Nakamura M, Iigo M & Okamura H (2003). Bimodal circadian secretion of melatonin from the pineal gland in a living CBA mouse. *Proceedings of the National Academy of Sciences* **100**: 9584-9589.

Nathan PJ, Burrows GD & Norman TR (1999). Melatonin sensitivity to dim white light in affective disorders. *Neuropsychopharmacology* **21**: 408-413.

Nathans J (1999). The evolution and physiology of human color vision: insights from molecular genetic studies of visual pigments. *Neuron* **24**: 299-312.

Navara KJ & Nelson R (2007). The dark side of light at night: physiological, epidemiological and ecological consequences. *Journal of Pineal Research* **43**: 215-224.

Negoro H, Kanematsu A, Doi M, Suadicani SO, Matsuo M, Imamura M, Okinami T, Nishikawa N, Oura T, Matsui S, Seo K, Tainaka M, Urabe S, Kiyokage E, Todo T, Okamura H, Tabata Y & Ogawa O (2012). Involvement of urinary bladder Connexin43 and the circadian clock in coordination of diurnal micturition rhythm. *Nature Communications* **3**: 809.

Nel JAJ (1975). Aspects of the social ethology of some Kalahari Rodents. *Zeitschrift für Tierpsychologie* **37**: 322–331.

Noh JY, Han DH, Yoon JA, Kim MH, Kim SE, Ko IG, Kim KH, Kim, CJ & Cho S (2011). Circadian rhythms in urinary functions: possible roles of circadian clocks? *International Neurourology Journal* **15**: 64-73.

Noguchi H & Sakaguchi T (1999). Effect of illuminance and color temperature on lowering of physiological activity. *Applied Human Science* **18**: 117-123.

Nowak R, McMillen IC, Redman J & Short RV (1987). The correlation between serum and salivary melatonin concentrations and urinary 6-hydroxymelatonin sulphate excretion rates: two non-invasive techniques for monitoring human circadian rhythmicity. *Clinical Endocrinology* **27**: 445-452.

Nunez AA, Bult A, McElhinny TL & Smale L (1999). Daily rhythms of Fos expression in hypothalamic targets of the suprachiasmatic nucleus in diurnal and nocturnal rodents. *Journal of Biological Rhythms* **14**: 300-306.

O'Connor TG, Bergman K, Sarkar P & Glover V (2013). Prenatal cortisol exposure predicts infant cortisol response to acute stress. *Developmental Psychobiology* **55**: 145-155.

Ogawa S, Chan J, Gustafsson JA, Korach KS & Pfaff DW (2003). Estrogen increases locomotor activity in mice through estrogen receptor α: specificity for the type of activity. *Endocrinology* **144**: 230-239.

Oster H, Avivi A, Joel A, Albrecht U & Nevo E (2002). A switch from diurnal to nocturnal activity in *S. ehrenbergi* is accompanied by an uncoupling of light input and the circadian clock. *Current Biology* **12**: 1919-1922.

Oster H, Damerow S, Kiessling S, Jakubcakova V, Abraham D, Tian J, Hoffmann MW & Eichele G (2006). The circadian rhythm of glucocorticoids is regulated by a gating mechanism residing in the adrenal cortical clock. *Cell Metabolism* **4**: 163–173.

Palme R, Rettenbacher S, Touma C, El-Bahr SM & Möstl E (2005). Comparative aspects regarding metabolism, excretion, and noninvasive measurement in fecal samples. *Annals New York Academy of Science* **1040**: 162-171.

Panke ES, Rollag MD & Reiter RJ (1978). Pineal melatonin concentrations in the Syrian hamster. *Endocrinology* **104**: 194-197.

Park SJ & Tokura H (1999). Bright light exposure during the daytime affects circadian rhythms of urinary melatonin and salivary immunoglobulin A. *Chronobiology International* **16**: 359-71.

Paul MJ, Zucker I & Schwartz WJ (2008). Tracking the seasons: the internal calendars of vertebrates. *Philosophical Transactions of the Royal Society B: Biological Sciences*: **363**: 341-361.

Peek CB, Affinati AH, Ramsey KM, Kuo HY, Yu W, Sena LA, Ilkayeva O, Marcheva B, Kobayashi Y, Omura C, Levine DC, Bacsik DJ, Gius D, Newgards CB, Goetzman E, Chandel NS, Denu JM, Mrksich M & Bass J (2013). Circadian clock NAD+ cycle drives mitochondrial oxidative metabolism in mice. *Science* **342**: 1243417.

Peichl L & Moutairou K (1998). Absence of short-wavelength sensitive cones in the retinae of seals (Carnivora) and African giant rats (Rodentia). *European Journal of Neuroscience* **10**: 2586-2594.

Peichl L (2005). Diversity of mammalian photoreceptor properties: adaptations to habitat and lifestyle? *The Anatomical Record Part A: Discoveries in Molecular, Cellular, and Evolutionary Biology* **287**: 1001-1012.

Peichl L, Némec P & Burda H (2004). Unusual cone and rod properties in subterranean African mole-rats (Rodentia, Bathyergidae). *European Journal of Neuroscience* **19**: 1545-1558.

Petry HM, Erichsen JT & Szél Á (1993). Immunocytochemical identification of photoreceptor populations in the tree shrew retina. *Brain Research* **616**: 344-350.

Piccione G, Caola G & Refinetti R (2002). The circadian rhythm of body temperature of the horse. *Biological Rhythm Research*, **33**: 113-119.

Pittendrigh CS & Daan S (1976). A functional analysis of circadian pacemakers in nocturnal rodents. IV. Entrainment: Pacemaker as clock. Journal of Comparative Physiology **106**: 291–331.

Pittendrigh CS & Minis DH (1964). The entrainment of circadian oscillations by light and their role as photoperiodic clocks. *The American Naturalist* **98**: 261-294.

Provencio I, Cooper HM & Foster RG (1998). Retinal projections in mice with inherited retinal degeneration: implications for circadian photoentrainment. *Journal of Comparative Neurology* **395**: 417-439.

Provencio I, Rodriguez IR, Jiang G, Hayes WP, Moreira EF & Rollag MD (2000). A novel human opsin in the inner retina. *The Journal of Neuroscience* **20**: 600-605.

Rahman SA, Kollara A, Brown TJ & Casper RF (2008). Selectively filtering short wavelengths attenuates the disruptive effects of nocturnal light on endocrine and molecular circadian phase markers in rats. *Endocrinology* **149**: 6125-6135.

Rajaratnam SM & Redman JR (1999). Social contact synchronizes free-running activity rhythms of diurnal palm squirrels. *Physiolgy & Behavior* **66**: 21-26.

Ralph MR & Menaker M (1988). A mutation of the circadian system in golden hamster. *Science* **241**: 1225-1227.

Ralph MR, Foster RG, Davis FC & Menaker M (1990). Transplanted suprachiasmatic nucleus determines circadian period. *Science* **247**: 975–978.

Redlin U & Mrosovsky N (2004). Nocturnal activity in a diurnal rodent (*Arvicanthis niloticus*): the importance of masking. *Journal of Biological Rhythms* **19**: 58-67.

Refinetti R (2008). The diversity of temporal niches in mammals. *Biological Rhythm Research* **39**: 173-192.

Reiter RJ (1993). The melatonin rhythm: Both a clock and a calendar. *Experientia* **49**: 654–664.

Reiter RJ, King TS, Richardson BA & Hurlbut EC (1982). Studies on pineal melatonin levels in a diurnal species, the Eastern chipmunk (*Tamias striatus*): Effects of light at night, propranolol administration or superior cervical ganglionectomy. *Journal of Neural Transmission* **54**: 275-284.

Reiter RJ, Tan DX, Sanchez-Barcelo E, Mediavilla MD, Gitto E & Korkmaz A (2011). Circadian mechanisms in the regulation of melatonin synthesis: disruption with light at night and the pathophysiological consequences. *Journal of Experimental and Integrative Medicine* **1**: 13-22.

Reiter RJ, Tan DX, Terron MP, Flores LJ & Czarnocki Z (2007). Melatonin and its metabolites: new findings regarding their production and their radical scavenging actions. A*cta Biochimica Polonica - English Edition* **54**: 1-9.

Reppert SM & Weaver DR (2001). Molecular analysis of mammalian circadian rhythms. *Annual Review of Physiology* **63**: 647-676.

Reppert SM & Weaver DR (2002). Coordination of circadian timing in mammals. *Nature* **418**: 935-941.

Rieke F & Baylor DA (1998). Single-photon detection by rod cells of the retina. *Reviews of Modern Physics* **70**: 1027-1036.

Rittig S, Schaumburg HL, Siggaard C, Schmidt F & Djurhuus JC (2008). The circadian defect in plasma vasopressin and urine output is related to desmopressin response and enuresis status in children with nocturnal enuresis. *The Journal of Urology* **179**: 2389-2395.

Rocha FA, Ahnelt PK, Peichl L, Saito CA, Silveira LC & De Lima SM (2009). The topography of cone photoreceptors in the retina of a diurnal rodent, the agouti *(Dasyprocta aguti). Visual Neuroscience* **26**: 167–175.

Rodieck RW & Rushton WA (1976). Cancellation of rod signals by cones, and cone signals by rods in the cat retina. *Journal of Physiology* **254**: 775–785.

Röhlich P & Szél Á (1993). Binding sites of photoreceptor-specific antibodies COS-1, OS-2 and AO. *Current Eye Research* **12**: 935-944.

Röhlich P, van Veen T & Szél Á (1994). Two different visual pigments in one retinal cone cell. *Neuron* **13**: 1159–1166.

Roll U, Dayan T & Kronfeld-Schor N (2006). On the role of phylogeny in determining activity patterns of rodents. *Evolutionary Ecology* **20**: 479-490.

Ross CF & Kirk EC (2007). Evolution of eye size and shape in primates. *Journal of Human Evolution* **52**: 294-313.

Rotics S, Dayan T & Kronfeld-Schor N (2011). Effect of artificial night lighting on temporally partitioned spiny mice. *Journal of Mammalogy* **92**: 159-168.

Ruby NF, Dark J, Heller HC & Zucker I (1996). Ablation of suprachiasmatic nucleus alters timing of hibernation in ground squirrels. *Proceedings of the National Academy of Sciences* **93**: 9864-9868.

Ruby NF & Heller HC (1998). Phase shift magnitude and direction determine whether Siberian hamsters reentrain to the photocycle. *Journal of Biological Rhythms* **13**: 506-517.

Russo IR, Chimimba CT & Bloomer P (2010). Bioregion heterogeneity correlates with extensive mitochondrial DNA diversity in the Namaqua rock mouse, *Micaelamys namaquensis* (Rodentia: Muridae) from southern Africa - evidence for a species complex. *BMC Evolutionary Biology* **10**: 307.

Saïdi T, Mbarek S, Chaouacha-Chekir RB & Hicks D (2011). Diurnal rodents as animal models of human central vision: characterisation of the retina of the sand rat *Psammomys obsesus*. *Graefe's Archive for Clinical and Experimental Ophthalmology* **249**: 1029-1037.

Sand A, Schmidt TM & Kofuji P (2012). Diverse types of ganglion cell photoreceptors in the mammalian retina. *Progress in Retinal and Eye Research* **31**: 287-302.

Sato T & Kawamura H (1984). Circadian rhythms in multiple unit activity inside and outside the suprachiasmatic nucleus in the diurnal chipmunk (*Eutamias sibiricus*). *Neuroscience Research* **1**: 45-52.

Schiller PH (2010). Parallel information processing channels created in the retina. *Proceedings of the National Academy of Sciences* **107**: 17087–17094.

Schmidt TM, Chen SK & Hattar S (2011a). Intrinsically photosensitive retinal ganglion cells: many subtypes, diverse functions. *Trends in Neurosciences* **34**: 572-580.

Schmidt TM, Do MTH, Dacey D, Lucas R, Hattar S & Matynia A (2011b). Melanopsin-positive intrinsically photosensitive retinal ganglion cells: from form to function. *The Journal of Neuroscience* **31**: 16094-16101.

Schnapf JL, Kraft TW & Baylor DA (1987). Spectral sensitivity of human cone photoreceptors. *Nature* **325**: 439-441.

Schoorlemmer GHM, Johnson AK & Thunhorst RL (2001). Circulating angiotensin II mediates sodium appetite in adrenalectomized rats. *American Journal of Physiology - Regulatory, Integrative and Comparative Physiology* **281**: R723-R729.

Schradin C & Pillay N (2003). Paternal care in the social and diurnal striped mouse (*Rhabdomys pumilio*): laboratory and field evidence. Journal of Comparative Psychology **117**: 317–324.

Schradin C (2006). Whole-day follows of striped mice (*Rhabdomys pumilio*), a diurnal murid rodent. *Journal of Ethology* **24**: 37-43.

Schradin C, Krackow S, Schubert M, Keller C, Schradin B & Pillay N (2007). Regulation of activity in desert-living striped mice: The importance of basking. *Ethology* **113**: 606-614.

Schumann DM, Cooper HM, Hofmeyr MD & Bennett NC (2005). Circadian rhythm of locomotor activity in the four striped field mouse, *Rhabdomys pumilio*: A diurnal African rodent. *Physiology & Behavior* **85**: 231-239.

Schwartz WJ, Reppert SM, Eagan SM & Moore-Ede MC (1983). In vivo metabolic activity of the suprachiasmatic nuclei: a comparative study. *Brain Research* **274**: 184-187.

Sellix MT, Evans JA, Leise TL, Castanon-Cervantes O, Hill DD, DeLisser P, Block GD, Menaker M & Davidson AJ (2012). Aging differentially affects the re-entrainmentresponse of central and peripheral circadian oscillators. *The Journal of Neuroscience* **32**: 16193-16202.

Semo MA, Peirson S, Lupi D, Lucas RJ, Jeffery G & Foster RG (2003). Melanopsin retinal ganglion cells and the maintenance of circadian and pupillary responses to light in aged rodless/coneless (rd/rd cl) mice. *European Journal of Neuroscience* **17**: 1793-1801.

Sharma VK, Chandrashekaran MK, Singaravel M & Subbaraj R (1999). Relationship between light intensity and phase resetting in a mammalian circadian system. *Journal of Experimental Zoology* **283**: 181-185.

Singaravel M, Sharma VK, Subbaraj R & Nair NG (1996). Chronobiotic effect of melatonin following phase shift of light/dark cycles in the field mouse *Mus booduga*. *Journal of Biosciences* **21**: 789-795.

Skene DJ & Arendt J (2007). Circadian rhythm sleep disorders in the blind and their treatment with melatonin. *Sleep Medicine* **8**: 651-655.

Skinner JD & Chimimba CT (2005). The Mammals of the Southern African Subregion. Cambridge University Press, Cambridge, UK.

Smale L, Lee T & Nunez AA (2003). Mammalian diurnality: some facts and gaps. *Journal of Biological Rhythms* **18**: 356-366.

Sonna LA, Fujita J, Gaffin SL & Lilly CM (2002). Invited review: Effects of heat and cold stress on mammalian gene expression. *Journal of Applied Physiology* **92**: 1725-1742.

Srinivasan V, Smits M, Spence W, Lowe AD, Kayumov L, Pandi-Perumal SR, Parry B & Cardinali DP (2006). Melatonin in mood disorders. *World Journal of Biological Psychiatry* **7**: 138-151.

Stephan FK & Zucker I (1972). Circadian rhythms in drinking behavior and locomotor activity of rats are eliminated by hypothalamic lesions. *Proceedings of the National Academy of Sciences* **69**: 1583-1586.

Stevens RG & Rea MS (2001). Light in the built environment: potential role of circadian disruption in endocrine disruption and breast cancer. *Cancer Causes & Control* **12**: 279-287.

Stieglitz A, Spiegelhalte F, Klante G & Heldmaier G (1995). Urinary 6-sulphatoxymelatonin excretion reflects pineal melatonin secretion in the Djungarian hamster (*Phodopus sungorus*). *Journal of Pineal Research* **18**: 69-76.

Strauss O (2005). The retinal pigment epithelium in visual function. *Physiological Reviews* **85**: 845-881.

Sugita Y & Tasaki K (1988). The activation of cones in scotopic and rods in photopic vision. *Tohoku Journal of Experimental Medicine* **156**: 311–317.

Szél Á & Röhlich P (1992). Two cone types of rat retina detected by anti-visual pigment antibodies. *Experimental Eye Research* **55**: 47–52.

Szél Á, Csorba G, Caffe AR, Szél G, Röhlich P & Van Veen T (1994). Different patterns of retinal cone topography in two genera of rodents, Mus and Apodemus. *Cell and Tissue Research* **276**: 143-150.

Szél A, Röhlich P, Caffé AR & Van Veen T (1996). Distribution of cone photoreceptors in the mammalian retina. *Microscopy Research and Technique* **35**: 445-462.

Szél Á, Röhlich P, Gaffé AR, Juliusson B, Aguirre GV & van Veen T (1992). Unique topographical separation of two spectral classes of cones in the mouse retina. *Journal of Comparative Neurology* **325**: 327-342.

Tachinardi P, Bicudo JE W, Oda GA & Valentinuzzi VS (2014). Rhythmic 24 h variation of core body temperature and locomotor activity in a subterranean rodent (*Ctenomys* aff. *knighti*), the Tuco-Tuco. *PloS One* **9**: e85674.

Takasu N, Nigi H & Tokura H (2002). Effects of diurnal bright/dim light intensity on circadian core temperature and activity rhythms in the Japanese macaque. *Japanese Journal of Physiology* **52**: 573-578.

Tast A, Love RJ, Evans G, Andersson H, Peltoniemi OAT & Kennaway DJ (2001). The photophase light intensity does not affect the scotophase melatonin response in the domestic pig. *Animal Reproduction Science* **65**: 283-290.

Tendron-Franzin A, Gouyon JB, Guignard JP, Decramer S, Justrabo E, Gilbert T & Semama DS (2004). Long-term effects of in utero exposure to cyclosporin A on renal function in the rabbit. *American Journal of Physiology - Regulatory, Integrative and Comparative Physiology* **15**: 2687-2693.

Thapan K, Arendt J & Skene DJ (2001). An action spectrum for melatonin suppression: evidence for a novel non-rod, non-cone photoreceptor system in humans. *The Journal of Physiology* **535**: 261-267.

Thompson S, Foster RG, Stone EM, Sheffield VC & Mrosovsky N (2008). Classical and melanopsin photoreception in irradiance detection: negative masking of locomotor activity by light. *European Journal of Neuroscience* **27**: 1973-1979.

Thorpe JB, Rajabi N & de Catazaro D (2012). Circadian rhythm and response to an acute stressor of urinary corticosterone, testosterone, and creatinine in adult male mice. *Hormone and Metabolic Research* **44**: 429-435.

Topping MG, Millar JS & Goddard JA (1999). The effect of moonlight on nocturnal activity in bushy-tailed wood rats (*Neotoma cinerea*). *Canadian Journal of Zoology* **77**: 480-485.

Touma C, Sachser N, Möstl E & Palme R (2002). Effects of sex and time of day on metabolism and excretion of corticosterone in urine and feces of mice. *General and Comparative Endocrinology* **130**: 267-278.

Trent BK, Tucker ME & Lockard JS (1977). Activity changes with illumination in slow loris *Nycticebus coucang*. *Applied Animal Ethology* **3**: 281-286.

Van der Meer E, van Loo PLP & Baumans V (2004). Short-term effects of a disturbed light-dark cycle and environmental enrichment on aggression and stress-related parameters in male mice. *Laboratory Animals* **38**: 376-383.

Van der Merwe I, Oosthuizen MK, Bennett NC & Chimimba CT (2011). Circadian rhythms of locomotor activity in captive eastern rock sengi. *Journal of Zoology* **286**: 250-257.

Van Diepen HC, Ramkisoensing A, Peirson SN, Foster RG & Meijer JH (2013). Irradiance encoding in the suprachiasmatic nuclei by rod and cone photoreceptors. *The FASEB Journal* **27**: 4204-4212.

Vasicek CA, Oosthuizen MK, Cooper HM & Bennett NC (2005). Circadian rhythms of locomotor activity in the subterranean Mashona mole rat, *Cryptomys darlingi*. *Physiology & Behavior* **84**: 181-191.

Vásquez RA (1994). Assessment of predation risk via illumination level: facultative central place foraging in the cricetid rodent *Phyllotis darwini*. *Behavioral Ecology and Sociobiology* **34**: 375-381.

Vivanco P, Rol MÁ & Madrid JA (2009). Two steady-entrainment phases and graded masking effects by light generate different circadian chronotypes in *Octodon degus*. *Chronobiology International* **26**: 219-241.

Von Schantz M, Argamaso-Hernan SM, Szél Á & Foster RG (1997). Photopigments and photoentrainment in the Syrian golden hamster. *Brain Research* **770**: 131–138.

Von Schantz M, Provencio I & Foster RG (2000). Recent developments in circadian photoreception: more than meets the eye. *Investigative Ophthalmology & Visual Science* **41**: 1605-1607.

Wehr TA, Schwartz PJ, Turner EH, Feldman-Naim S, Drake CL & Rosenthal NE (1995). Bimodal patterns of human melatonin secretion consistent with a two-oscillator model of regulation. *Neuroscience Letters* **194**: 105-108.

Weibel L, Maccari S & Van Reeth O (2002). Circadian clock functioning is linked to acute stress reactivity in rats. *Journal of Biological Rhythms* **17**: 438-446.

Welsh DK, Takahashi JS & Kay SA (2010). Suprachiasmatic nucleus: cell autonomy and network properties. *Annual Review of Physiology* **72**: 551.

Weng S, Estevez ME & Berson DM (2013). Mouse ganglion-cell photoreceptors are driven by the most sensitive rod pathway and by both types of cones. *PloS One* **8**: ee66480.

Williams GA, Calderone JB & Jacobs GH (2005). Photoreceptors and photopigments in a subterranean rodent, the pocket gopher (*Thomomys bottae*). *Journal of Comparative Physiology A* **191**: 125–134.

Wong DL (2006). Epinephrine biosynthesis: hormonal and neural control during stress. *Cellular and Molecular Neurobiology* **26:** 891–900.

Yan J, Wang H, Liu Y & Shao C (2008). Analysis of gene regulatory networks in the mammalian circadian rhythm. *PLoS Computational Biology* **4**: e1000193.

Zheng B, Larkin DW, Albrecht U, Sun ZS, Sage M, Eichele G, Lee CC & Bradley A (1999). The *mPer2* gene encodes a functional component of the mammalian circadian clock. *Nature* **400**: 169-173.

Zubidat AE, Ben-Shlomo R & Haim A (2007). Thermoregulatory and endocrine responses to light pulses in short-day acclimated social voles (*Microtus socialis*). *Chronobiology International* **24**: 269-288.

Zubidat AE, Nelson RJ & Haim A (2009). Photosensitivity to different light intensities in blind and sighted rodents. *Journal of Experimental Biology* **212**: 3857-3864.

Zubidat AE, Nelson RJ & Haim A (2010a). Differential effects of photophase irradiance on metabolic and urinary stress hormone concentrations in blind and sighted rodents. *Journal of Experimental Biology* **212**: 3857-3864.

Zubidat AE, Nelson RJ & Haim A (2010b). Photoentrainment in blind and sighted rodent species: responses to photophase light with different wavelengths. *The Journal of Experimental Biology* **213**: 4213-4222.

Zubidat AE, Nelson RJ & Haim A (2011). Spectral and duration sensitivity to light-at-night in 'blind' and sighted rodent species. *The Journal of Experimental Biology* **214**: 3206-3217.